A search for $\mu^+ \to e^+\gamma$ with the highest sensitivity beyond the MEG experiment

(MEG実験を超える最高感度での$\mu^+ \to e^+\gamma$探索)

Kensuke Yamamoto

PhD Defence
Fri. 20th June 2025

Abstract

- A search for $\mu^+ \to e^+\gamma$ with the 2021-2022 MEG II dataset
  - Statistics are higher by a factor of 5 than those for the first MEG II result
    - Maintaining excellent detector performance over long-term data-taking
  - With algorithm updates in photon reconstruction

- The sensitivity is the highest ever: 2.2×10^{-13}
  - Better by a factor of 2.4 than that in the MEG experiment

- No signal was found
- The most stringent upper limit set to $\mathcal{B}(\mu^+ \to e^+\gamma) < 1.5 \times 10^{-13}$ (90% C.L.)

Timeline and my contribution summary

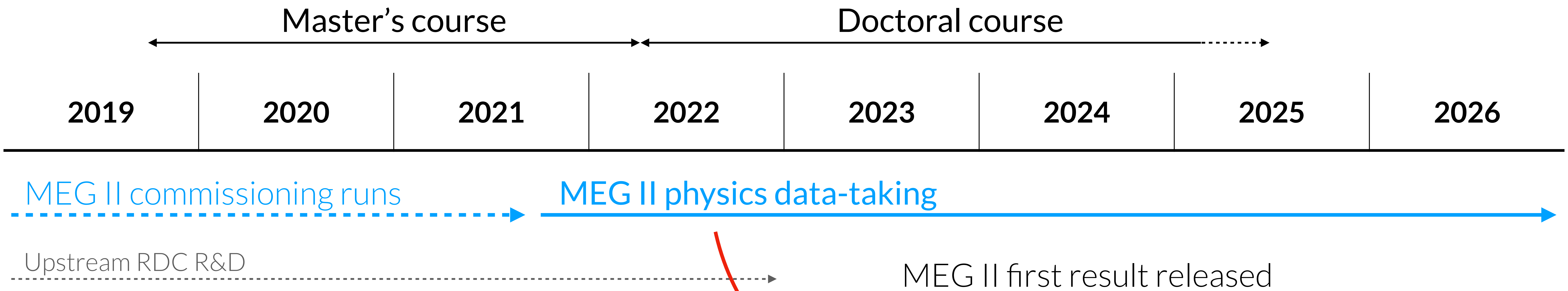

MEG II first result released
(Paper published in Feb. 2024)

Analysis updates:
- Photon and RDC reconstructions

Detector calibrations:
- LXe γ detector
  - 4,760 photosensors
  - Energy scale
- RDC

MEG II 2021-22 result released
(Paper submitted to PRL in Apr.)

Likelihood analysis to search for $\mu^+ \to e^+\gamma$

Achievement summary

- RDC operation and quick feedback to beam
- Feedback to LXe detector calibration DAQ
- New photon pileup unfolding algorithm increased signal efficiency by 2% and reconstruction reliability
- RDC analysis updates increased detection efficiency by 17%
- Photon energy scale uncertainty suppressed down to 0.18% thanks to careful calibration

Contents

Contents

Physics behind $\mu^+ \to e^+\gamma$

- The Standard Model of particle physics has achieved remarkable success so far
- But, considered as a low-energy approximation of more fundamental theory

- **The charged-lepton-flavour-violating decay $\mu \to e\gamma$ is an interesting probe to search for new physics beyond the SM**
  - **Its discovery would be clear evidence of new physics**

$\mathcal{B}(\mu \to e\gamma) \sim 10^{-54}$ SM + ν oscillation

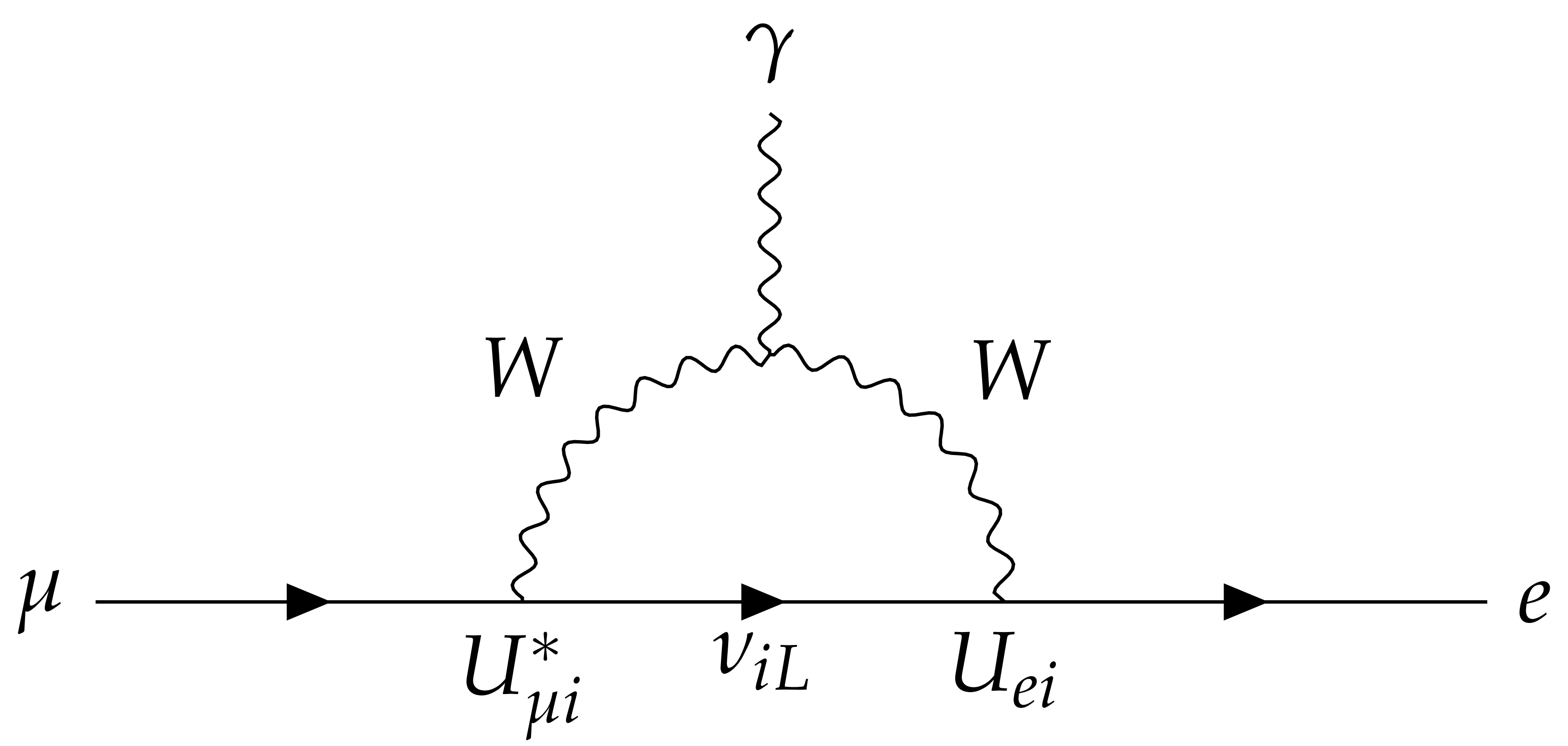

SUSY models $\mathcal{B}(\mu \to e\gamma) \sim 10^{-12} - 10^{-14}$

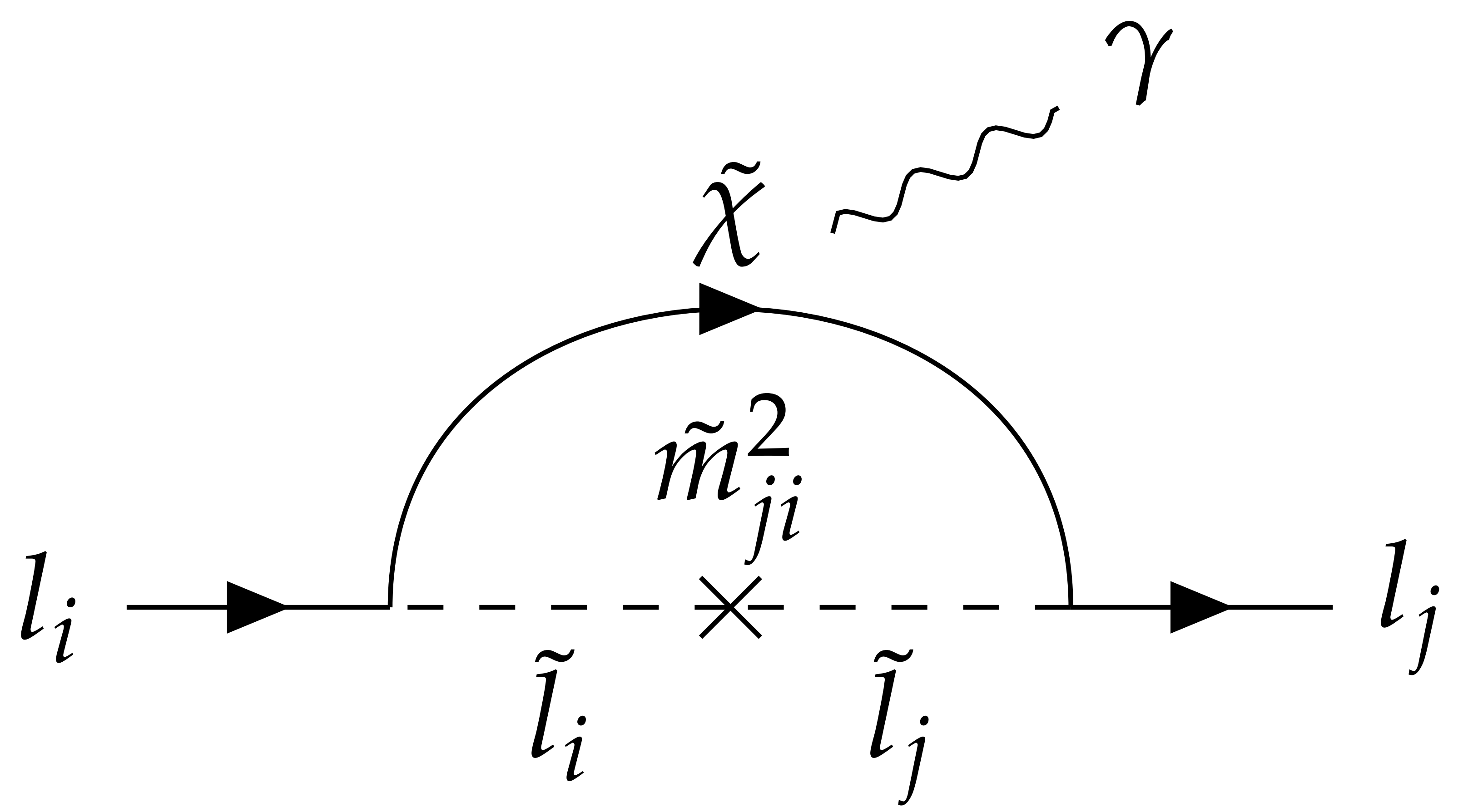

$\mu^+ \to e^+\gamma$ signature and background

	Signal	Accidental background $\gg$	RMD background
	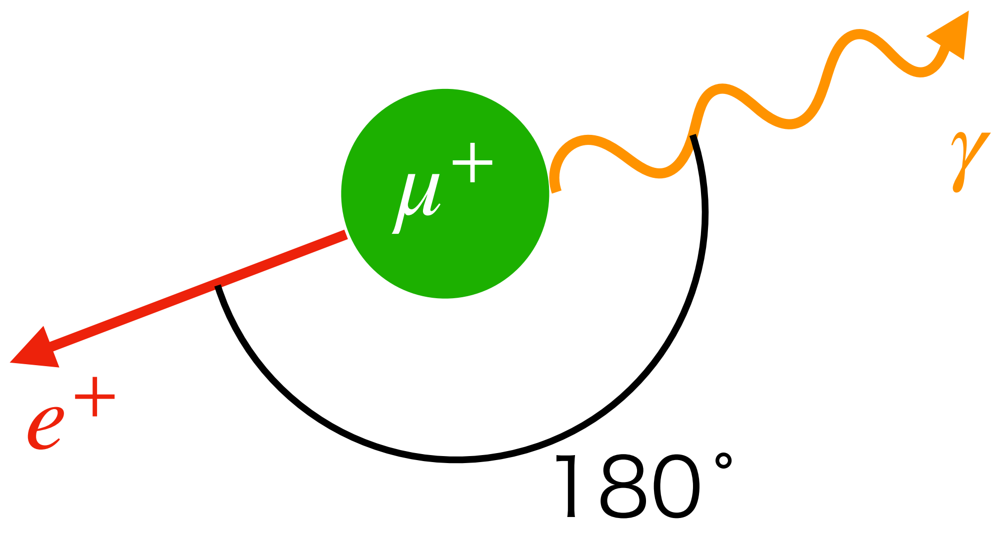	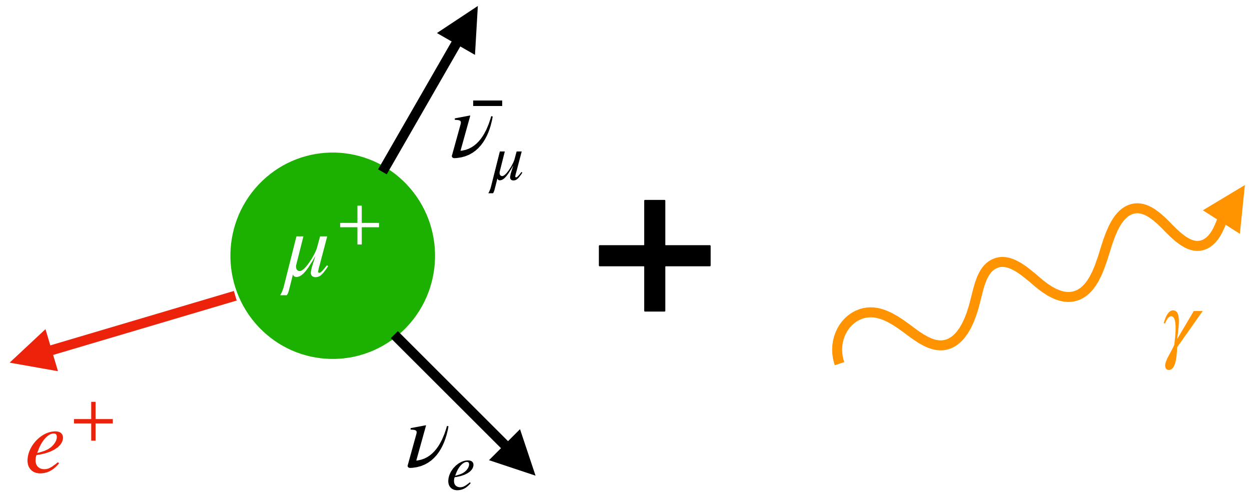	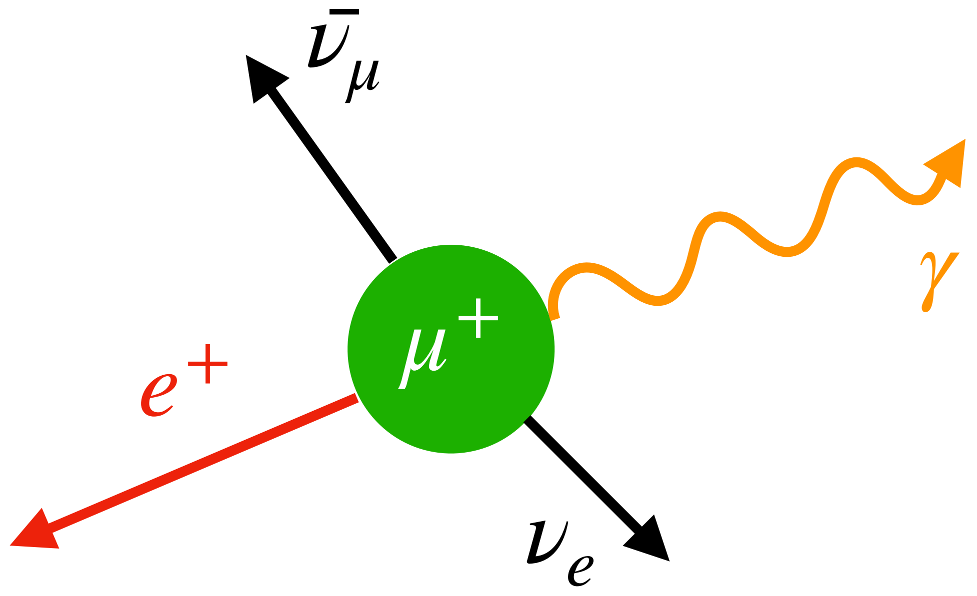
E_γ	52.8 MeV	<52.8 MeV	<52.8 MeV
E_e	52.8 MeV	<52.8 MeV	<52.8 MeV
$t_{e\gamma} = t_\gamma - t_e$	0 s	Flat	0 s
Opening angle	180°	<180°	<180°

Precise kinematics measurement required to distinguish signal from backgrounds

Keys to accidental background suppression

$$N_{\mathrm{ACC}} \propto \underline{R_\mu^2} \cdot \underline{\sigma_{E_e} \cdot \sigma_{E_\gamma}^2 \cdot \sigma_{t_{e\gamma}} \cdot \sigma_{\Theta_{e\gamma}}^2}$$

Continuous beam   Detector resolutions

$0.9 < y\,(= 2E_\gamma/m_\mu) < 1.0$

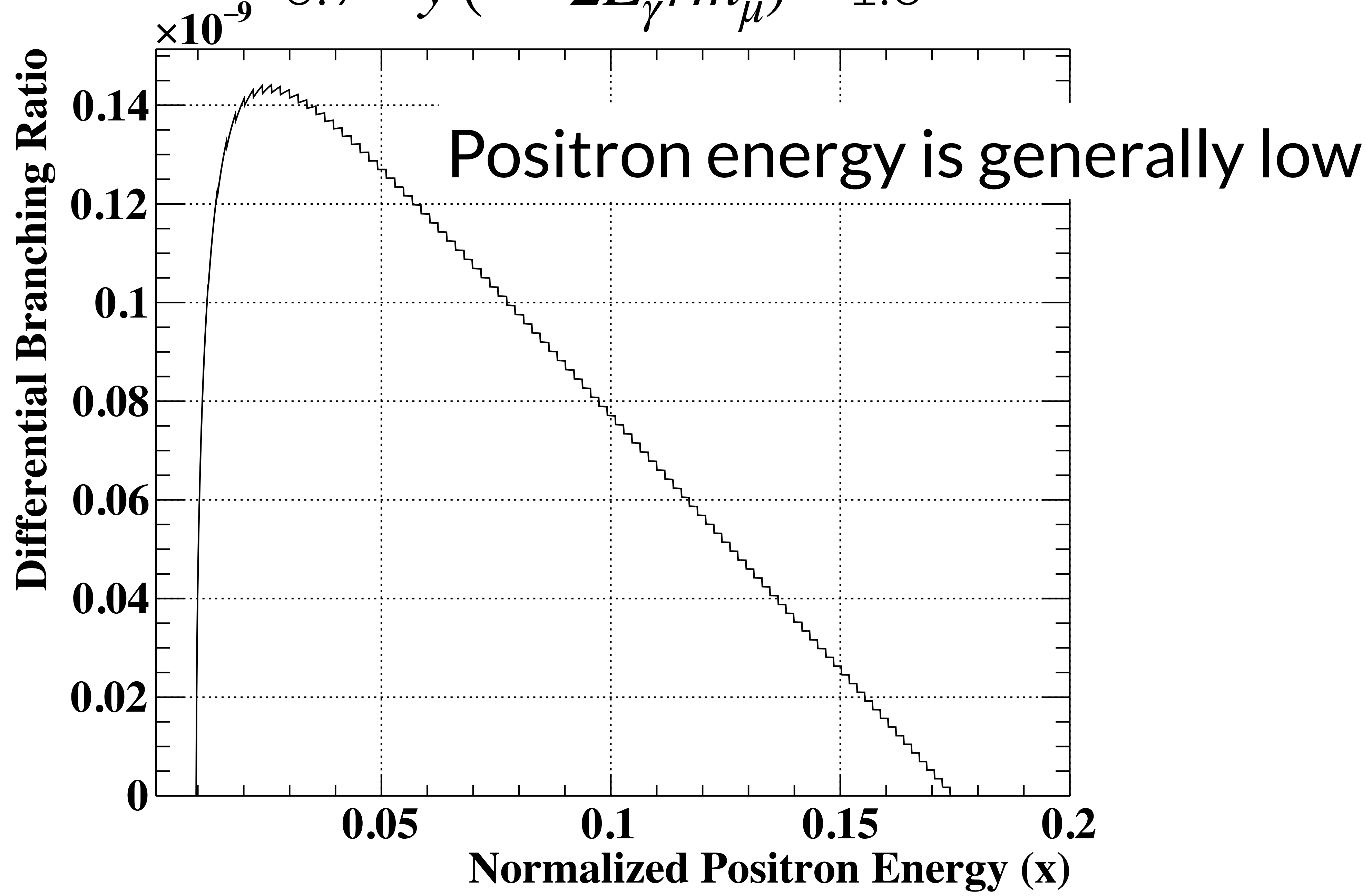

$x\,(= 2E_e/m_\mu)$

Active background tagging

High-energy RMD photon tagging
by detecting accompanying low-energy positron

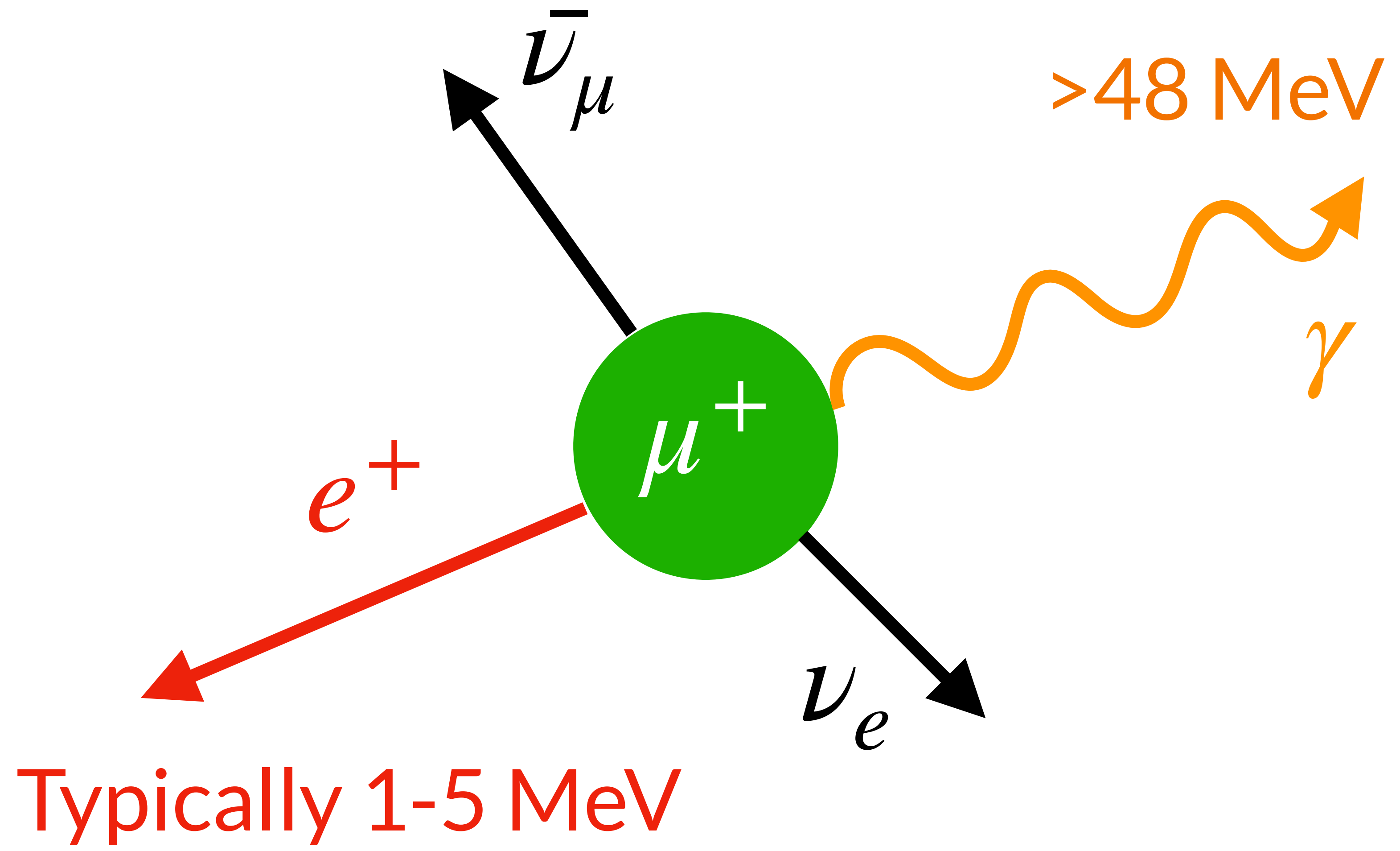

Contents

MEG II apparatus & reconstruction overview

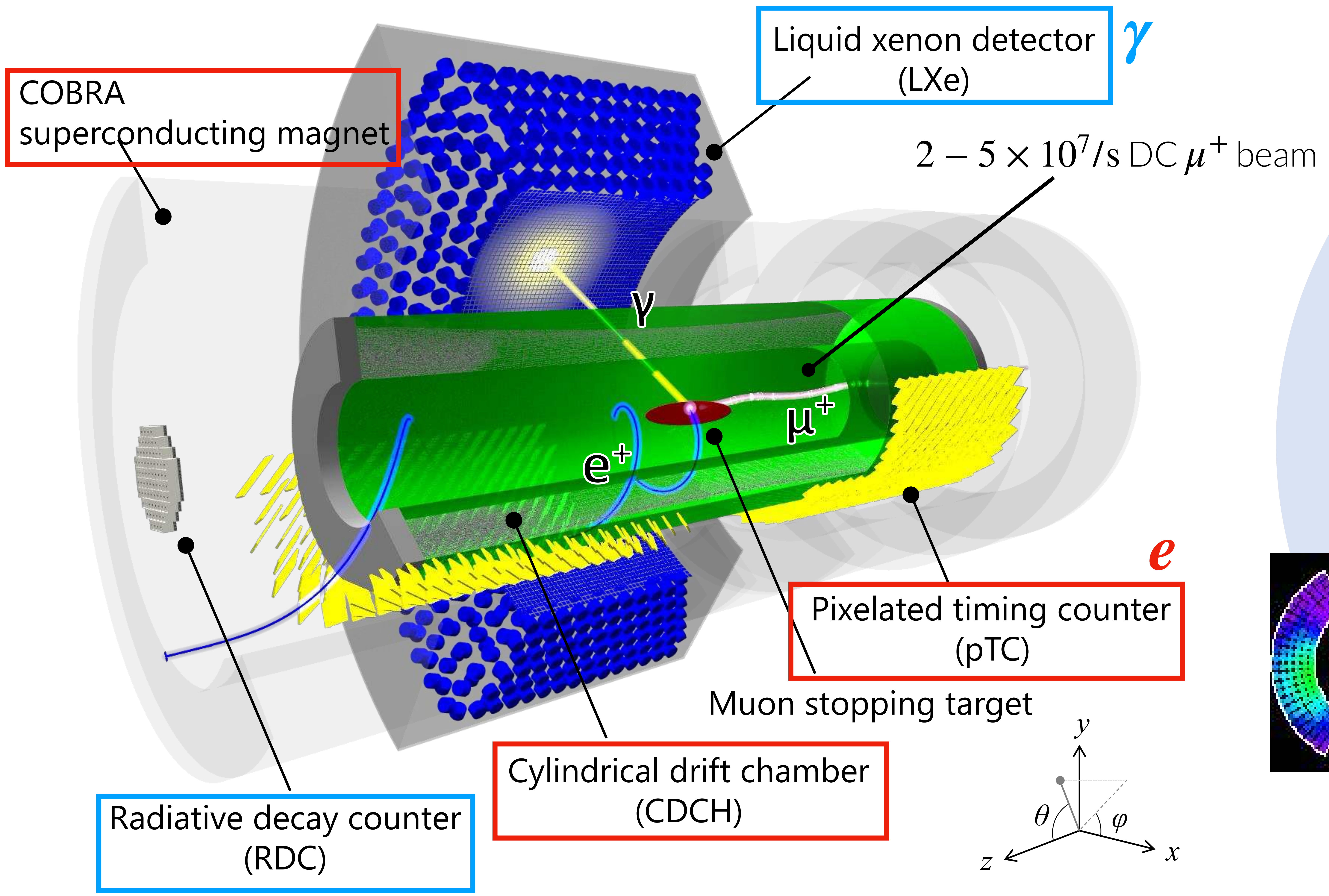

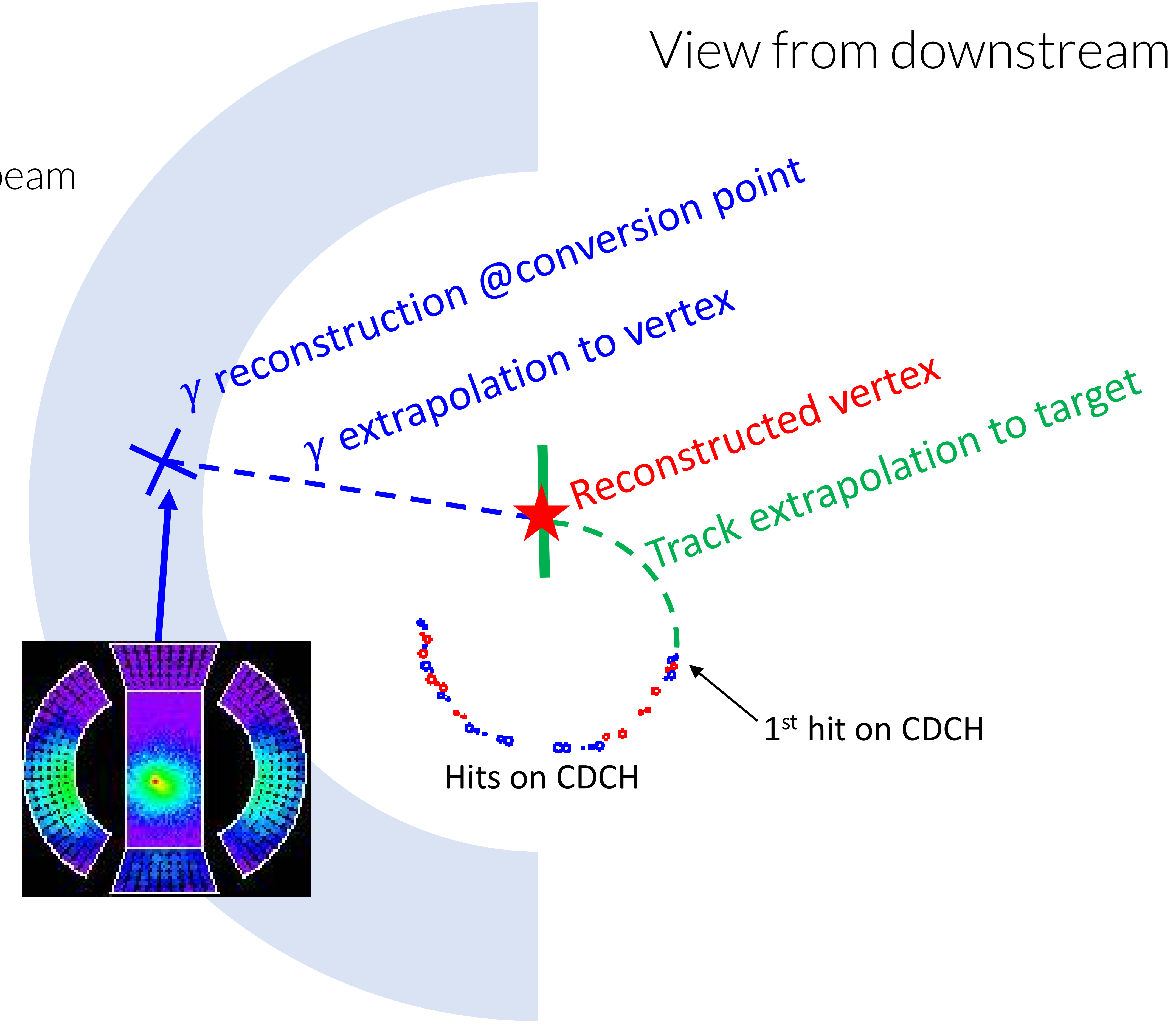

High-intensity DC muon beam × Innovative high-resolution detector

Positron spectrometer

- Designed to detect 52.8 MeV positrons under a high-rate environment

- Superconducting COBRA magnet
  - Constant bending radius of positrons
  - Provide gradient magnetic field (0.5-1.3 T)

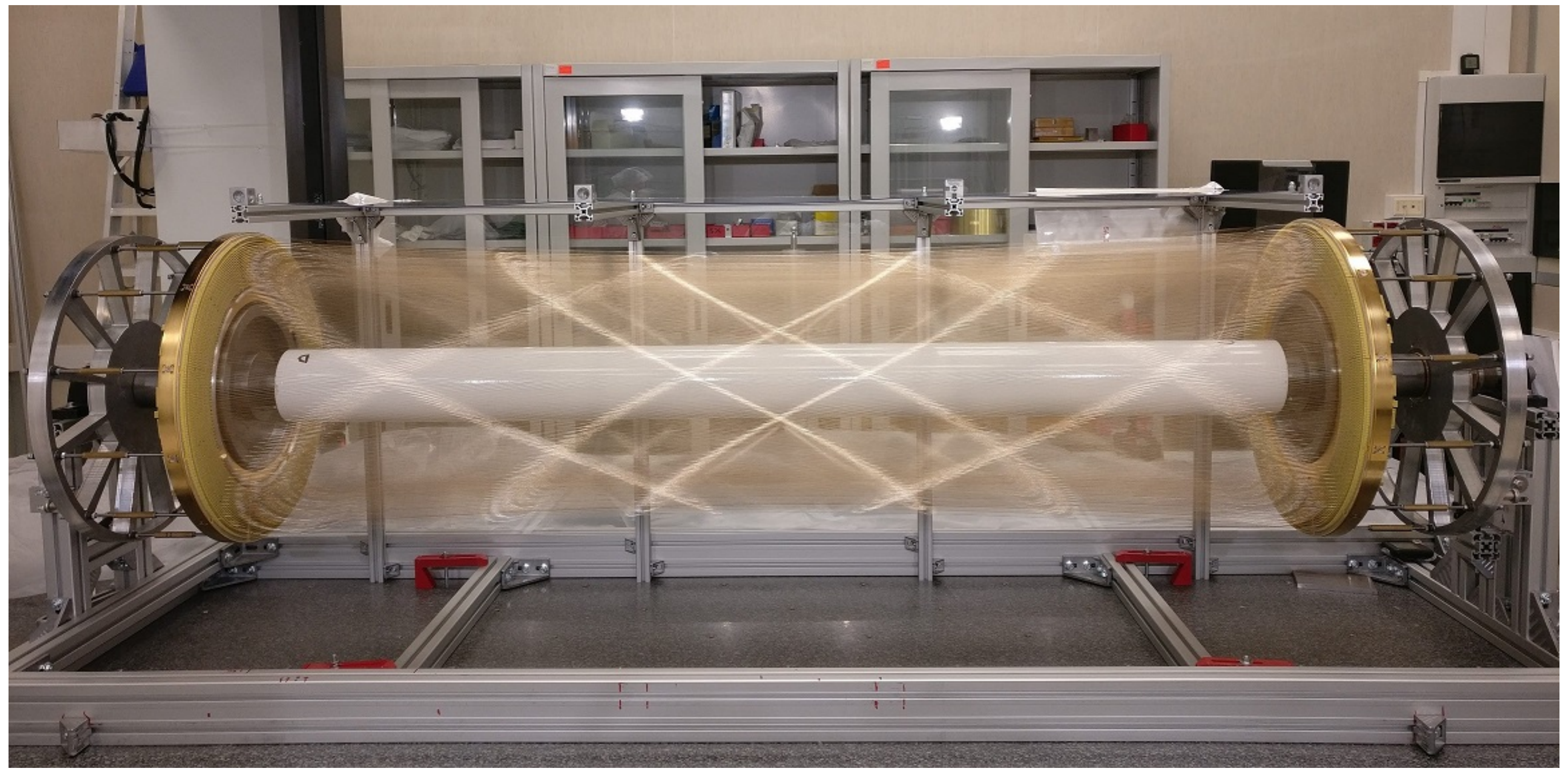

- Single-volume cylindrical drift chamber (CDCH)
  - Ultra-low-mass design
  - Wires arranged in a stereo configuration

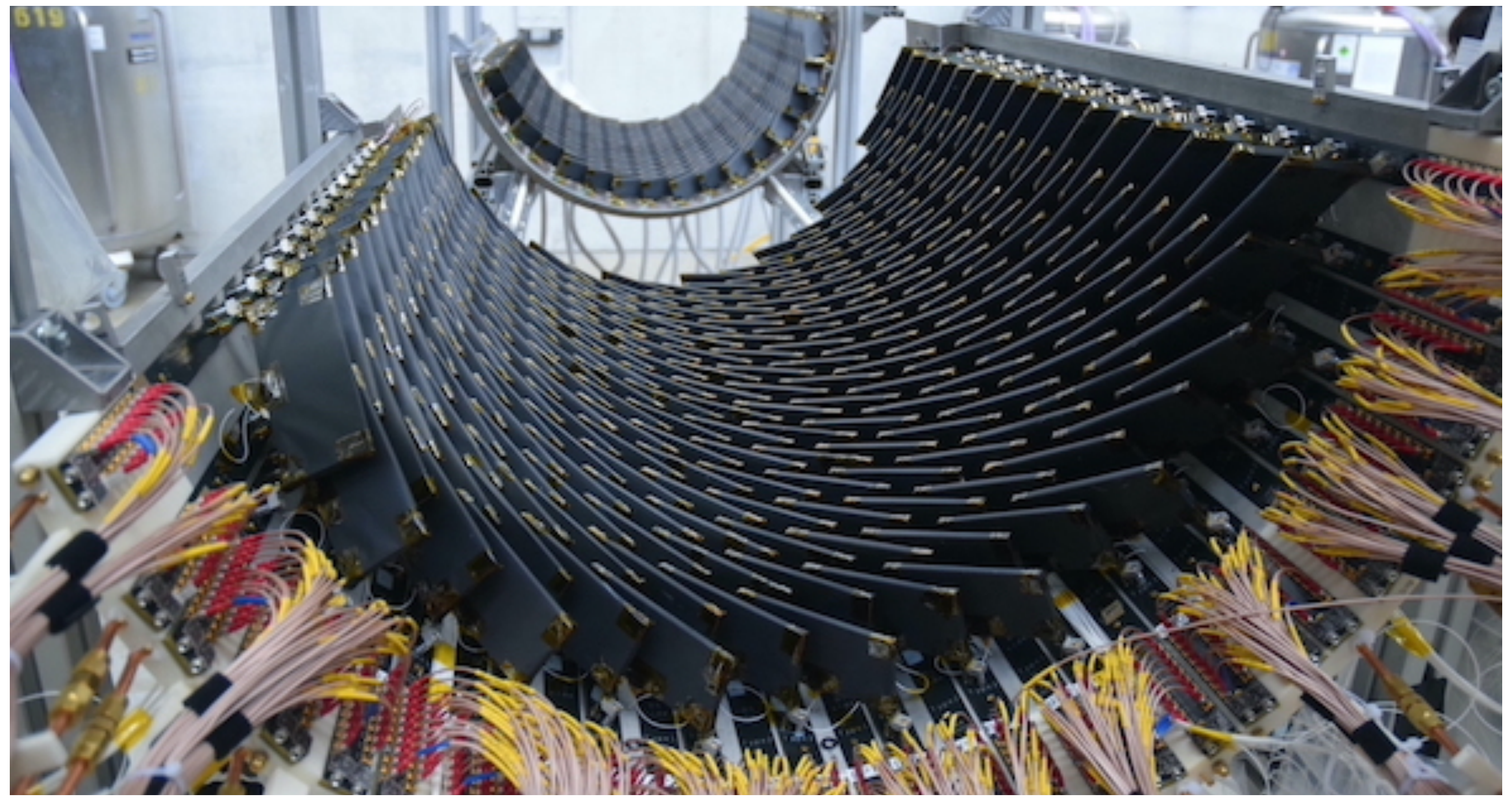

- Pixelated timing counter (pTC)
  - 256 scintillation counters in each sub-module
  - Multiple hits improve resolution $\sigma_{t_e} = \frac{\sigma_{\mathrm{single}}}{\sqrt{n_{\mathrm{pTC}}}}$

Homogeneous liquid xenon photon detector

- 900 L of liquid xenon
- 4,760 VUV-sensitive photosensors (4,092 MPPCs + 668 PMTs)

- Reconstruct photon kinematics
  - $\vec{x}_\gamma$ and E_γ based on scintillation light distribution
  - t_γ based on detected pulse timing

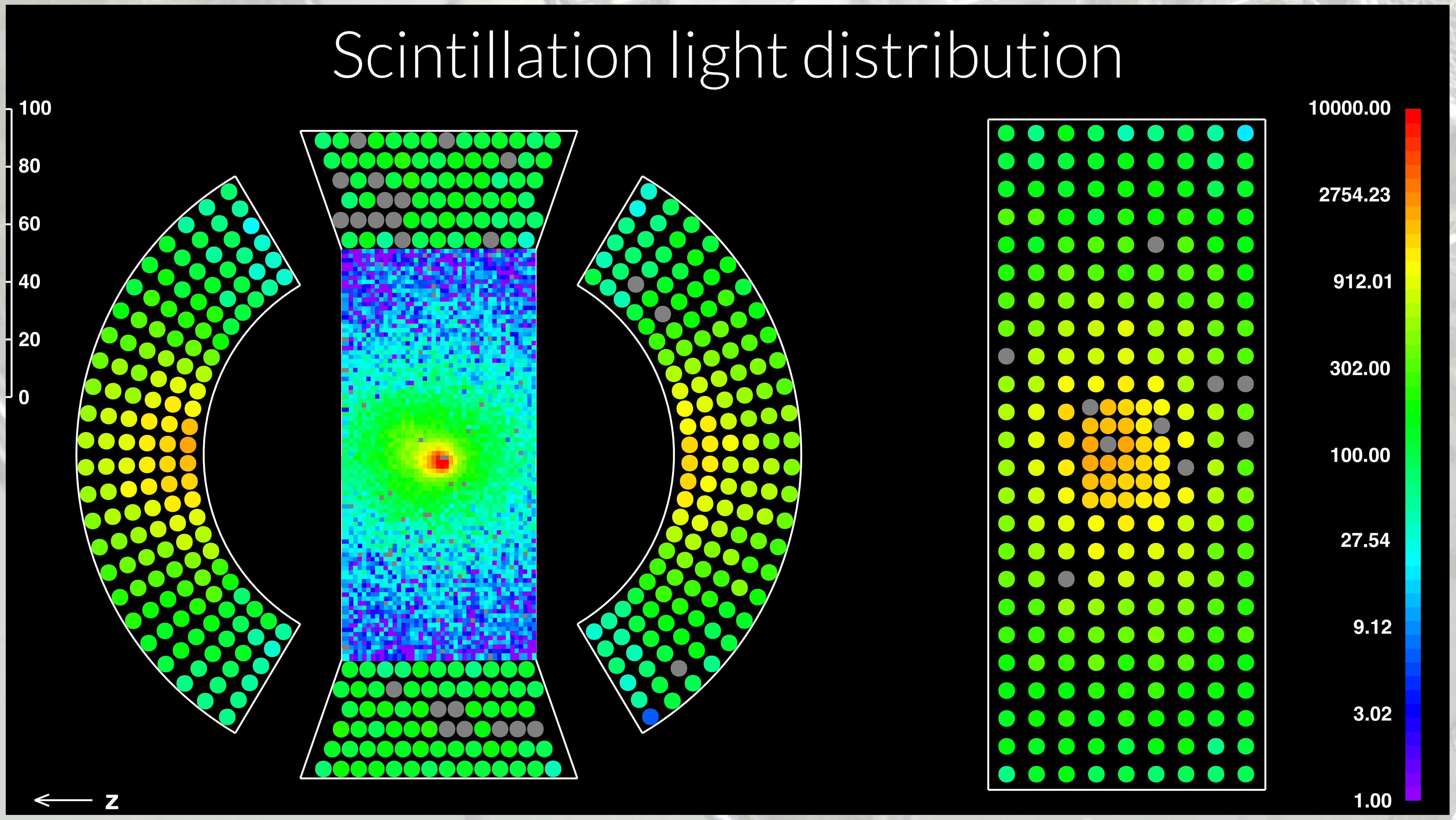

Radiative decay counter

- Detect low-energy positrons to tag high-energy photons detected by LXe detector
- Measure
  - Positron timing t_{RDC} with plastic scintillators and
  - Positron energy E_{RDC} with LYSO crystals

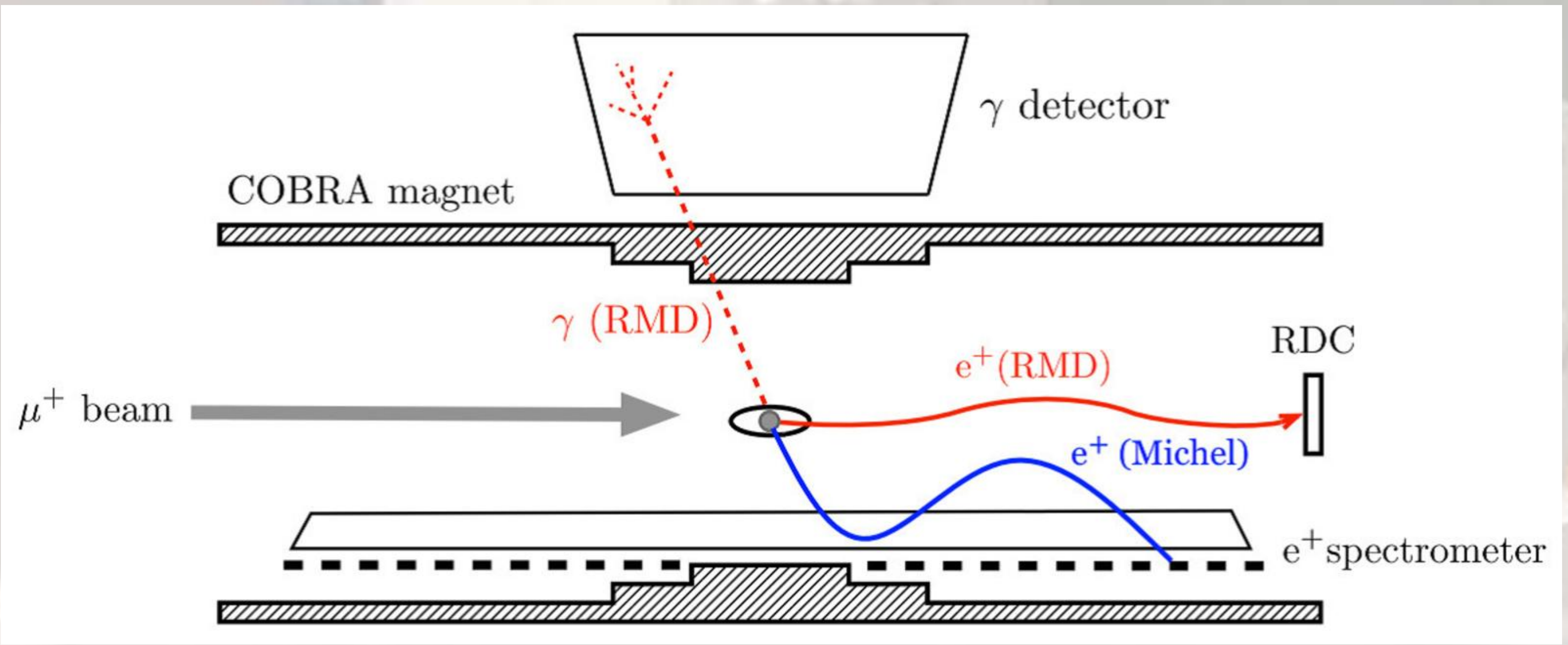

Positron hits at the edge of RDC

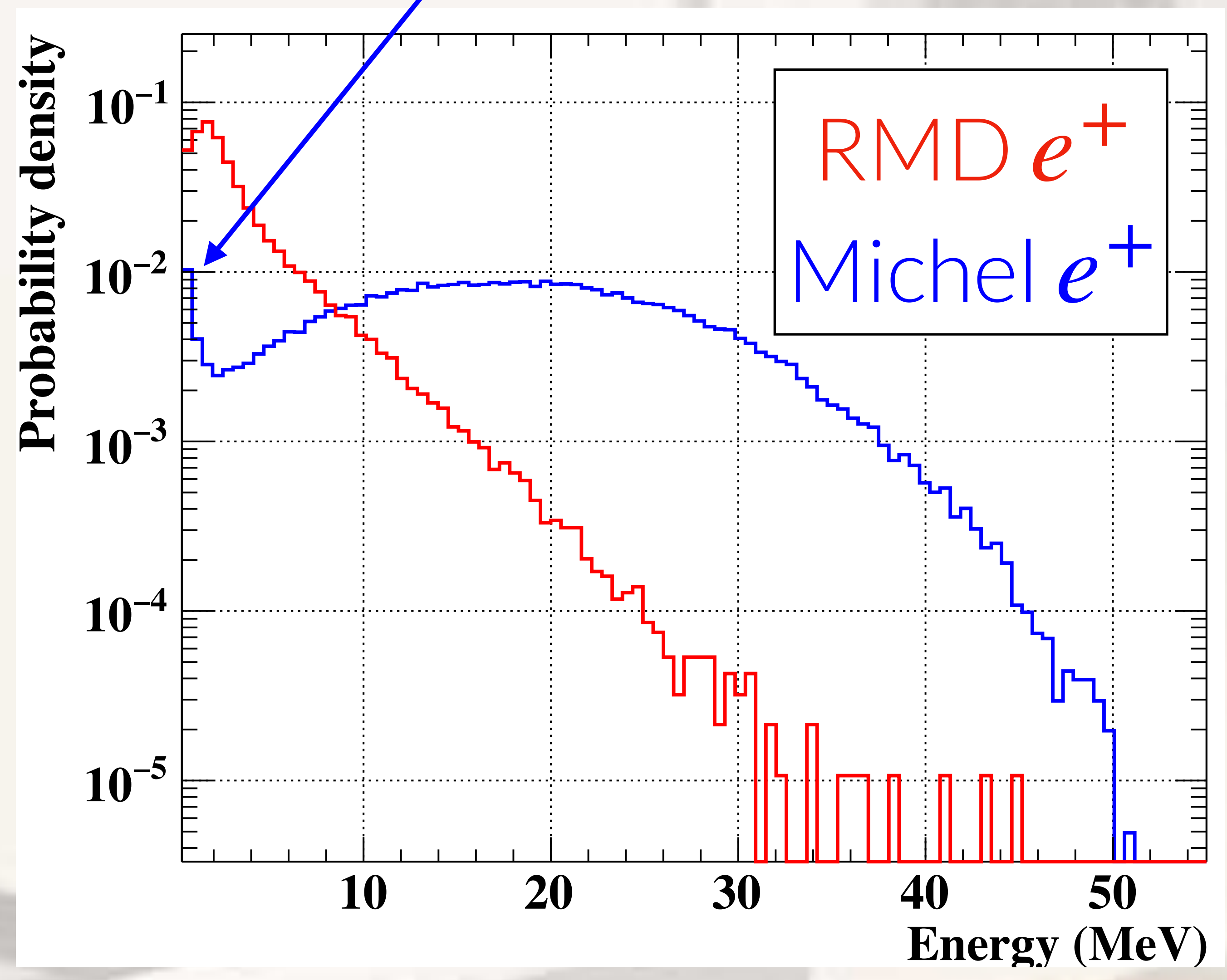

Run

- Physics and calibration data successfully collected in 2021 and 2022
  - Stable detector and DAQ conditions except for LXe purity

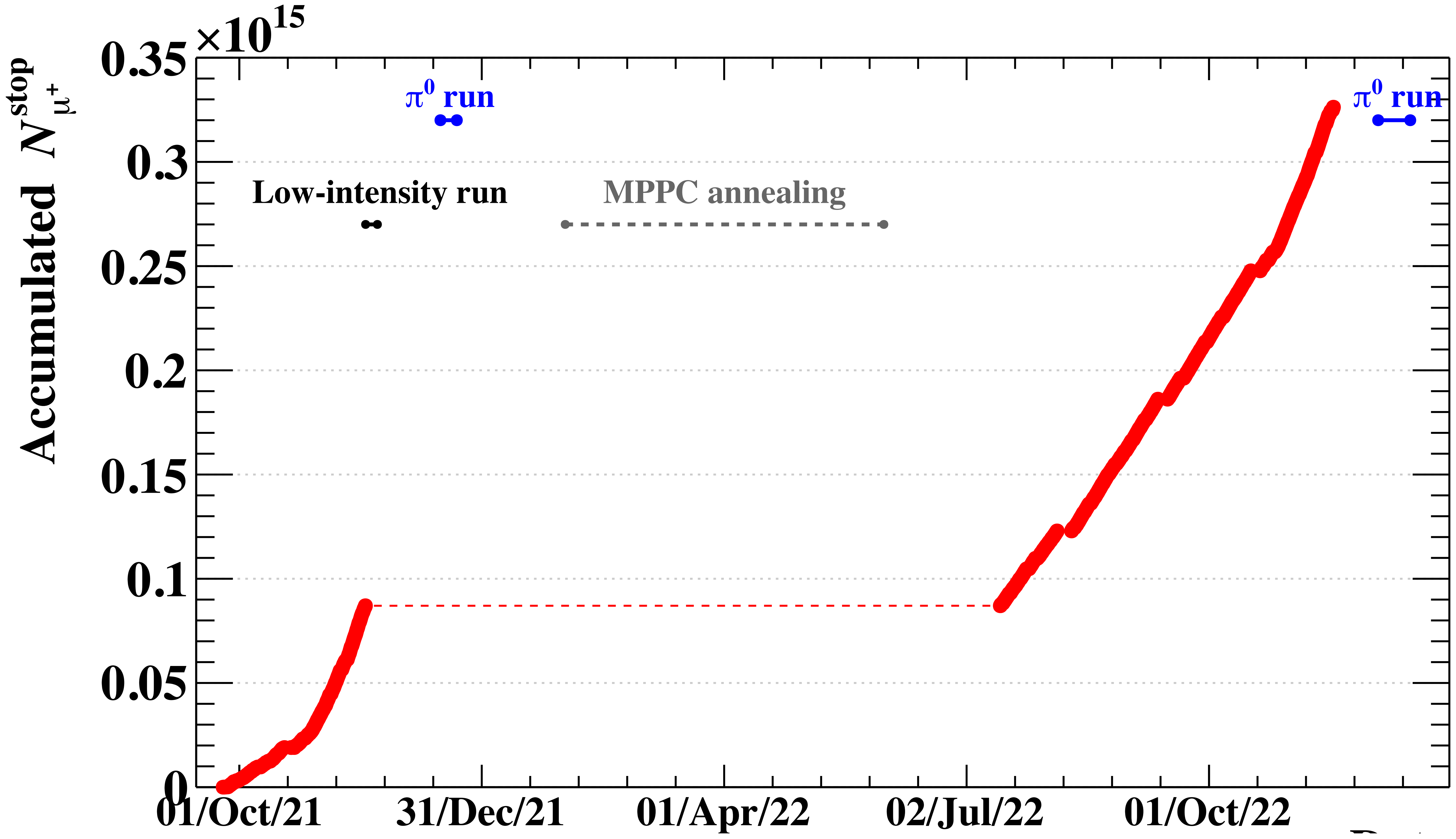

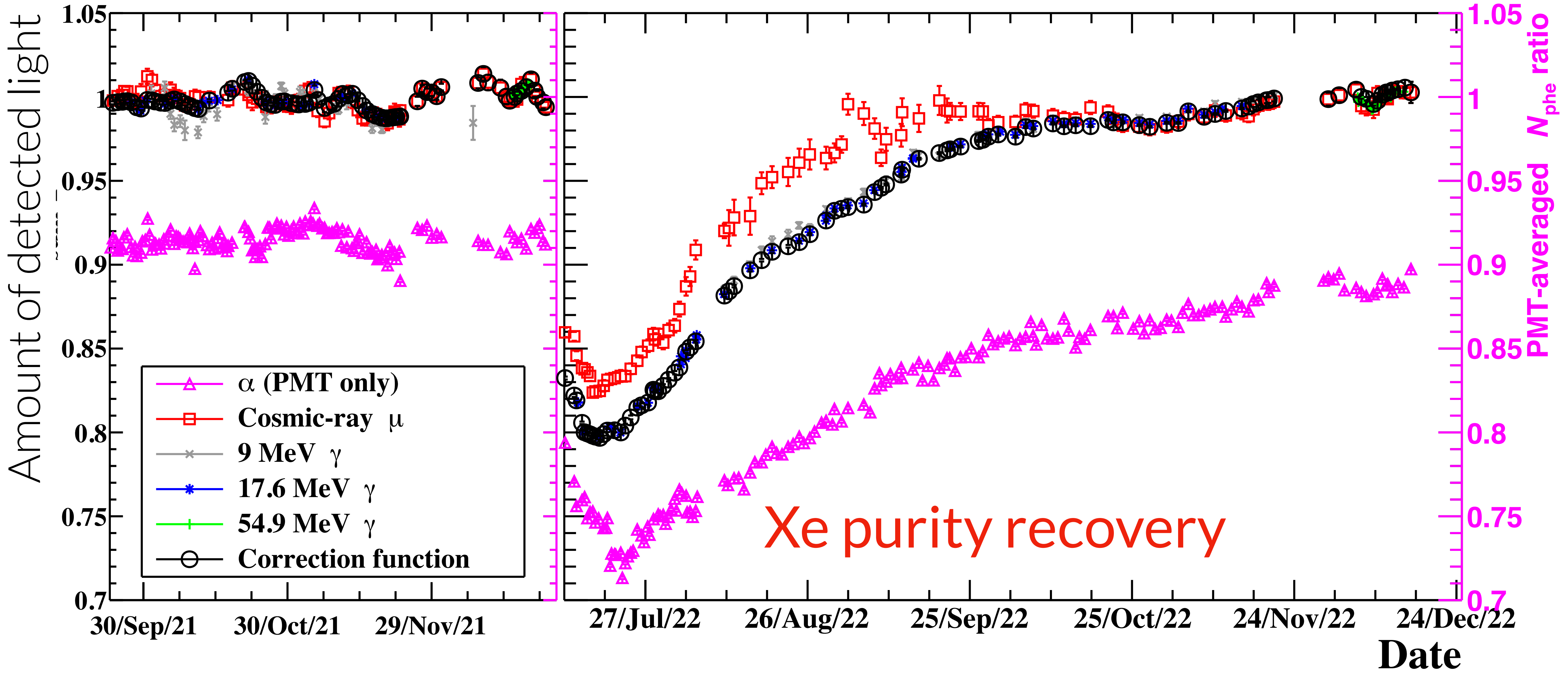

Contents

- Pileup unfolding algorithm improvement
- RDC reconstruction algorithm improvement

Pileup unfolding: a nutshell

- Template waveforms f are fitted to the sum of measured waveforms V by minimising

$$\chi^2_{\mathrm{wf}} = \sum_{\mathrm{MPPC,PMT}} \int \frac{\left(V(\tau) - \sum_i^{n_{\mathrm{pulse}}} f(\tau; A_i, T_i)\right)^2}{\sigma_f^2(\tau)} d\tau$$

- Initial parameter set $(n_{\mathrm{pulse}}; \underbrace{A_i}_{\text{Amplitude}}, \underbrace{T_i}_{\text{Timing}})$ with three techniques
  - Waveform processing
  - Scintillation light distribution
  - **ADC signal ← NEW**

- **Calculate E_γ only for the main pulse**
  - Eliminate pileup pulses

An example of $n_{\mathrm{pulse}} = 2$

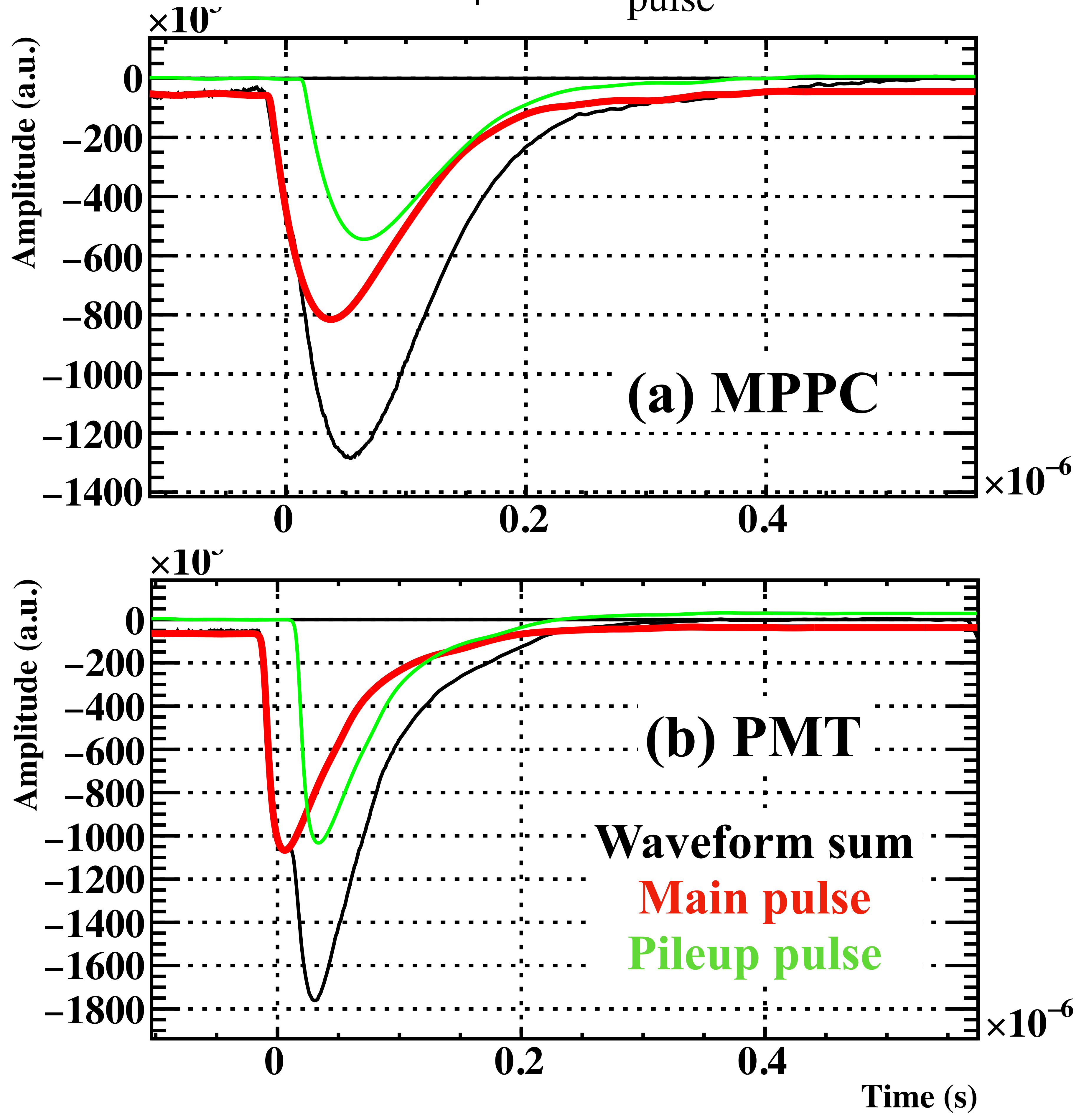

Pileup unfolding algorithm improvement

- **Fit convergence improved thanks to better pulse discrimination**
  - Simultaneous fit to use PMT timing information
  - Event fraction with larger χ^2_{wf} than threshold: 2-3% → <1%
- Reconstruction reliability
- **Signal efficiency improved by 2%**
  - (92 ± 2) % → (94.2 ± 0.5) %

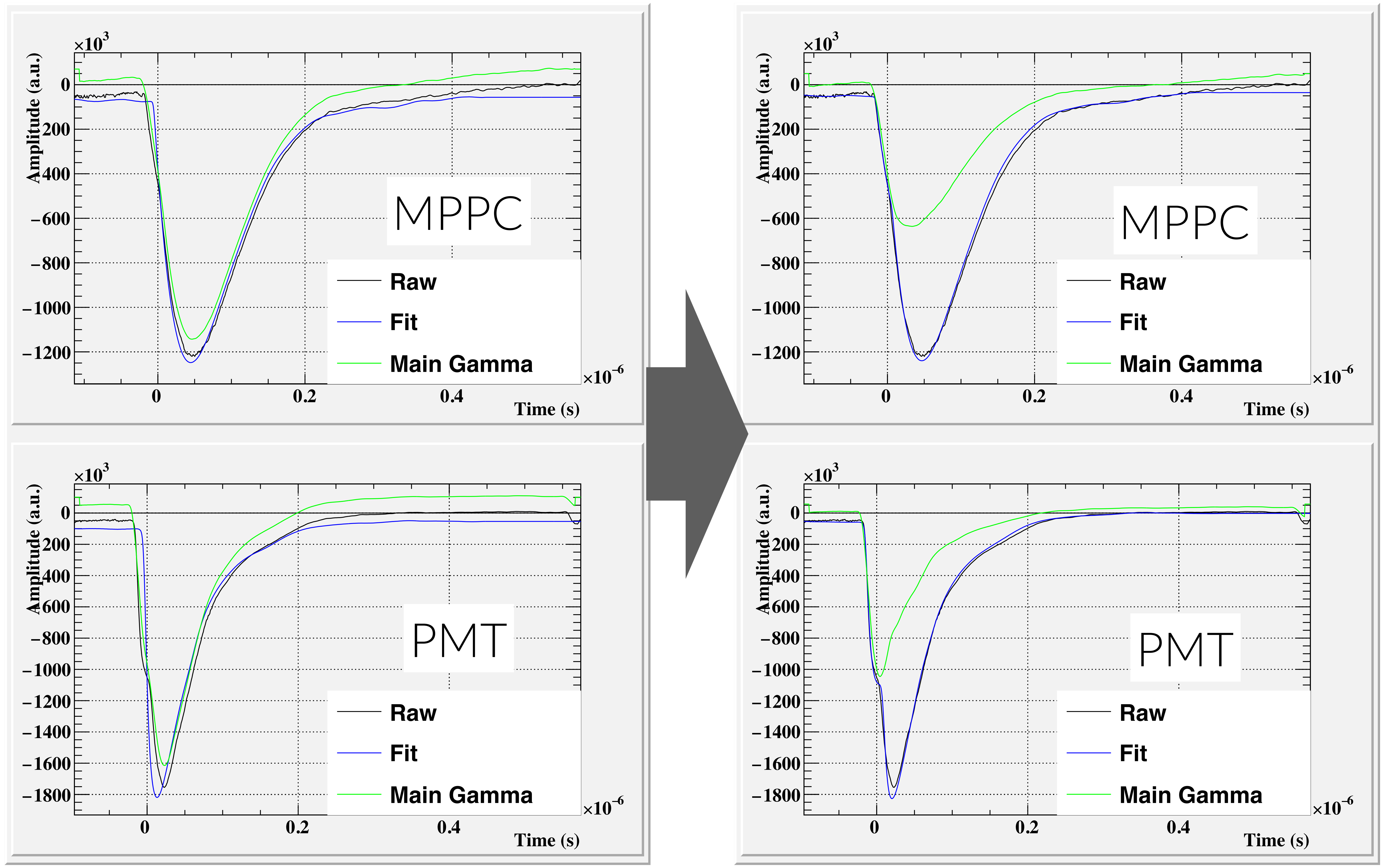

Pileup unfolding algorithm improvement

- ADC signal (originally for trigger) newly introduced
- Better identification and energy reconstruction in an event where pileup photon comes before the DRS time window

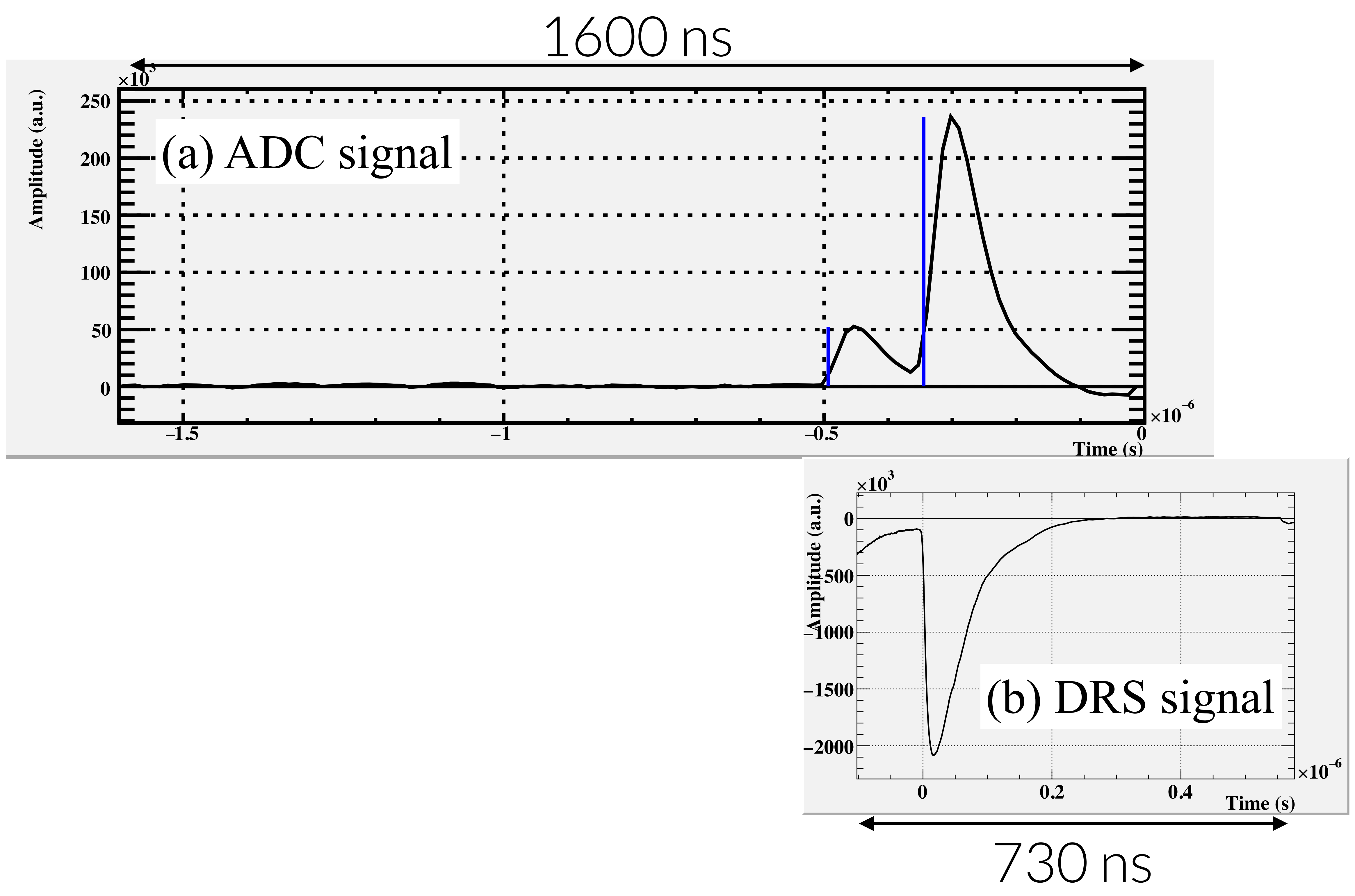

Response to 55 MeV γ for events with pre-window pileup

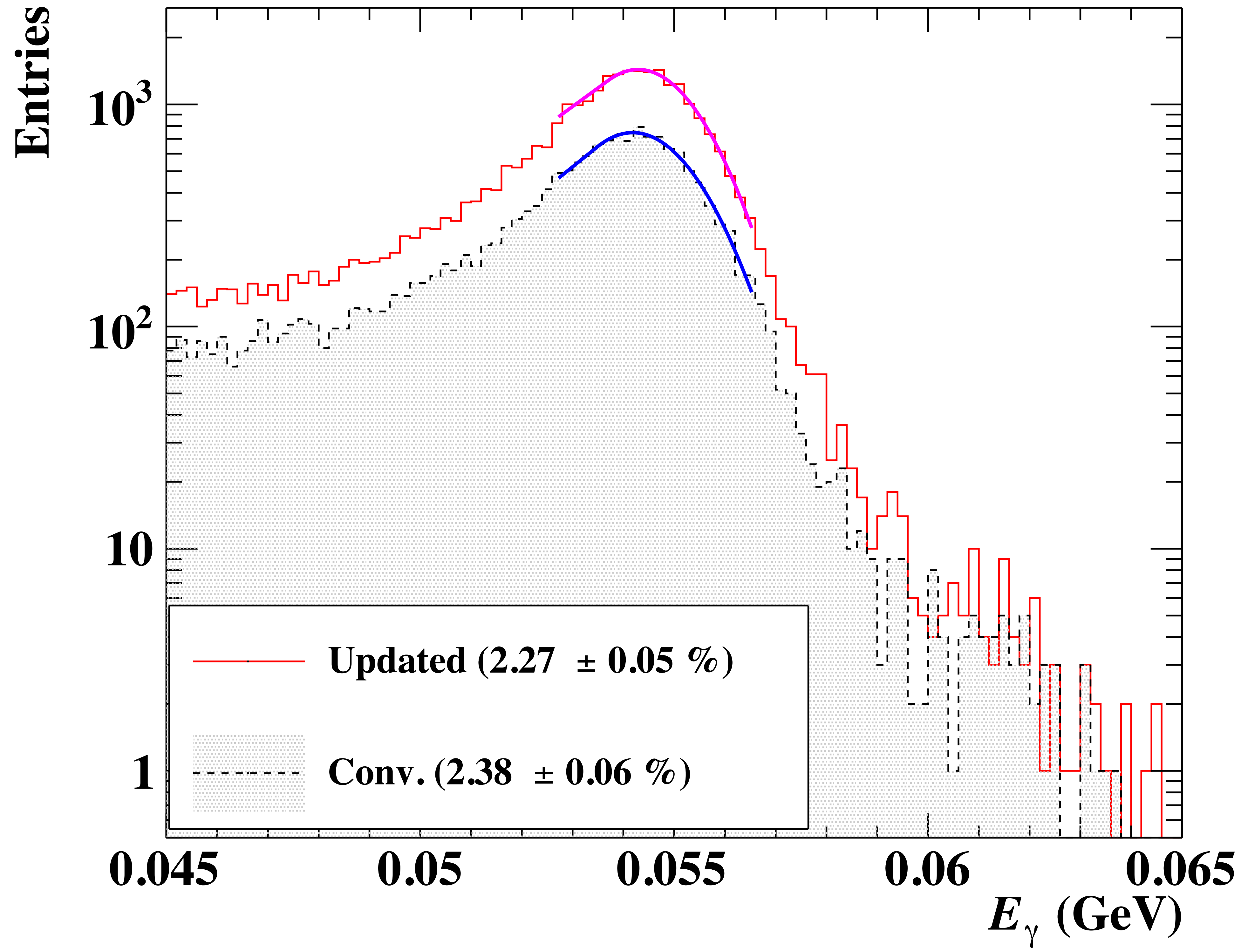

RDC reconstruction: a nutshell

- SiPMs attached
  - At both ends of the plastic scintillator
  - On the back side of the LYSO crystal
- Hits reconstructed in each scintillator independently
- Matching based on position and timing
- **Lower "tagged-RMD fraction" than MC in the 2021 dataset analysis**
  - Measurement (22%) vs Expectation (32%)

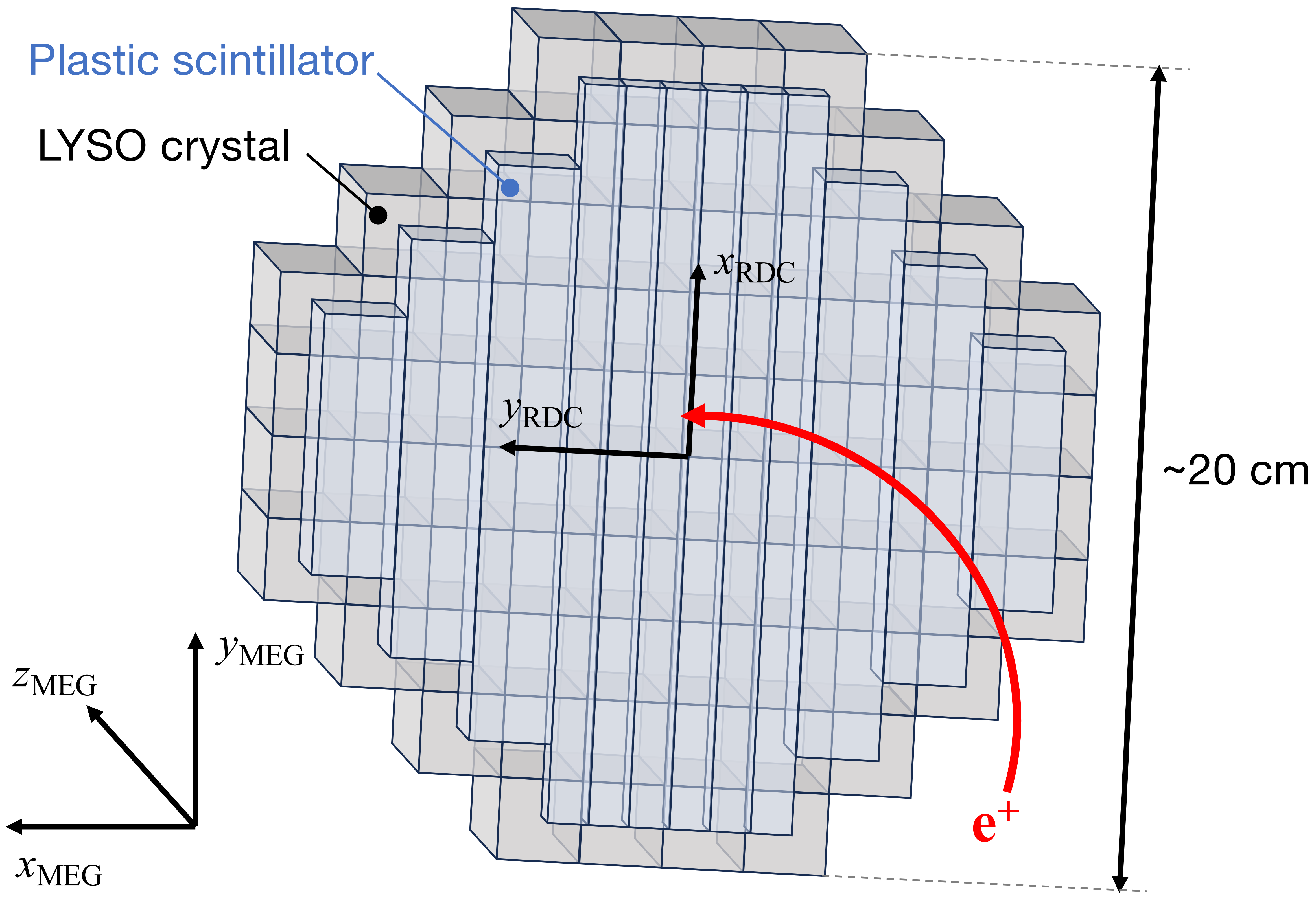

RDC detection efficiency improvement

- Detection efficiency improved by 17%
  - Thanks to offline waveform filter
  - Tagged-RMD fraction improved as well

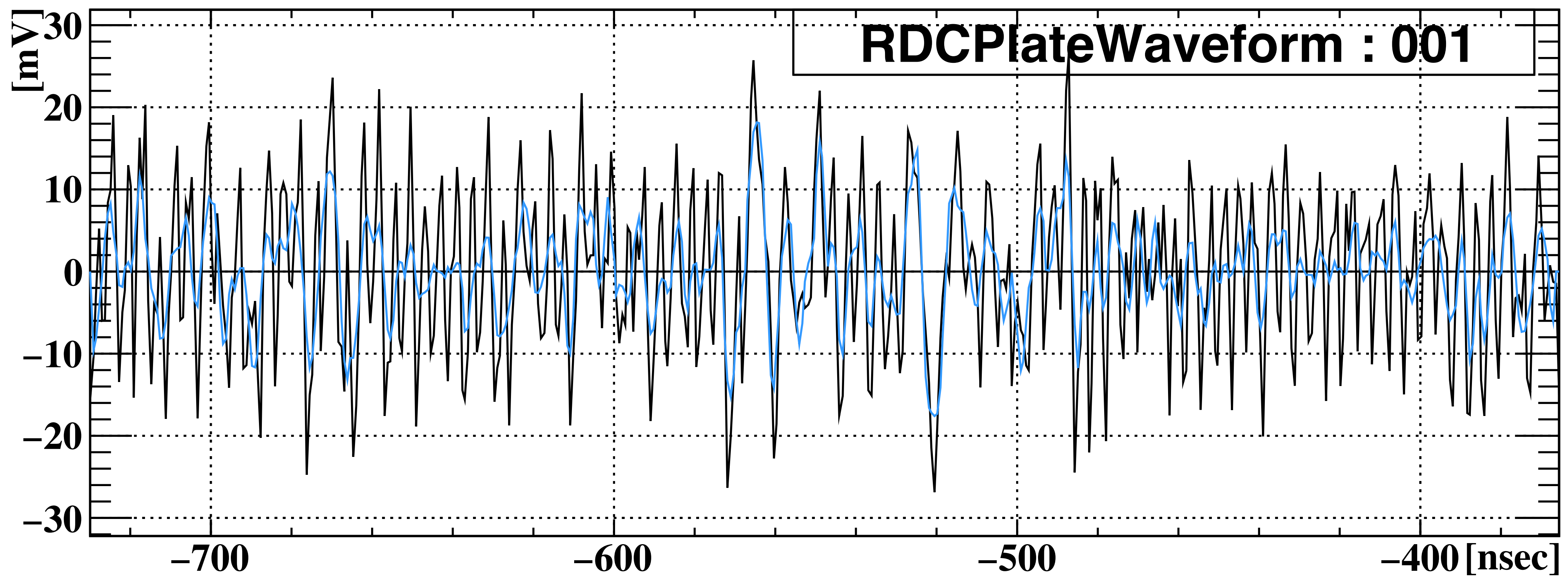

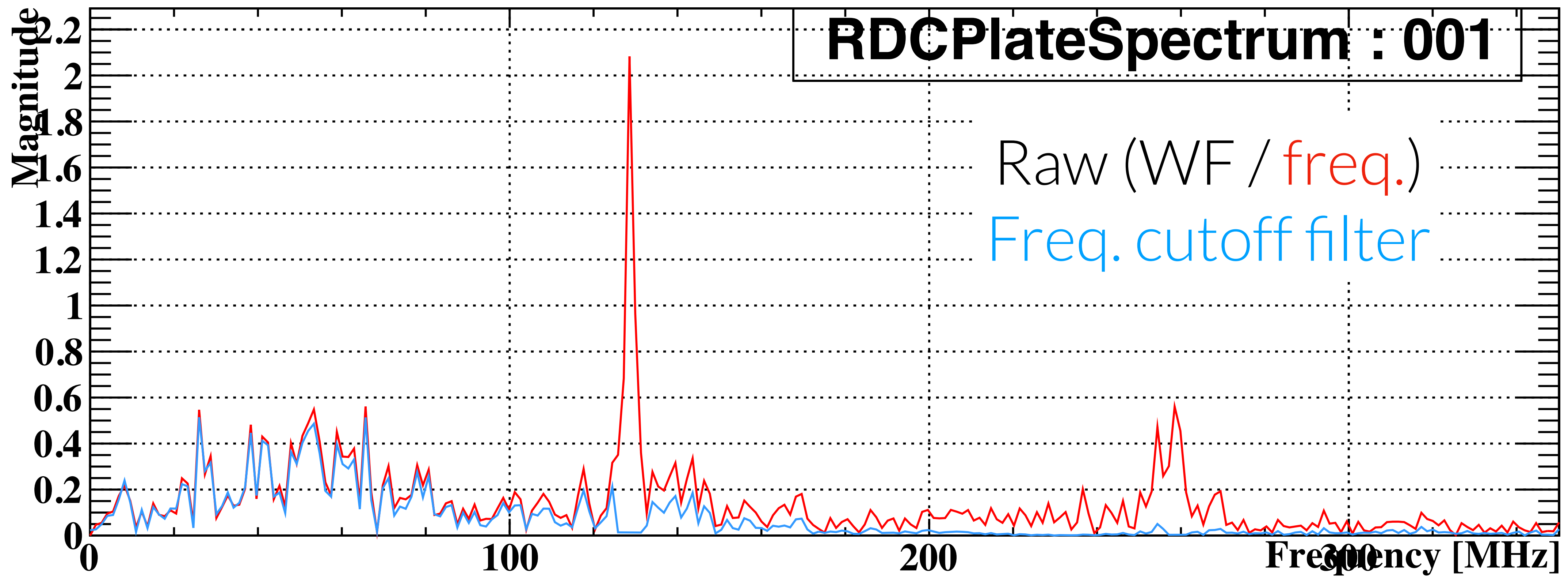

Tagged-RMD fraction as a function of E_γ

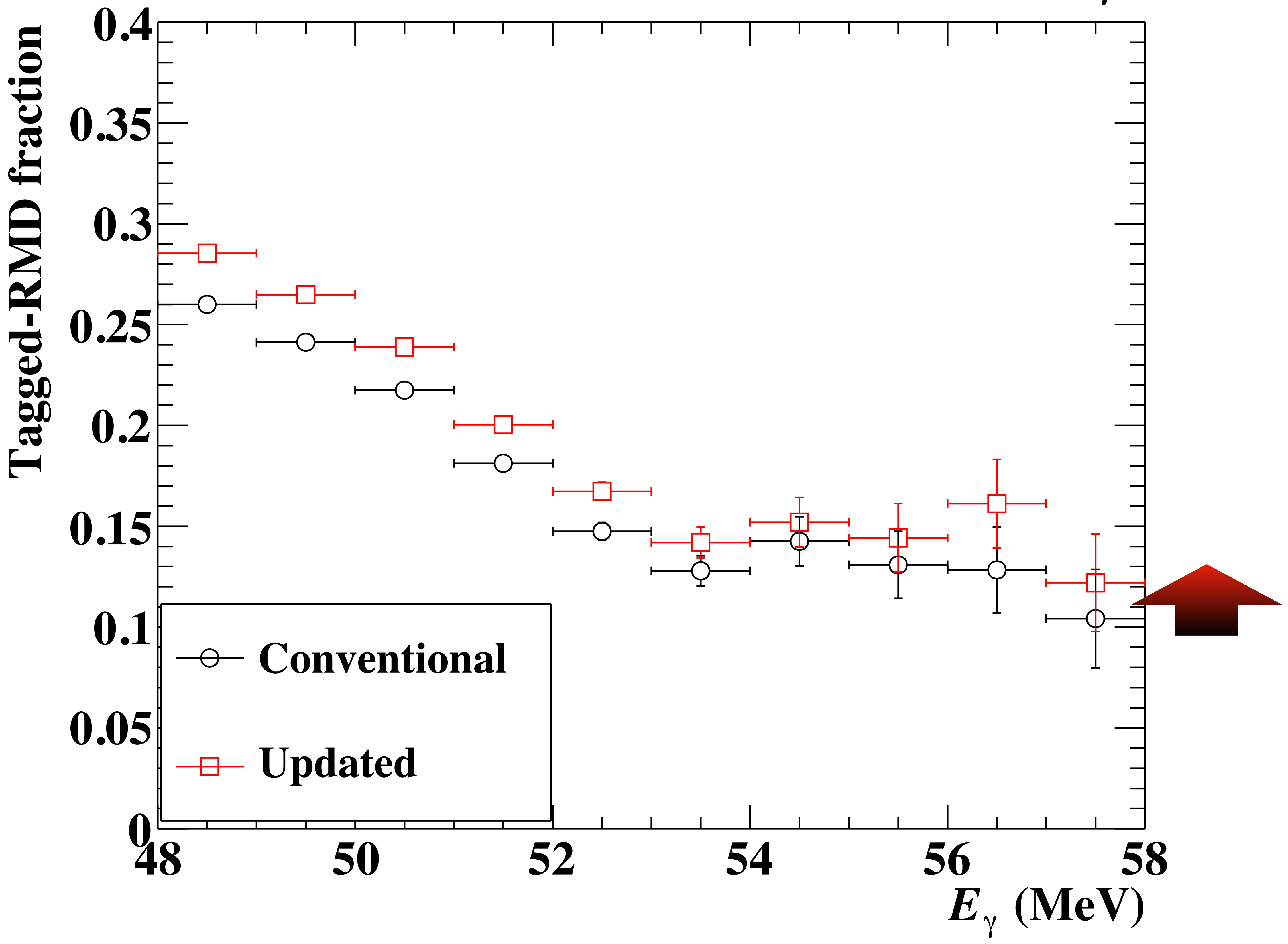

Contents

Analysis strategy

- Blind analysis
  - To prevent any biases in the analysis
  - Blind box fully covers analysis window

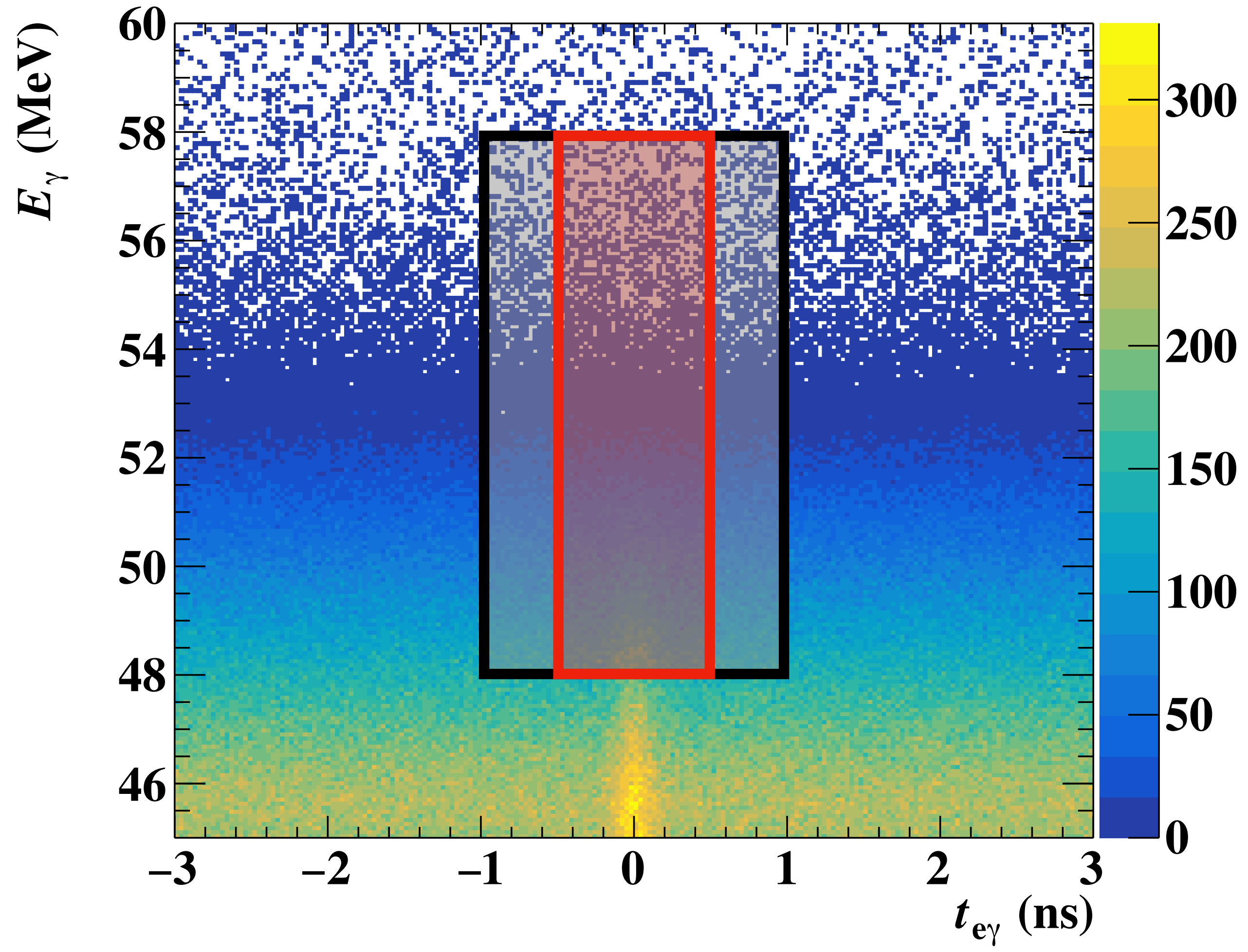

Analysis window
- 48 MeV < E_γ < 58 MeV
- 52.2 MeV < E_e < 53.5 MeV
- $|t_{e\gamma}|$ < 0.5 ns
- $|\theta_{e\gamma}|$ < 40 mrad
- $|\phi_{e\gamma}|$ < 40 mrad

- Maximum likelihood analysis estimates the number of signal events N_{sig}

$$\mathcal{L}(N_{\mathrm{sig}}, N_{\mathrm{ACC}}, N_{\mathrm{RMD}}, X_{\mathrm{T}}) = \underbrace{C(N_{\mathrm{ACC}}, N_{\mathrm{RMD}}, X_{\mathrm{T}})}_{\text{Gaussian constraints}} \times \frac{e^{-N}}{N_{\mathrm{obs}}!} \prod_{i=1}^{N_{\mathrm{obs}}} \left[N_{\mathrm{sig}} S(\vec{x}_i) + N_{\mathrm{ACC}} A(\vec{x}_i) + N_{\mathrm{RMD}} R(\vec{x}_i) \right]$$

- N_{sig} converted to $\mathcal{B}(\mu \to e\gamma)$ by number of effectively measured muons k

- Confidence interval calculated by the Feldman-Cousins approach with profile-likelihood ordering
  - N_{sig} 90% C.L. upper (lower) limit normalised to $\mathcal{B}$ 90% C.L. upper (lower) limit

Probability density functions

- "Event-by-event PDFs" to account for dependences on resolutions
- Built based on data with some MC-based corrections
  - Resolution evaluation
  - Side-band data

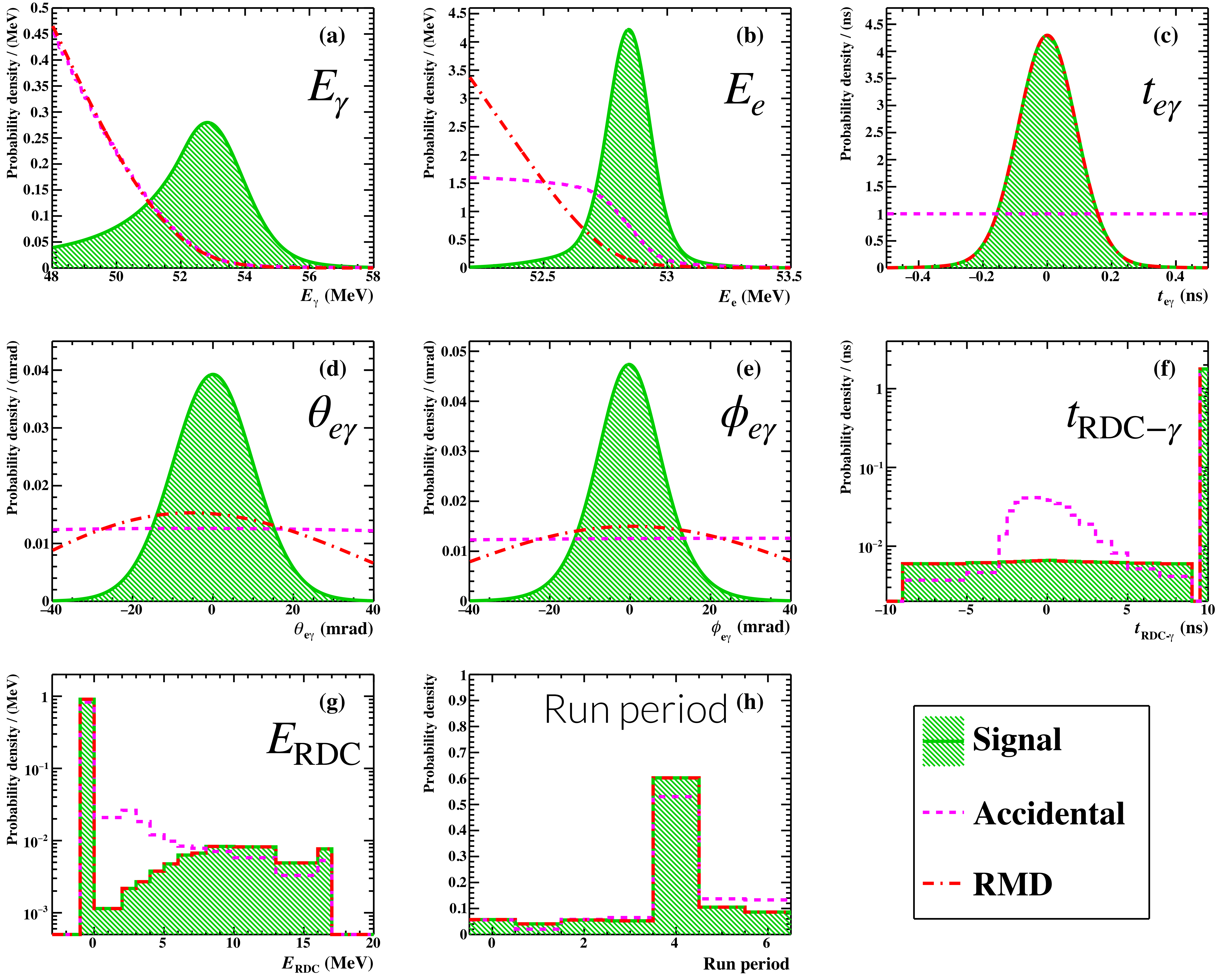

Observables $\vec{x}_i$

- E_γ
- E_e
- $t_{e\gamma}$
- n_{pTC}
- $\theta_{e\gamma}$
- $\phi_{e\gamma}$
- $t_{\mathrm{RDC}-\gamma}$
- E_{RDC}

Performance summary

		MEG [44]	MEG II first result	MEG II achieved in this work
	Resolutions			
γ	E_γ (%) $(w_\gamma < 2\,\mathrm{cm})/(w_\gamma > 2\,\mathrm{cm})$	2.4/1.7	2.0/1.8	2.4/1.9
γ	$u_\gamma, v_\gamma, w_\gamma$ (mm)	5, 5, 6 →	2.5, 2.5, 5	2.5, 2.5, 5
γ	t_γ (ps)	67 [43]	65	63
e	E_e (keV)	380 →	90	89
e	θ_e, ϕ_e (mrad)	9.4, 8.7	7.2, 4.1 →	6.2, 5.2
e	z_e, y_e (mm)	2.4, 1.2	2.0, 0.7 →	1.76, 0.61
e	t_e (ps)	102 [43] →	~40	~40
	$t_{e\gamma}$ (ps)	122 →	84	78
	Efficiencies			
	ε_γ (%)	63	62	63
	ε_e (%)	30 →	67	67
	$\varepsilon_{\mathrm{TRG}}$ (%)	≈99	80 →	91

Performance summary

		MEG [44]	MEG II first result	MEG II achieved in this work
	Resolutions			
γ	E_γ (%) $(w_\gamma < 2\,\mathrm{cm})/(w_\gamma > 2\,\mathrm{cm})$	2.4/1.7	$\boxed{2.0/1.8}$	$\boxed{2.4/1.9}$
γ	$u_\gamma, v_\gamma, w_\gamma$ (mm)	5, 5, 6 →	2.5, 2.5, 5	2.5, 2.5, 5
γ	t_γ (ps)	67 [43]	65	63
e	E_e (keV)	380 →	90	89
e	θ_e, ϕ_e (mrad)	9.4, 8.7	7.2, 4.1 →	6.2, 5.2
e	z_e, y_e (mm)	2.4, 1.2	2.0, 0.7 →	1.76, 0.61
e	t_e (ps)	102 [43] →	~40	~40
	$t_{e\gamma}$ (ps)	122 →	84	78
	Efficiencies			
	ε_γ (%)	63	62	63
	ε_e (%)	30 →	67	67
	ε_{TRG} (%)	≈99	80 →	91

Photon energy resolution evaluation

- 55 MeV γ from $\pi^0 \rightarrow \gamma\gamma$ used
- MPPC non-linearity suspected, but not fully understood
  - **Thermal annealing recovered PDE from 6% to 14%**

2021: 2.1%/1.8%

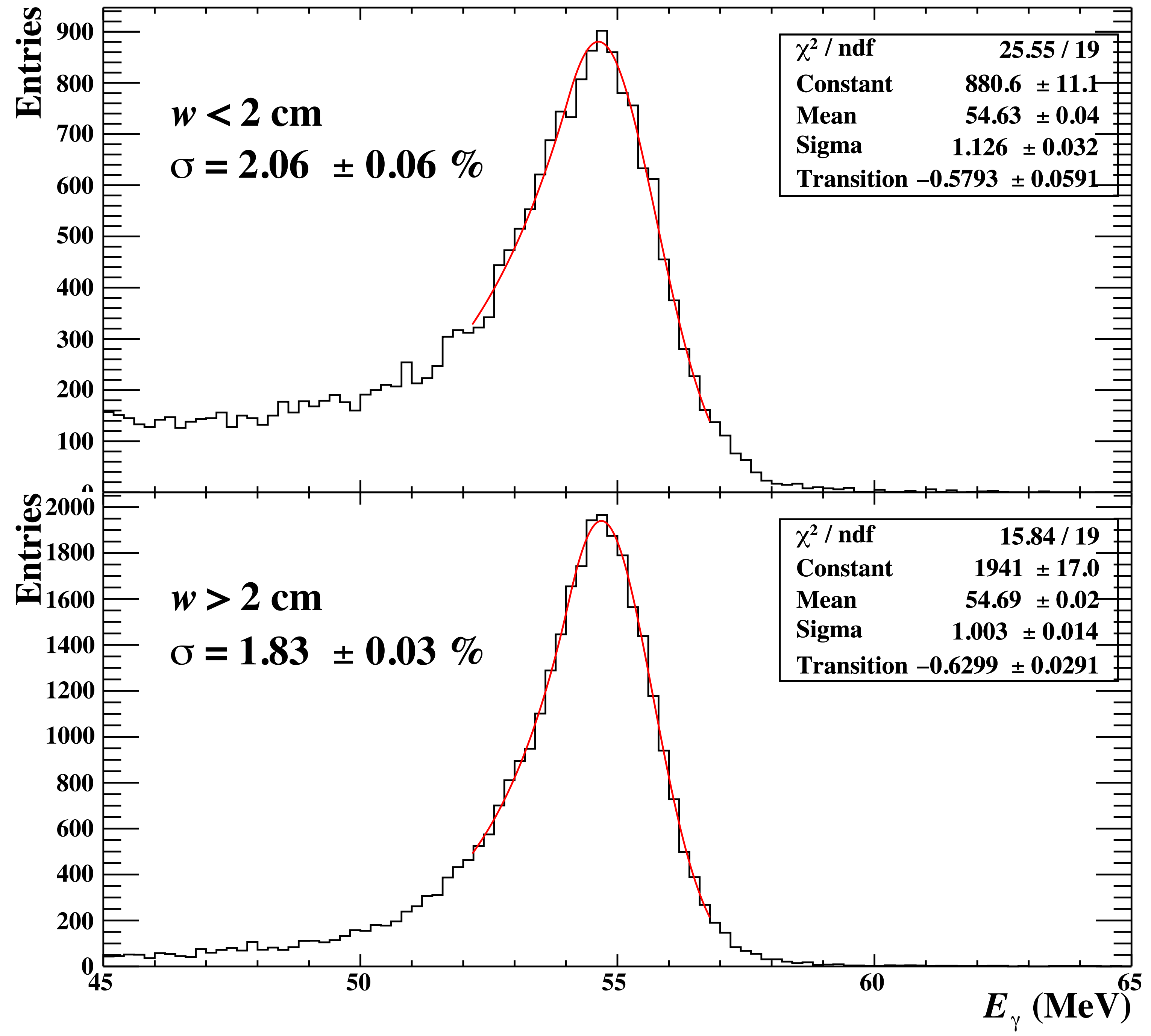

2022: 2.4%/1.9%

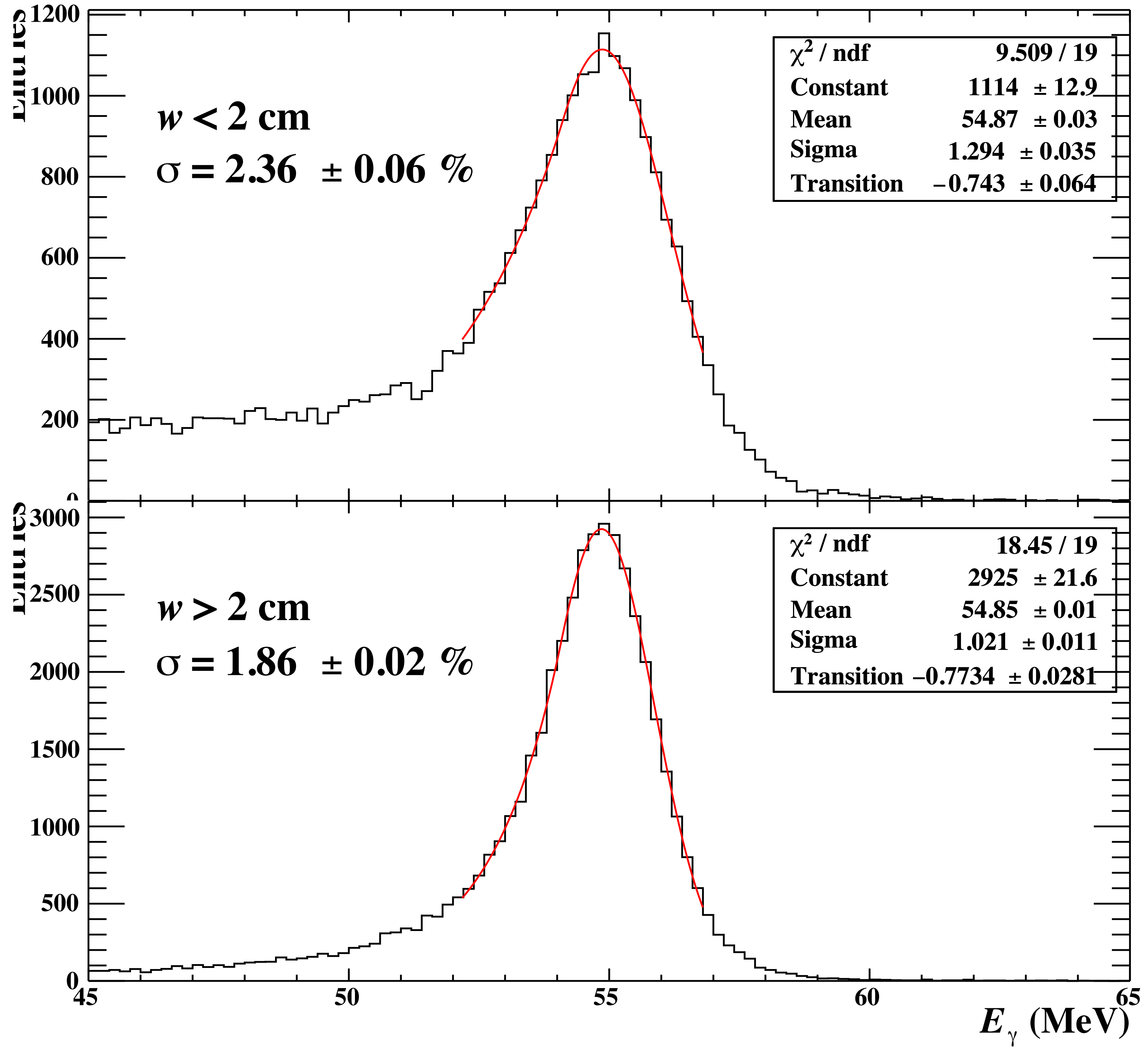

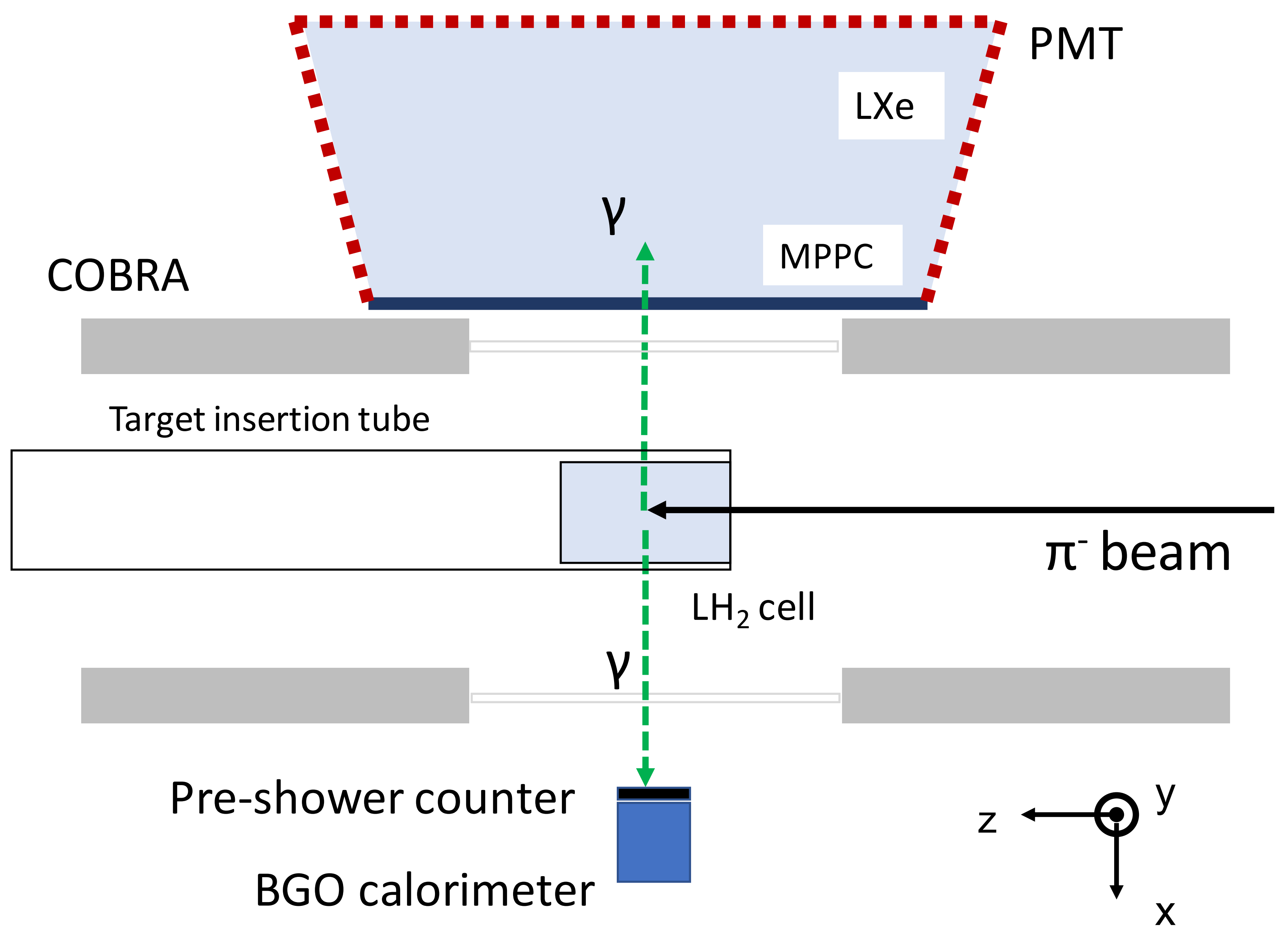

Careful detector calibration needed

- Signal response examined with $\pi^0 \to \gamma\gamma$
- **Must correct temporal variations** of
  - Energy scale
  - Position dependence of the energy scale
  - Resolution

Response to monochromatic γ

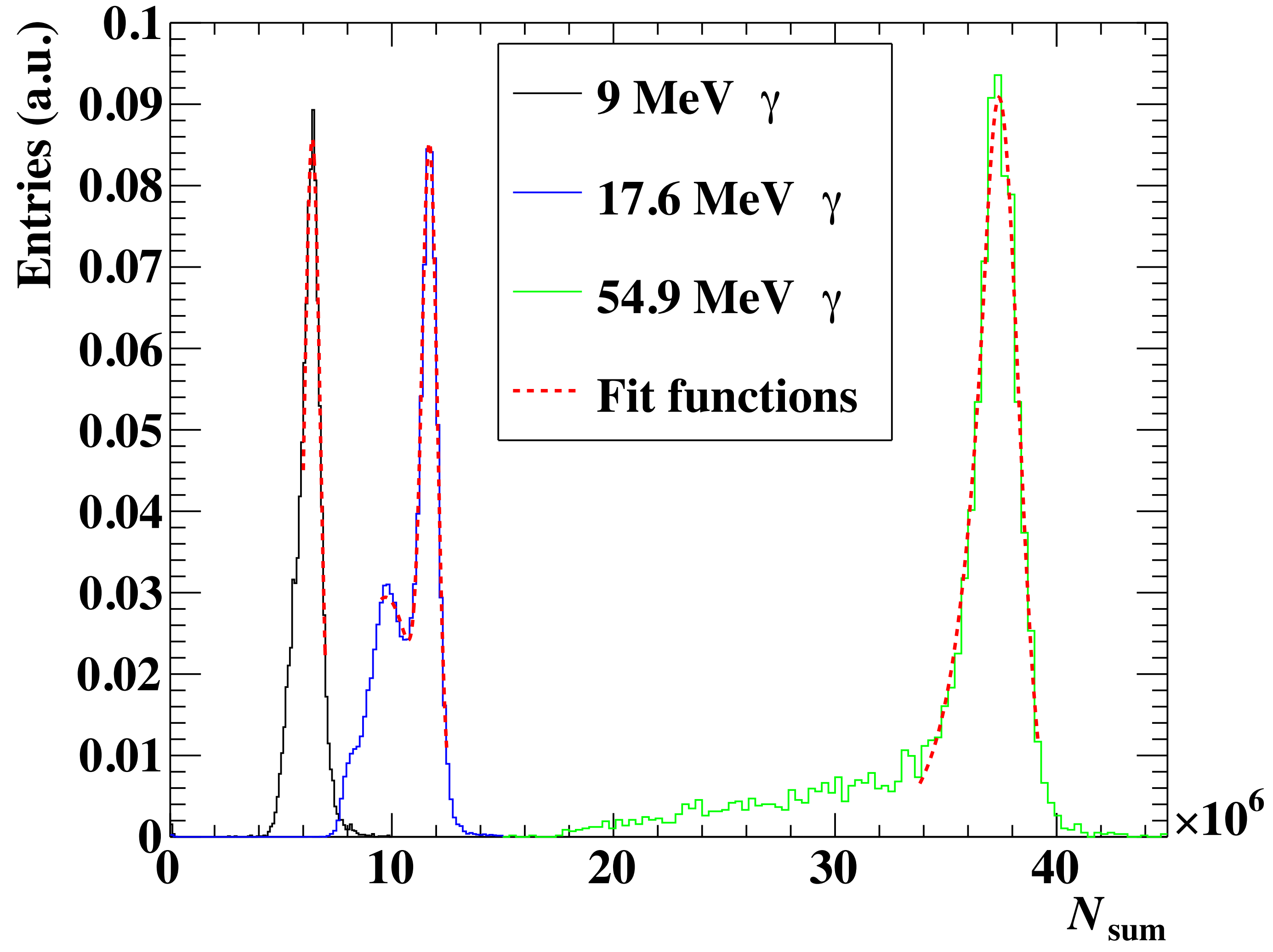

Response to background γ

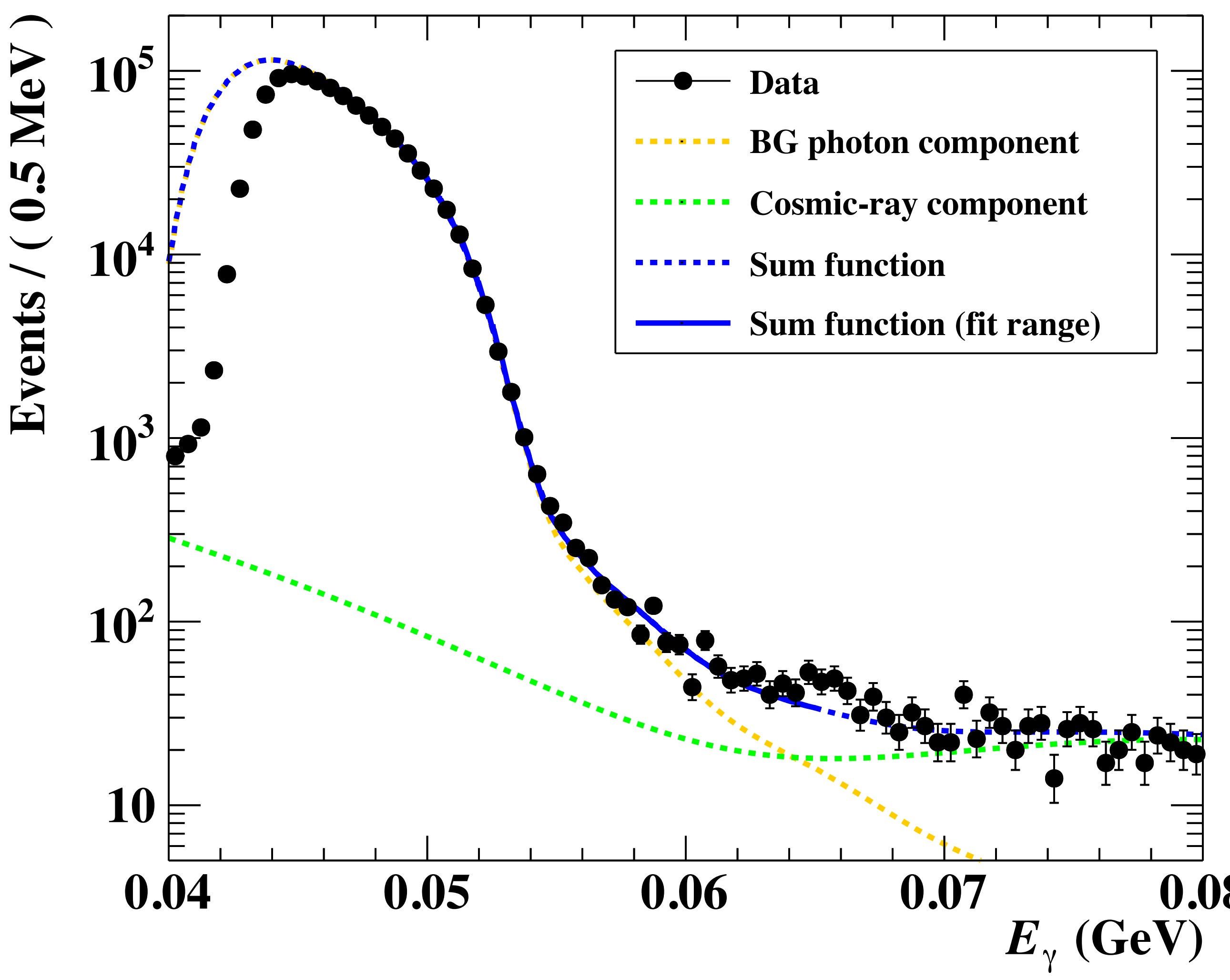

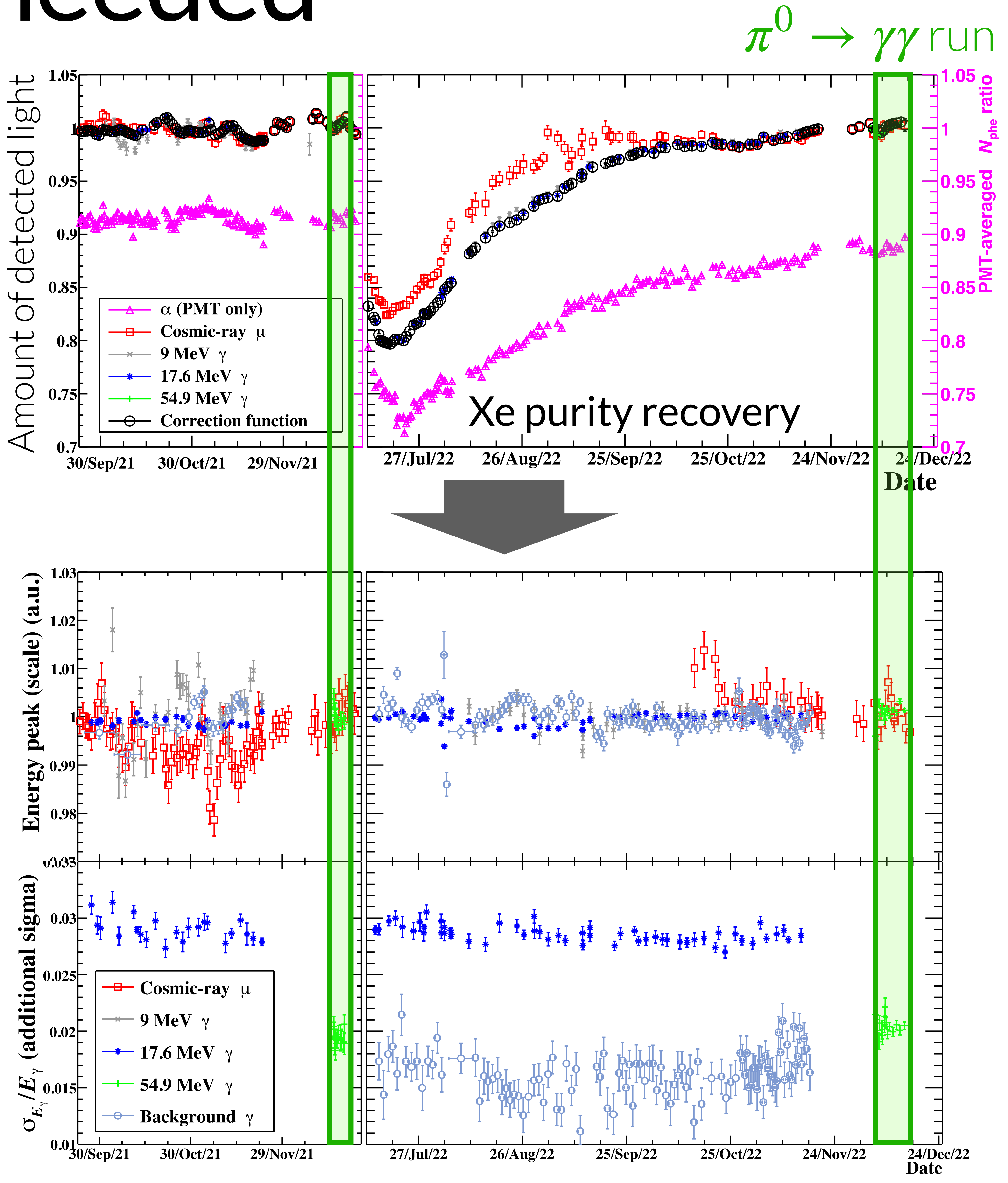

Uncertainty on the energy scale

- Temporal variation dominates the uncertainty of 0.18%
  - 0.3% in the last publication with the 2021 data

Temporal variation during the physics run

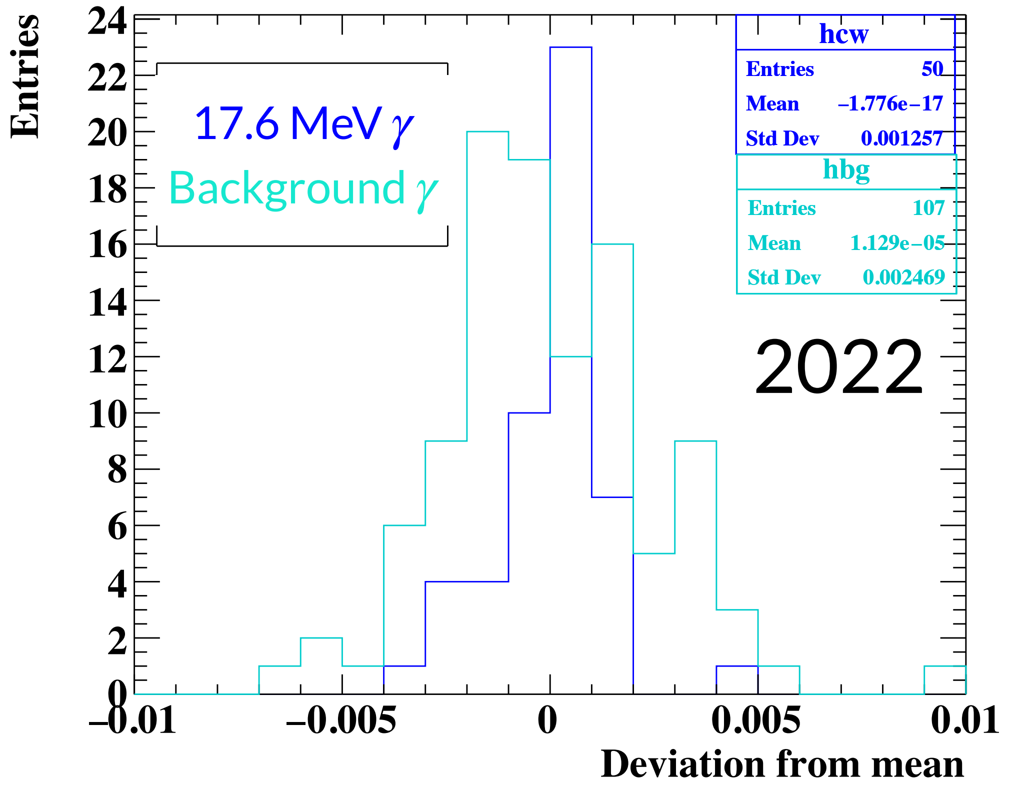

2021	0.14%
2022	0.11%

Connection between the physics & π^0 run

2021	0.11%
2022	0.14%

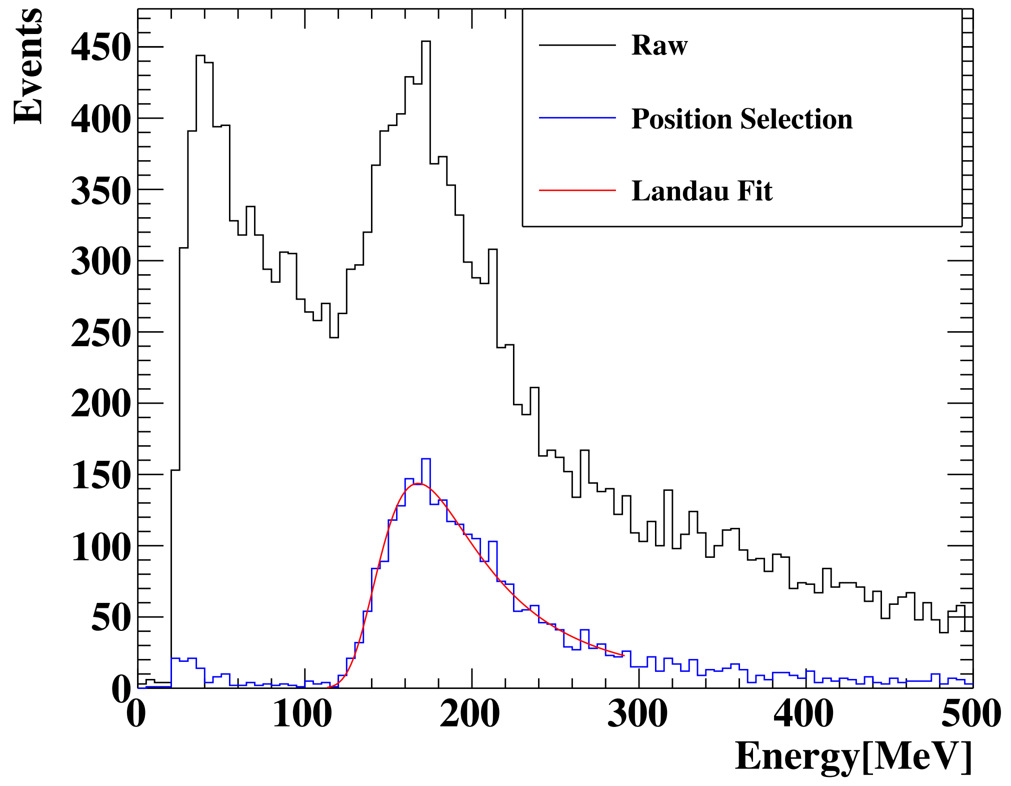

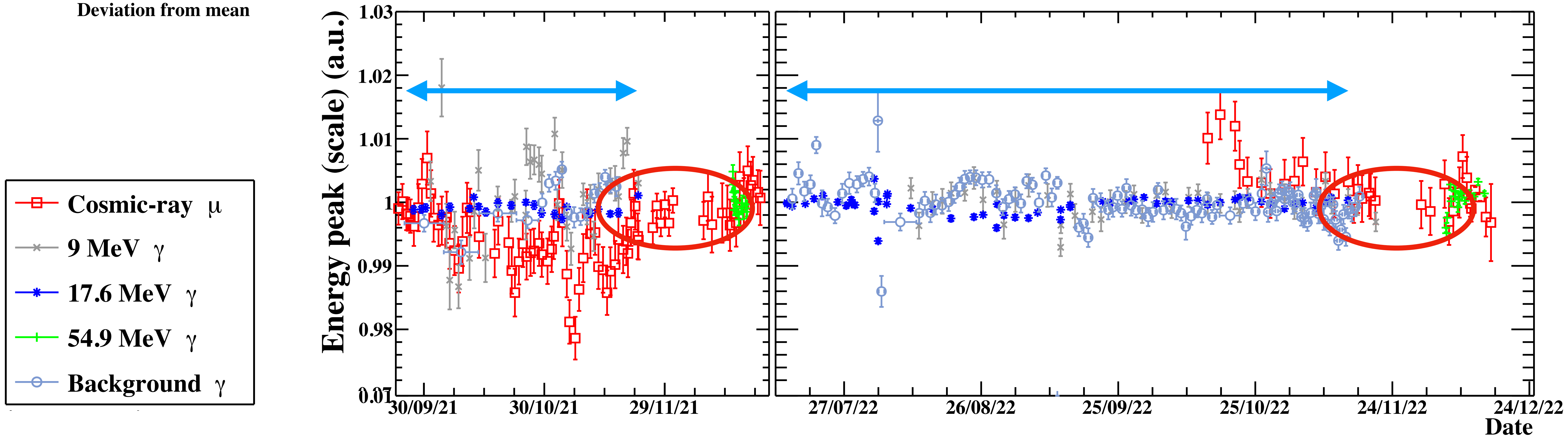

Statistical uncertainty on Landau peak extraction for cosmic-ray muons

Other remarks on E_γ PDFs

- Strong depth dependence on resolution

➡ **Segment fiducial volume for event-by-event PDFs**

- **Accidental BG PDFs based on time side-band data**
  - Parameterised with MC + cosmic-ray + acceptance

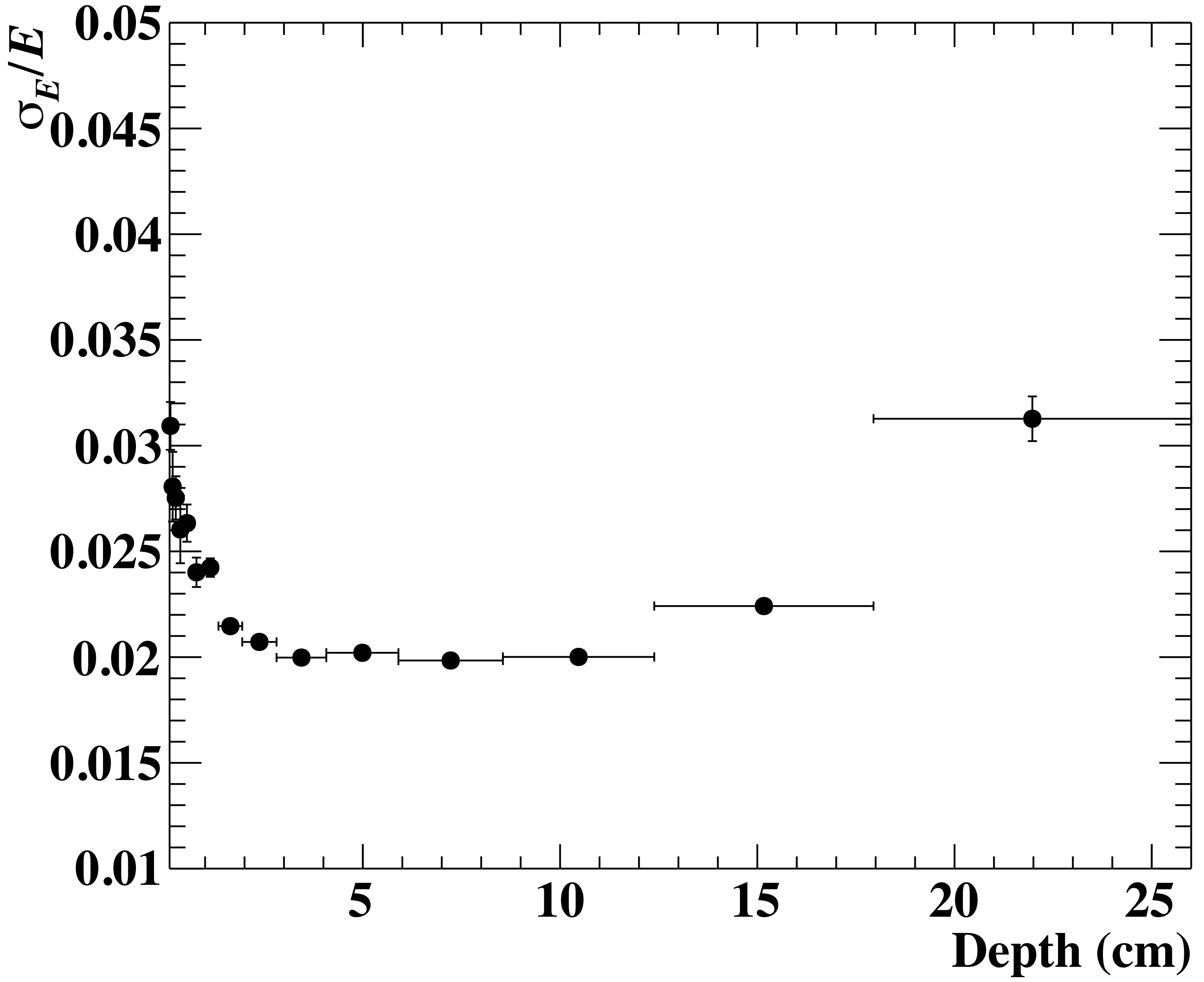

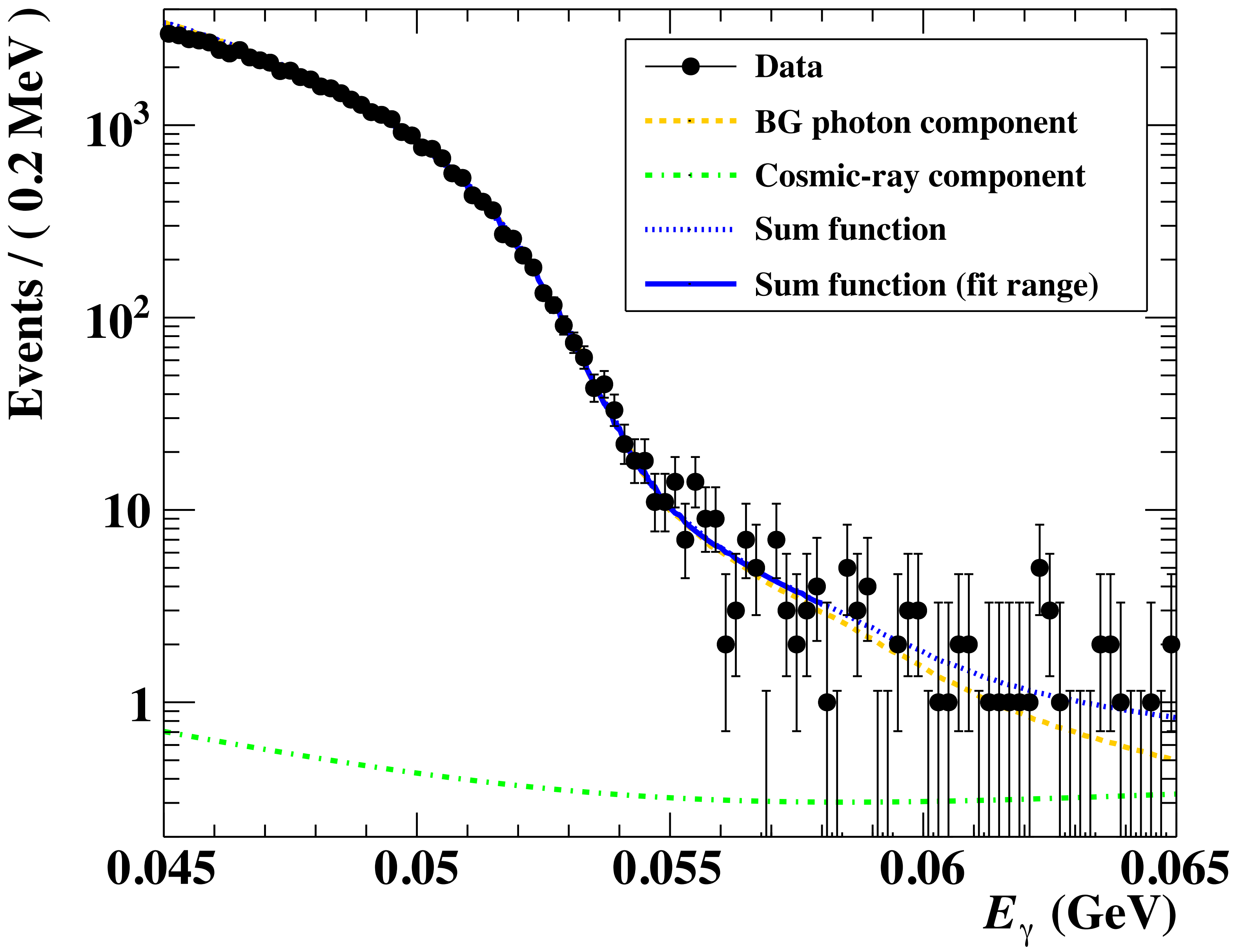

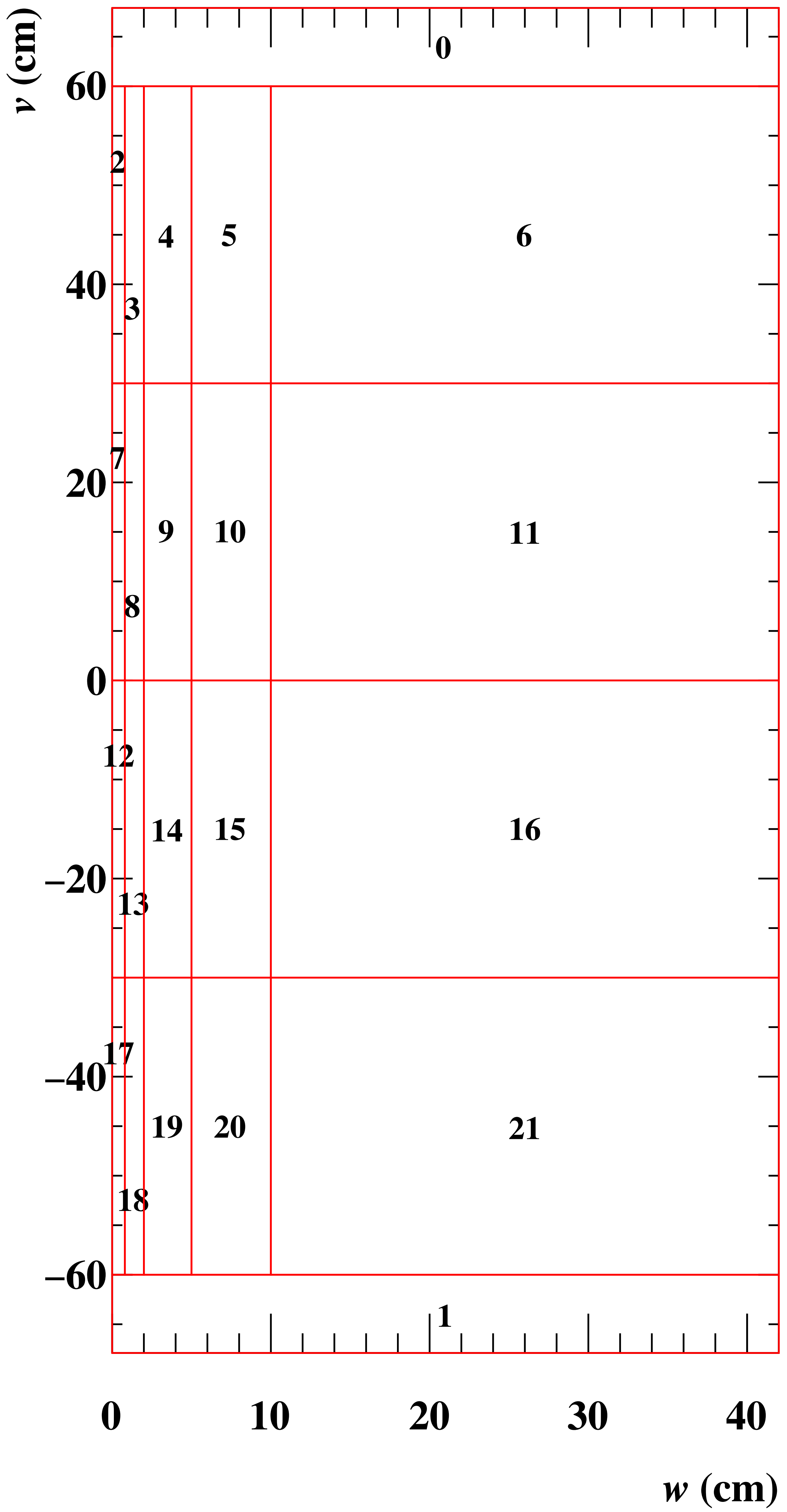

E_e PDFs

- Based on fitting to edge of Michel spectrum

$$(\mathcal{F}_{\mathrm{Michel}} \times \mathcal{A}_e) \otimes \mathcal{G}_{E_e}$$

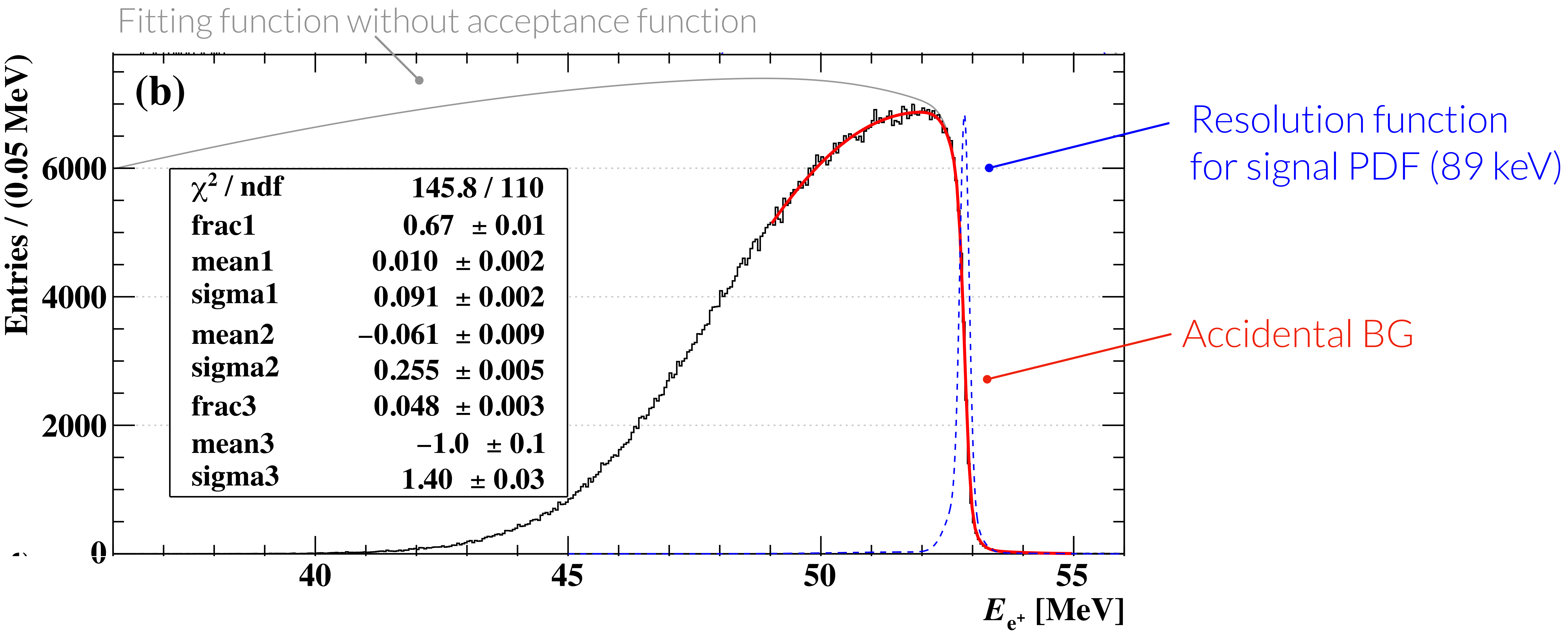

RDC PDFs

- Signal PDF
  - Accidental Michel *e* detection
- Accidental BG PDF
  - RMD *e* + accidental Michel *e* detection

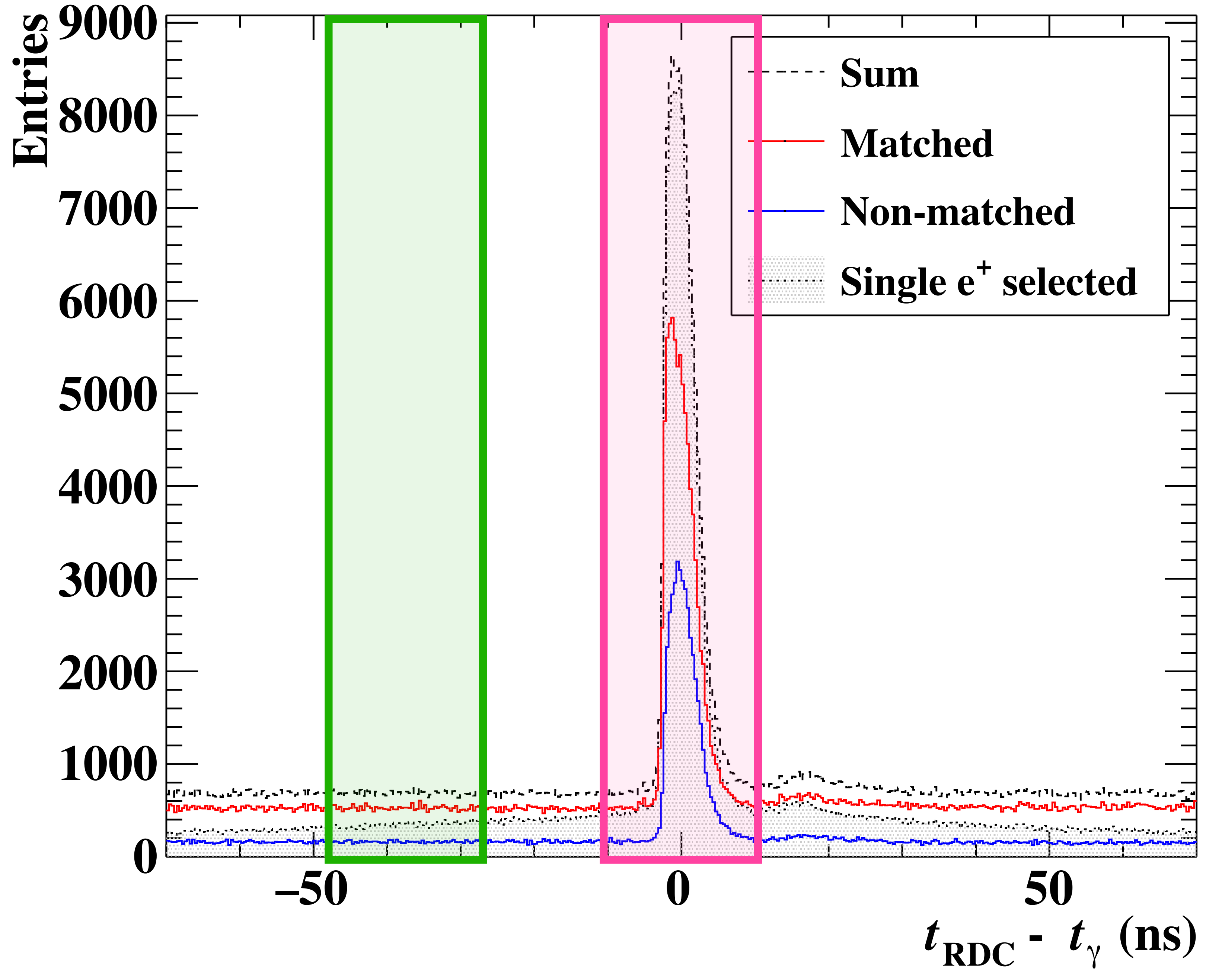

Non-detected events

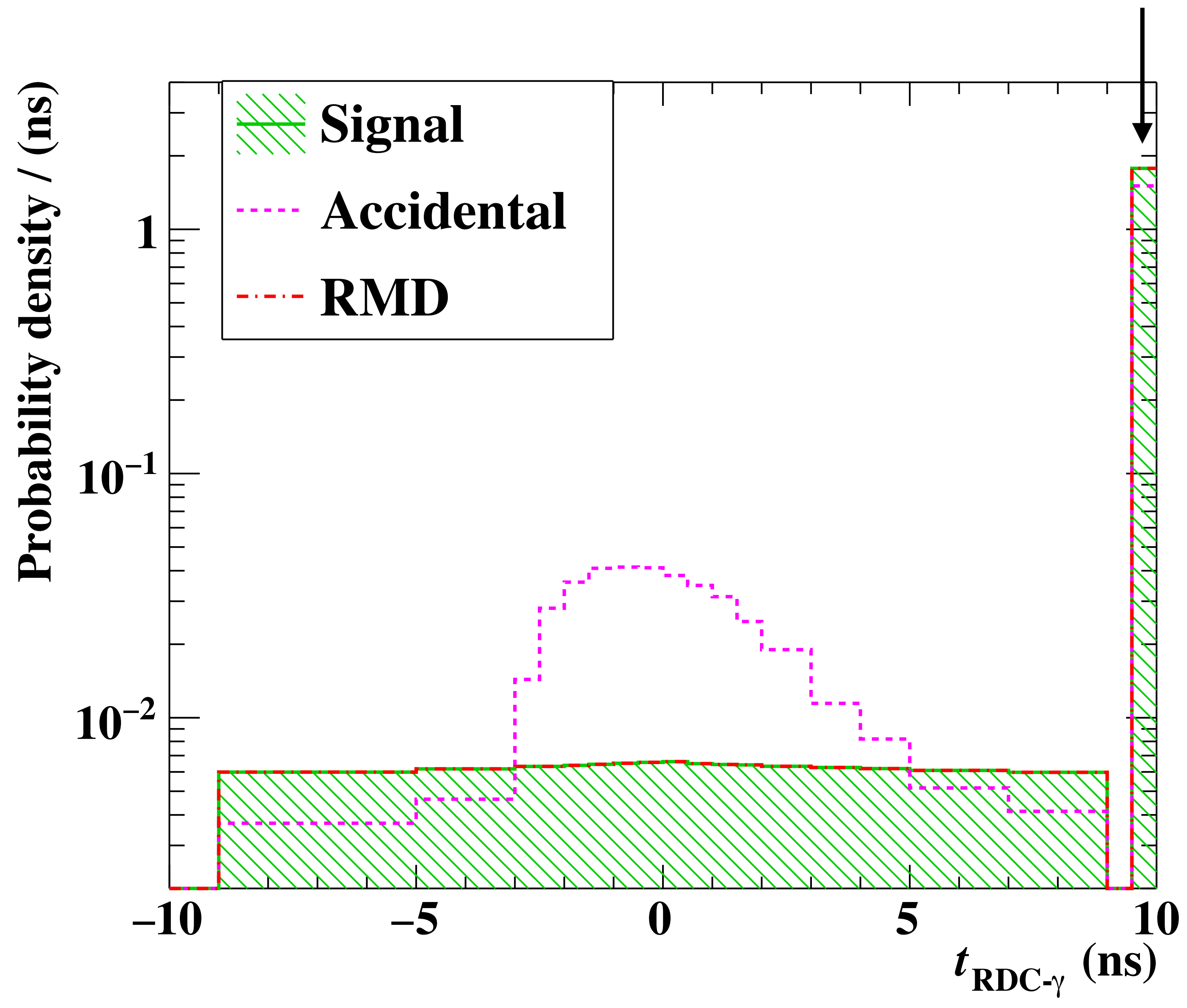

Non-detected events

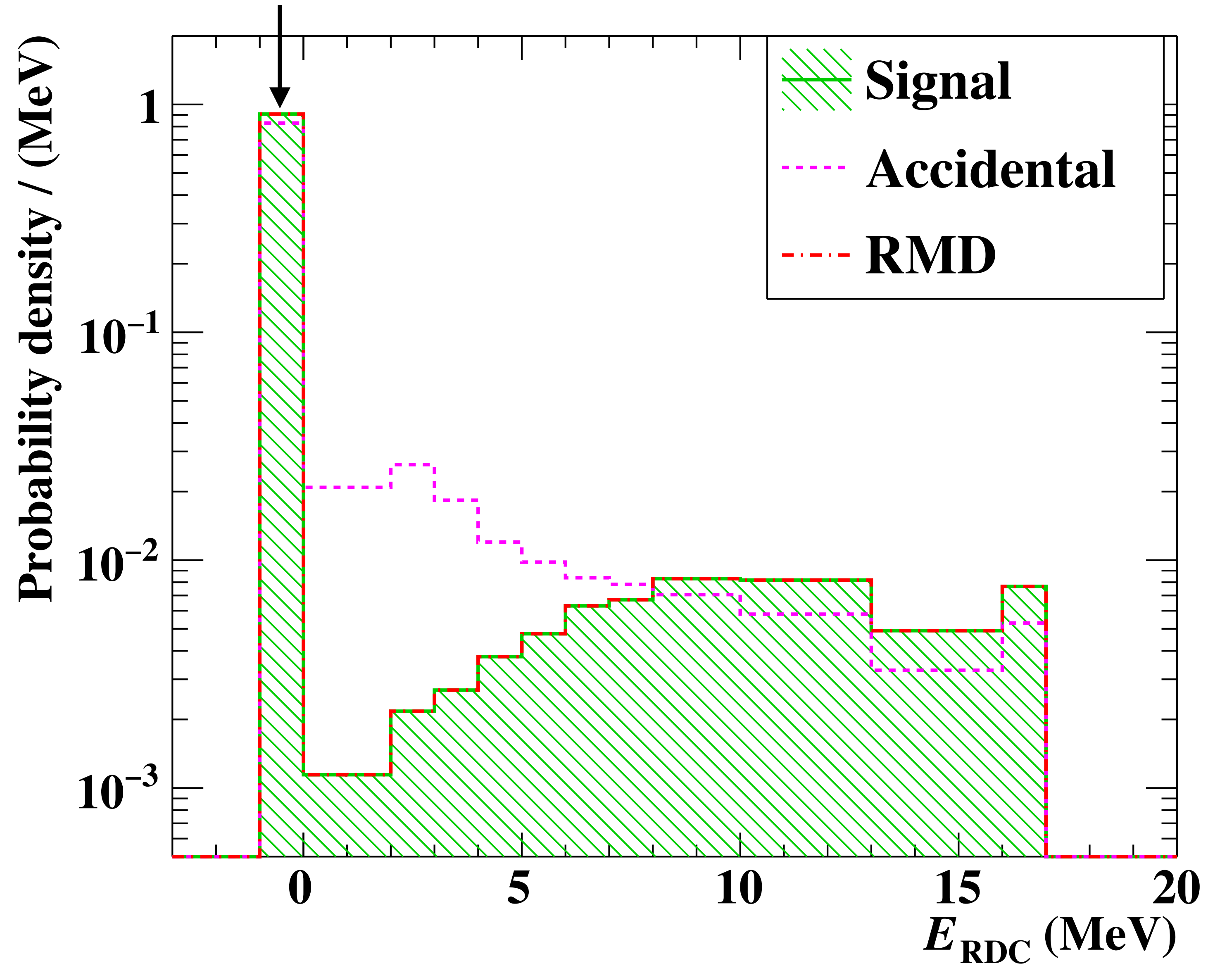

Normalisation k

- Count Michel positrons above 50 MeV and correct it

$$k_{\text{Michel}} = \frac{N^{e\nu\bar{\nu}}}{\mathcal{B}(\mu \to e\nu\bar{\nu})} \times \varepsilon_{\gamma} \times \frac{\varepsilon_{\text{TRG}}^{e\gamma}}{\varepsilon_{\text{TRG}}^{e\nu\bar{\nu}}} \times \text{Corrections} = \mathbf{(1.34 \pm 0.07) \times 10^{13}}$$

Difference between $\mu \to e\gamma$ and $\mu \to e\nu\bar{\nu}$

- Photon efficiency ε_{γ} improvement
  - Analysis efficiency improvement (92±2 % → 93±1 %)

- Trigger efficiency $\varepsilon_{\text{TRG}}^{e\gamma}$ update
  - Improvement in direction match trigger efficiency estimation: MC-based → data-driven
    - 2021 dataset: 80±1 % → 88±2 %
  - Improvement in trigger logic
    - 2021 (88±2 %) → 2022 (91±2 %)

Contents

Sensitivity & fit to side-bands

- Thousands of toy samples with a null-signal hypothesis

➡ **Median 90% C.L. upper limit on $\mathcal{B}$ is defined as sensitivity**

$$S_{90} = 2.2 \times 10^{-13}$$

- MEG final: 5.3×10^{-13}
- MEG II 2021: 8.8×10^{-13}

- Fit to $t_{e\gamma}$ side-bands for sensitivity cross-check

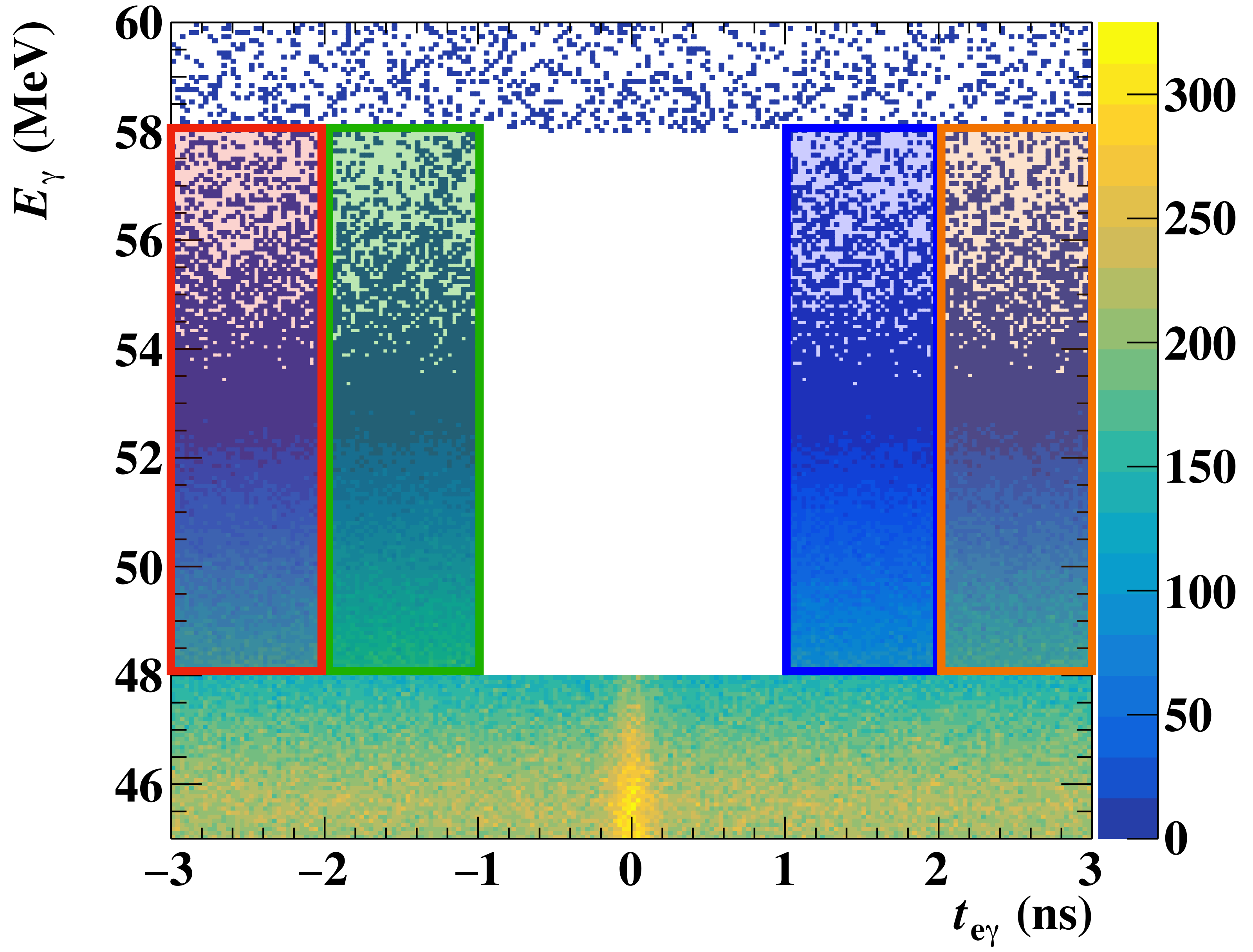

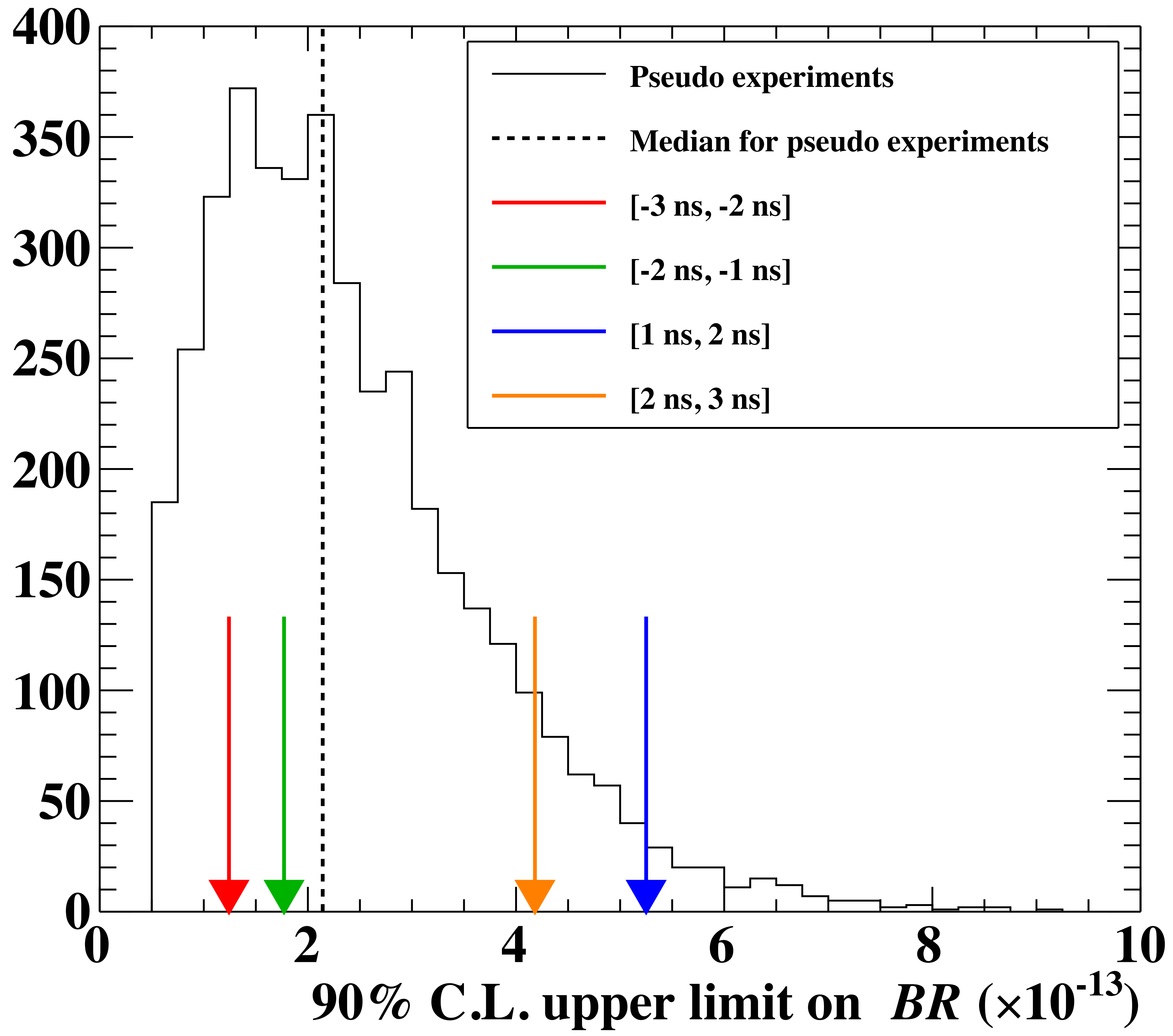

Unblind results: Event distribution

- No signal excess observed

Colour bar: Relative signal likelihood

$$R_{\mathrm{sig}}(\vec{x}_i) = \log_{10}\left(\frac{S(\vec{x}_i)}{(1-r)\cdot A(\vec{x}_i) + r\cdot R(\vec{x}_i)}\right)$$

$$r = \frac{N_{\mathrm{RMD}}}{N_{\mathrm{ACC}} + N_{\mathrm{RMD}}}$$

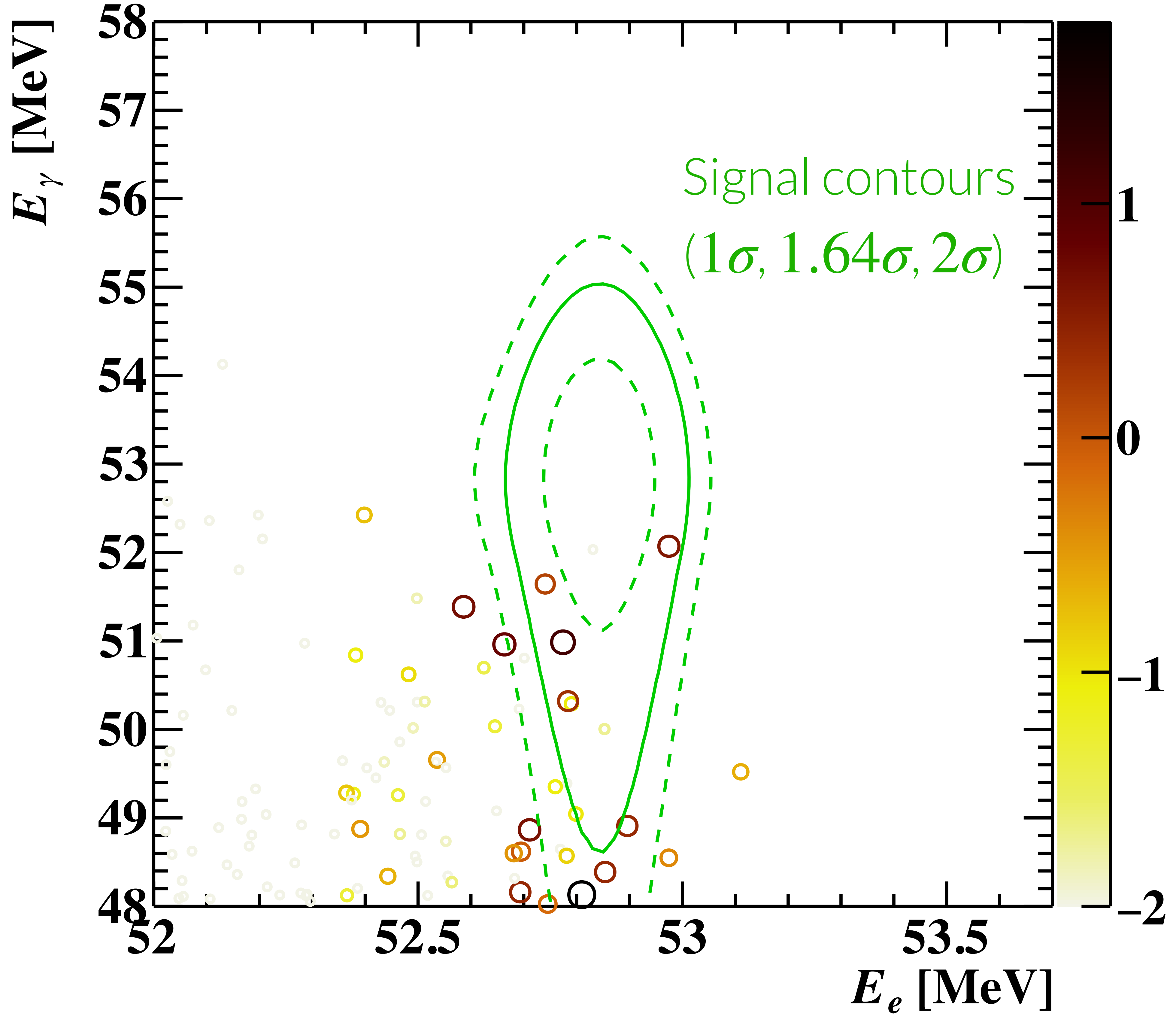

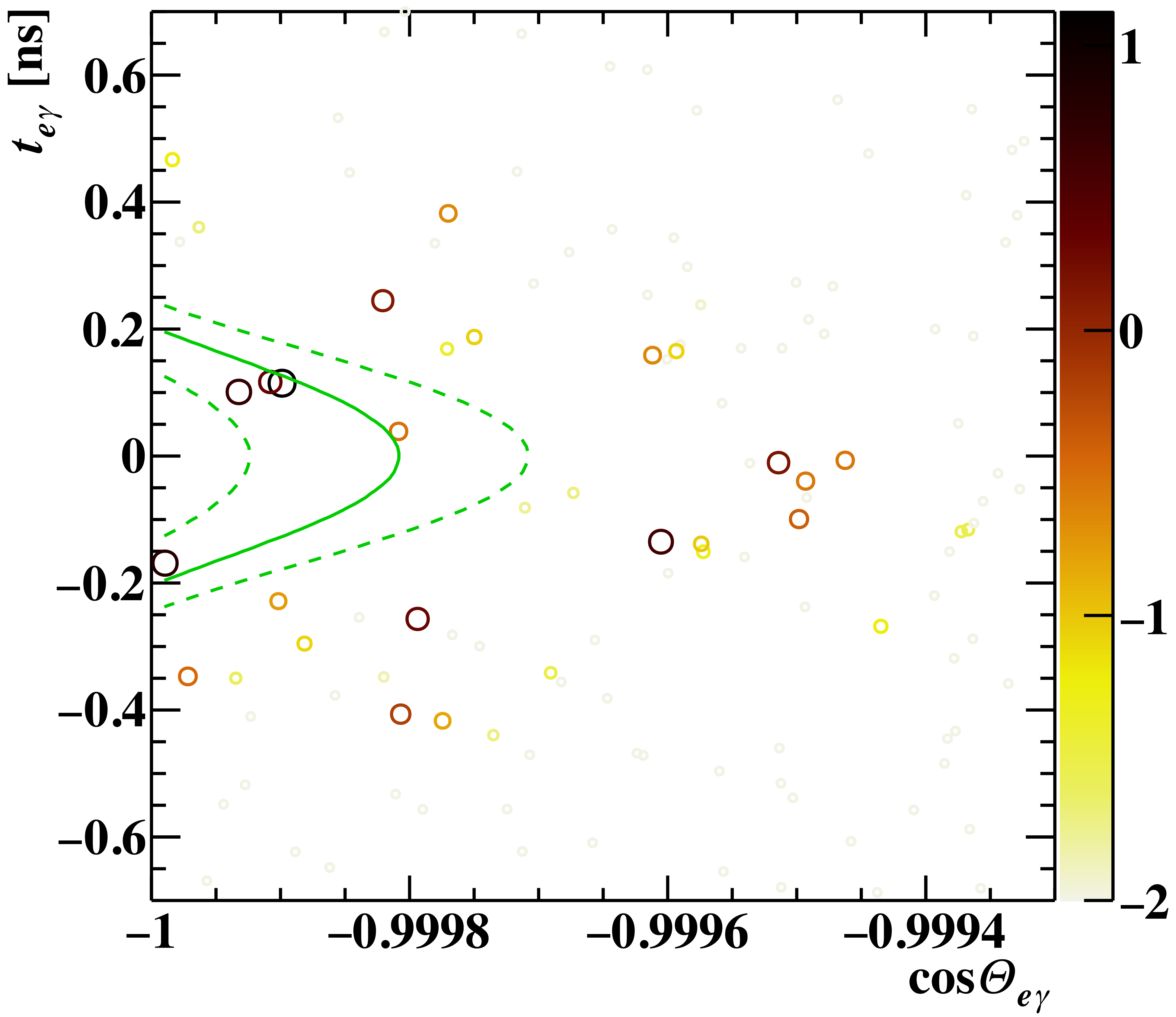

Unblind results: Fit results & confidence interval

- No signal excess observed
  - Clear in $R_{\rm sig}$ distribution (i)
- Set an upper limit on the branching ratio to 1.5×10^{-13} at 90% C.L.

	$N_{\rm sig}$	$N_{\rm RMD}$	$N_{\rm ACC}$
Expectation from side-bands		10.1 ± 1.7	364.00 ± 9.54
Without physical constraint	-5.01 ± 1.21	9.71 ± 1.68	361.91 ± 8.58
With physical constraint	0.00 ± 0.73	9.67 ± 1.68	360.94 ± 8.58

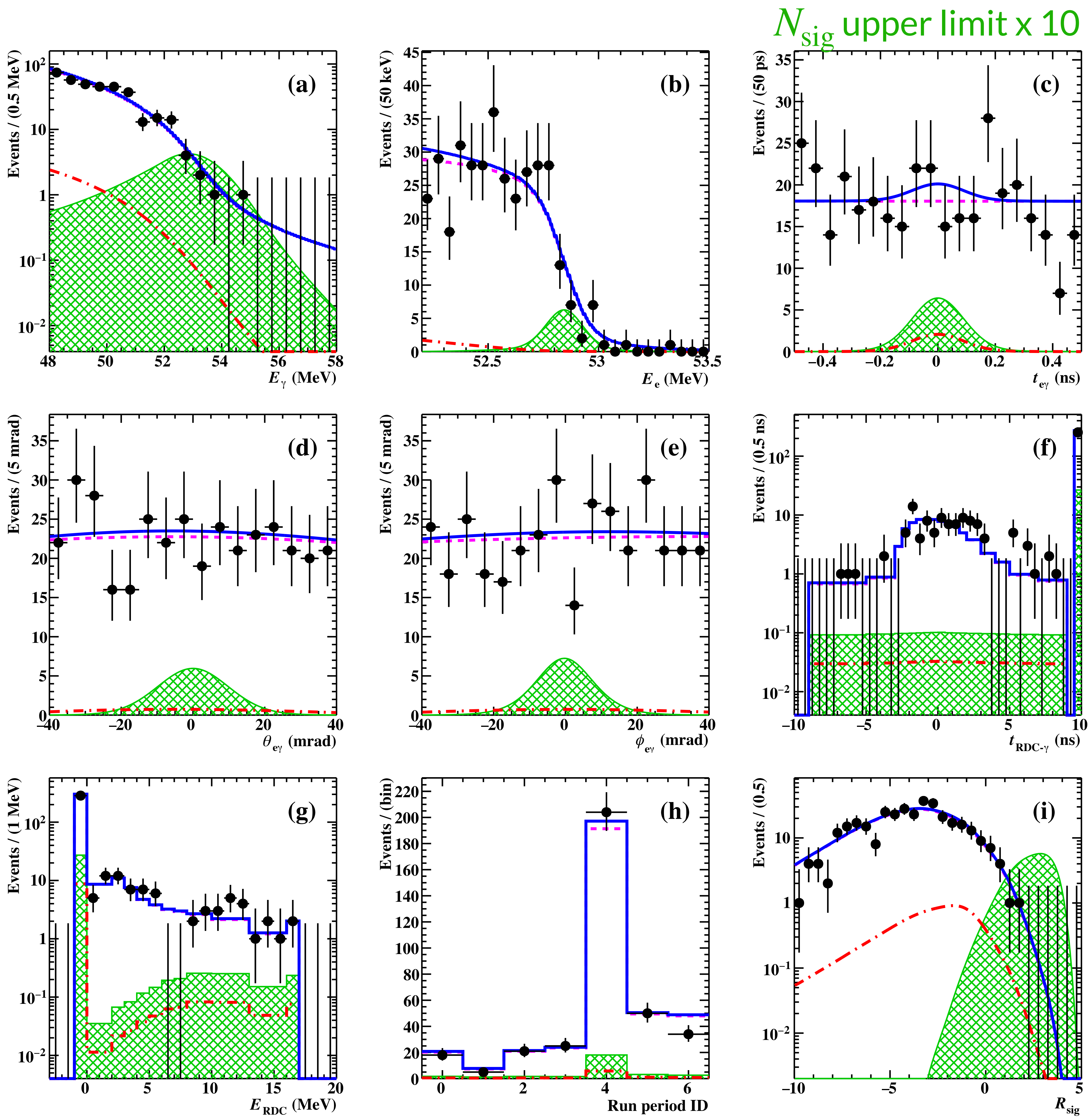

Discussion: Sensitivity improvement w.r.t. MEG

- Background suppression thanks to resolution improvements
- Similar statistics
  - k: 1.71×10^{13} (MEG) vs 1.34×10^{13} (MEG II 2021-2022)
  - Thanks to positron efficiency improvement and stable data-taking

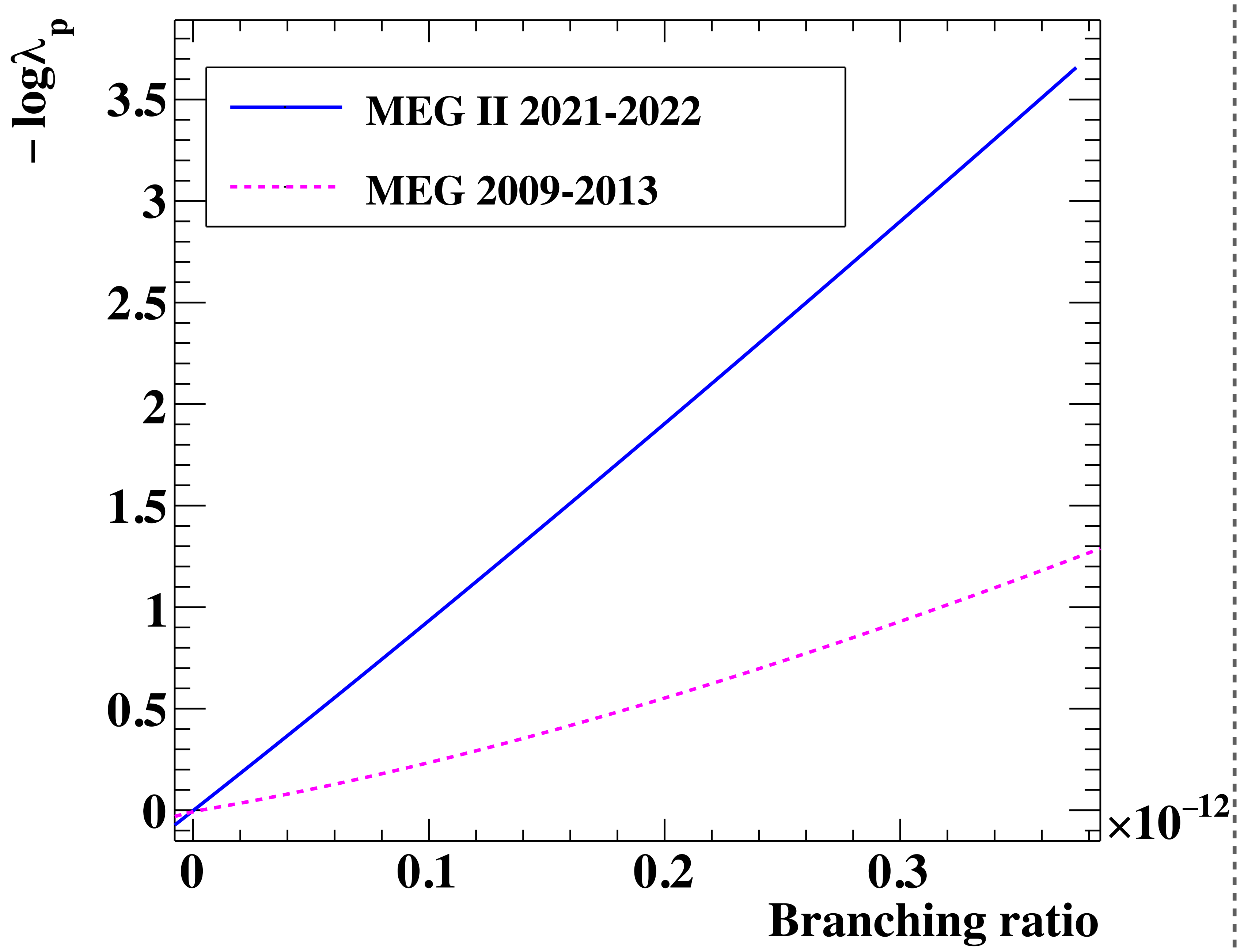

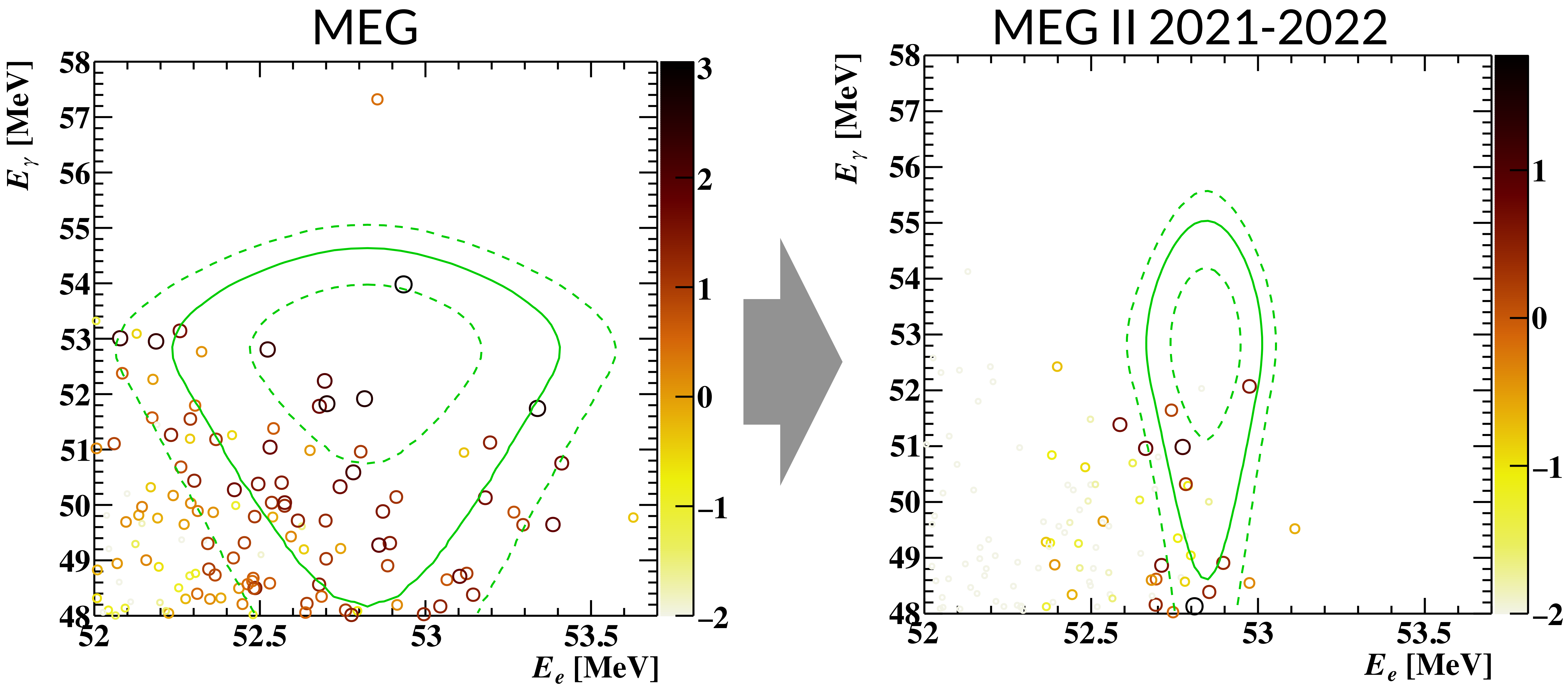

Discussion and prospects

- Demonstrate sensitivity improvement as statistics increase
  - With careful calibrations
- Encourage long-term data-taking

- **Statistics increase expected by a factor of 2.6 with the 2021-2024 dataset**

- Plan to take data in 2025-2026
- Will reach 6×10^{-14}
  - Even below with analysis improvements

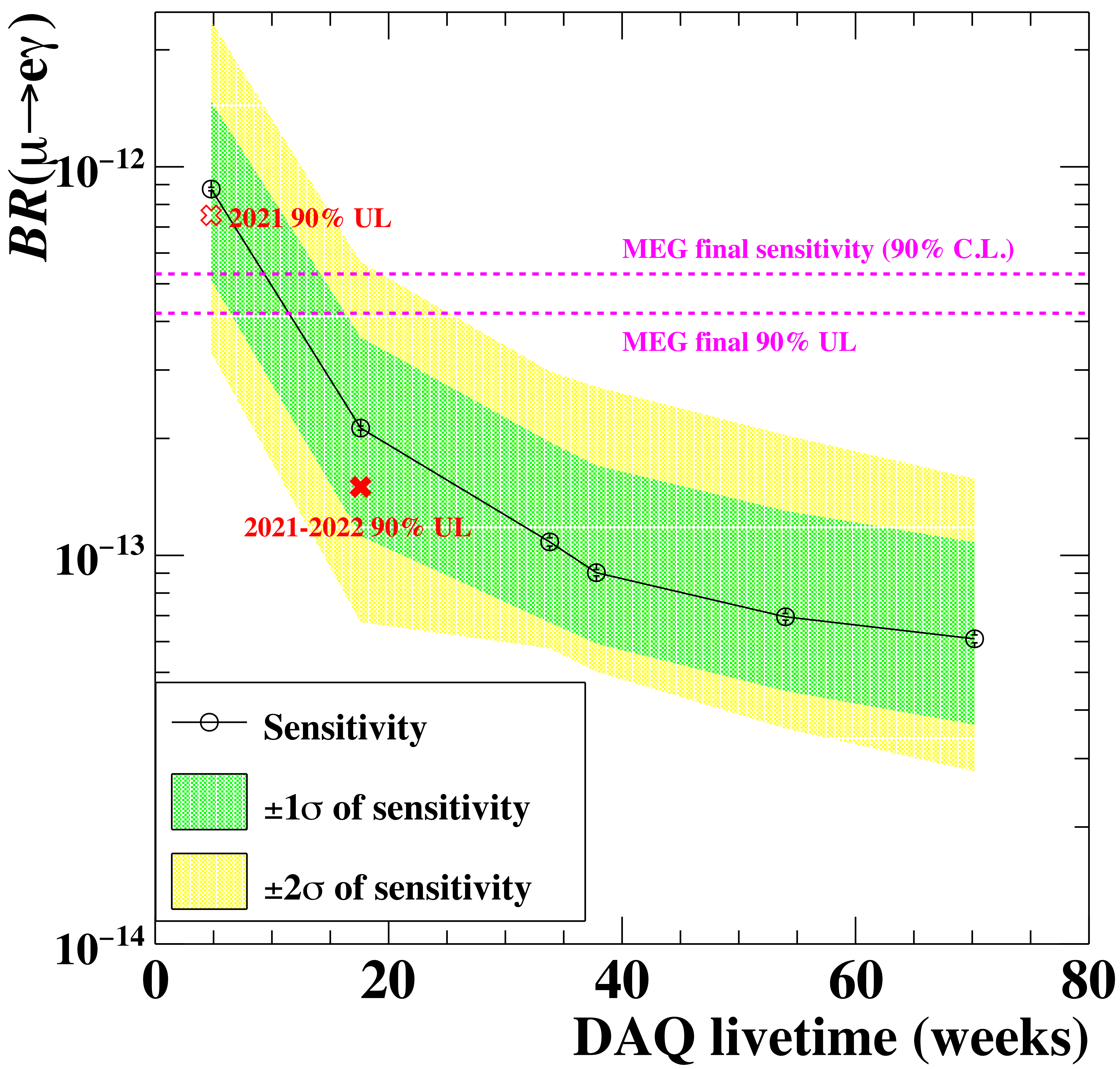

Contents

Conclusion

- A search for $\mu^+ \to e^+\gamma$ with the 2021-2022 MEG II dataset
  - Statistics is higher by a factor of 5 than that for the first result
  - New photon pileup unfolding algorithm increased signal efficiency by 2% and reconstruction reliability
  - RDC analysis updates increased detection efficiency by 17%
  - Photon energy scale uncertainty suppressed down to 0.18% thanks to careful calibration

- The sensitivity is the highest ever: 2.2×10^{-13}
  - Better by a factor of 2.4 than that in the MEG experiment

- No signal was found
- The most stringent upper limit set to $\mathcal{B}(\mu^+ \to e^+\gamma) < 1.5 \times 10^{-13}$ (90% C.L.)

Backup

$\mu^+ \to e^+\gamma$ in SUSY models

$$\frac{d\mathcal{B}(\mu^+ \to e^+\gamma)}{d(\cos\theta_e)} = 192\pi^2 \left[\underline{|A_R|^2(1 - P_\mu \cos\theta_e)} + \underline{|A_L|^2(1 + P_\mu \cos\theta_e)} \right]$$

SUSY-seesaw

- Slepton mixing only in **left**-handed slepton sector

➡ $A_R \neq 0$ and $A_L \sim 0$ for e^+ (i.e. Right-handed e^+ emitted)

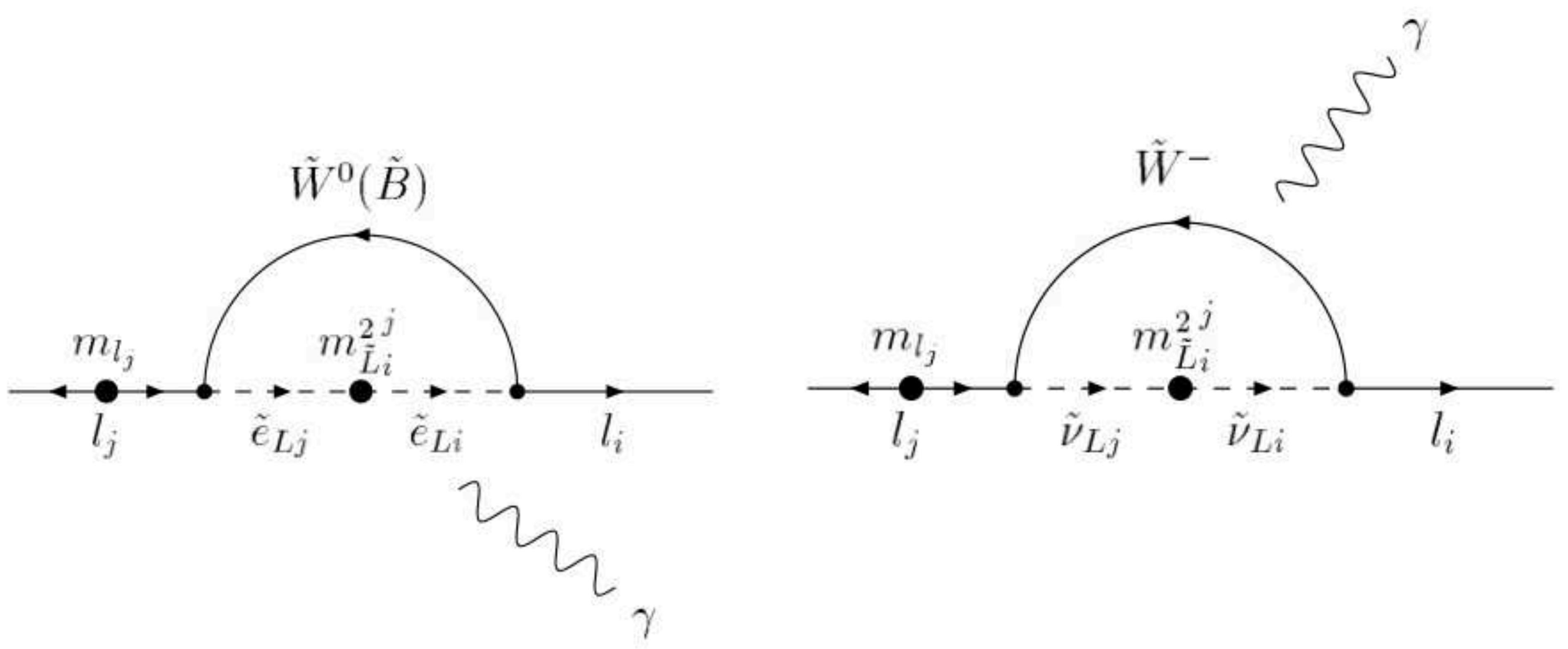

SU(5) SUSY-GUT

- Slepton mixing only in **right**-handed slepton sector

➡ $A_R \sim 0$ and $A_L \neq 0$ for e^+ (i.e. Left-handed e^+ emitted)

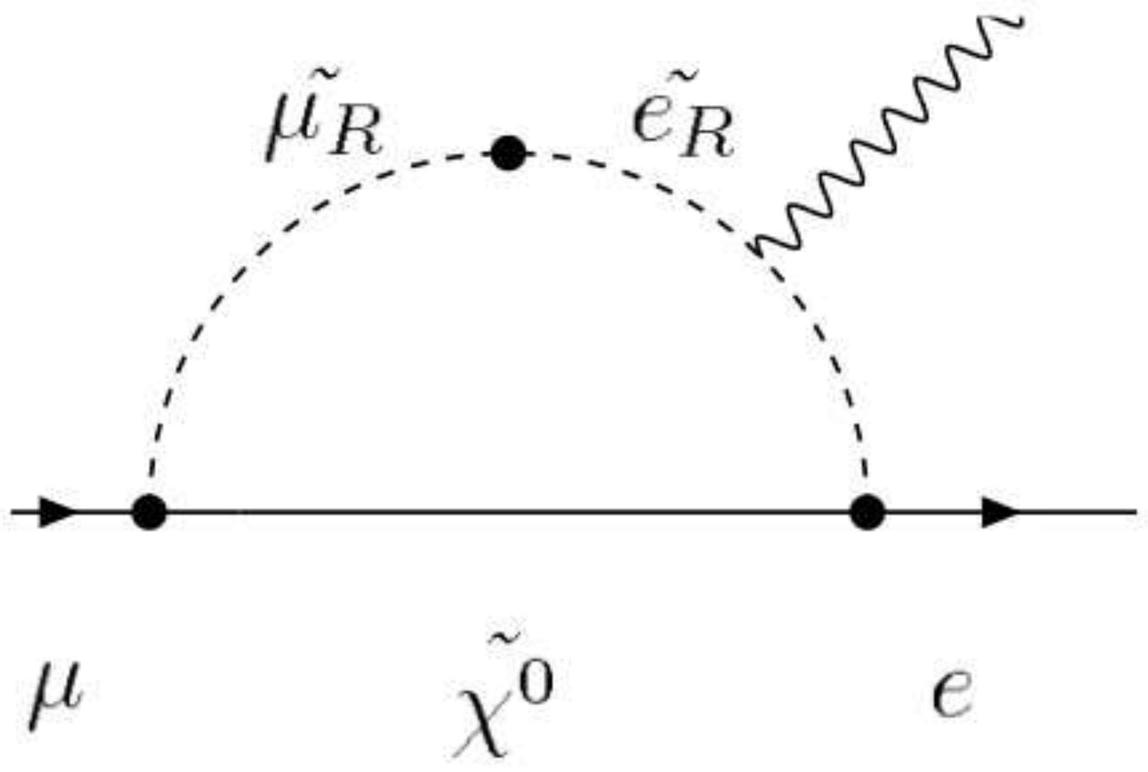

SO(10) SUSY-GUT

- Slepton mixing in both **left**- and **right**-handed slepton sectors

➡ $A_R \neq 0$ and $A_L \neq 0$

$\mu^+ \to e^+\gamma$ and CLFV channels with muons

- No CLFV discovery so far

Chronology of upper limits on CLFV processes

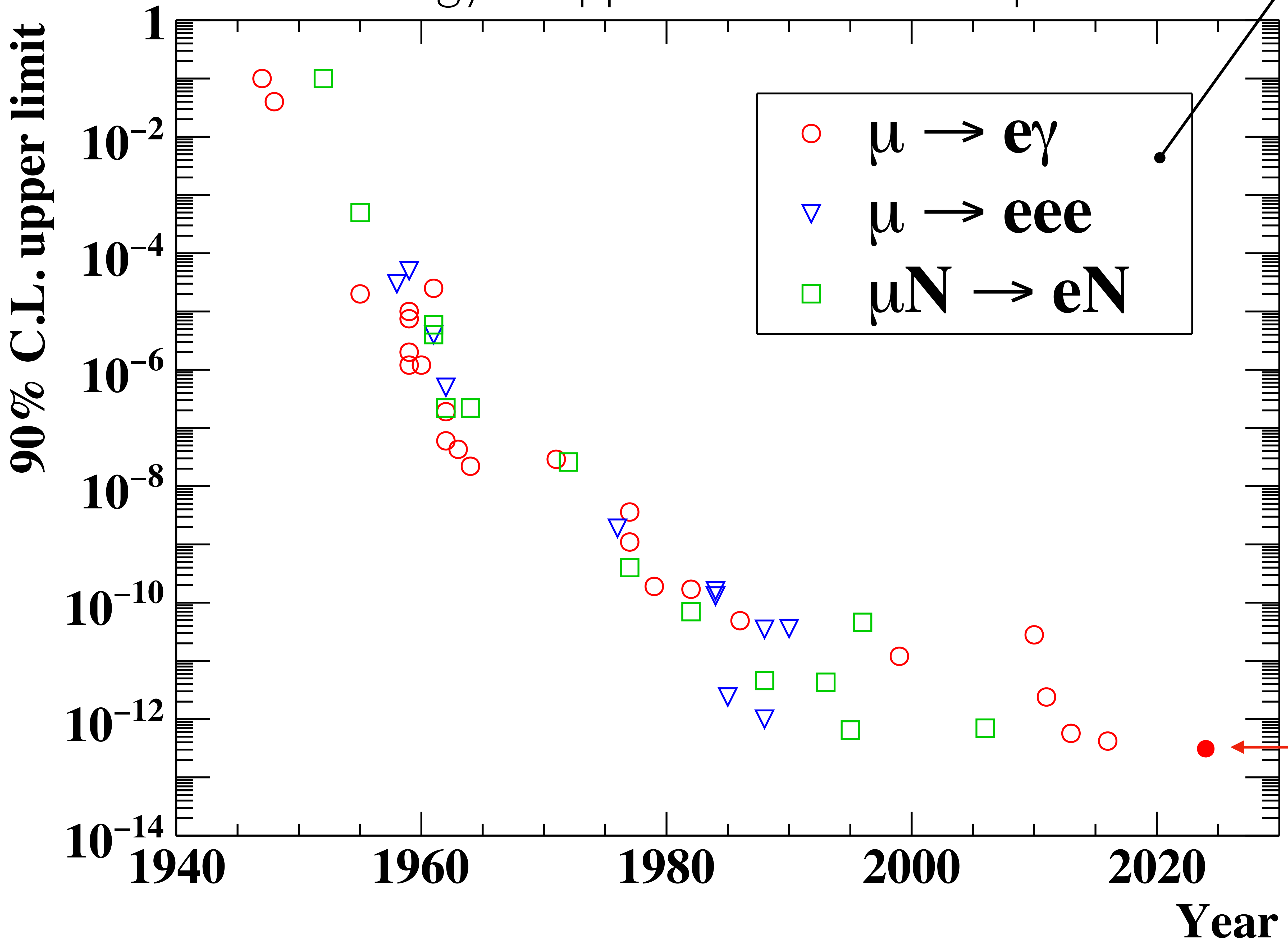

3.1×10^{-13} (90% C.L.)
(MEG full + MEG II 2021)

Complementary to each other

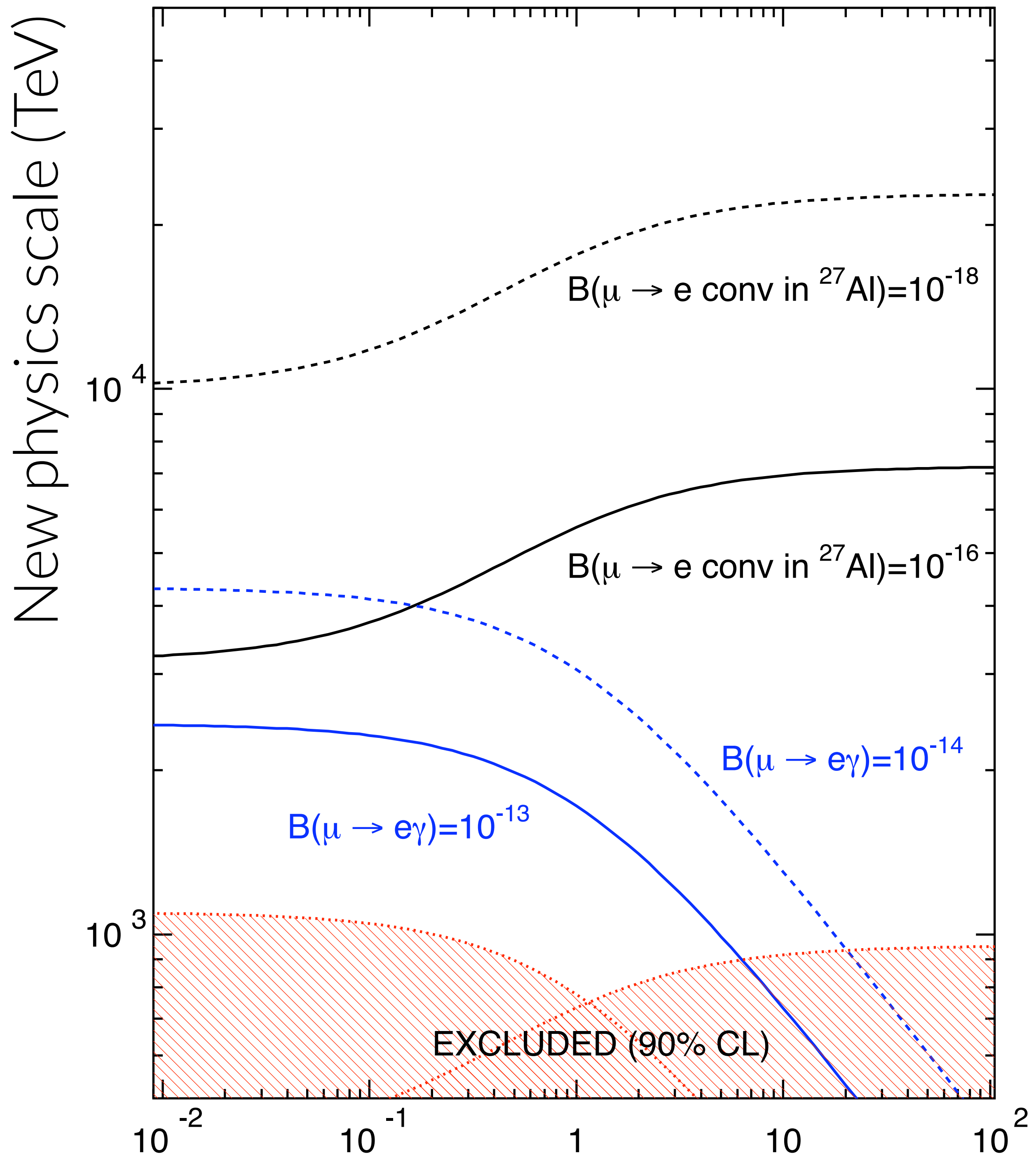

Interaction type parameter

Keys to accidental background suppression

$$N_{\mathrm{ACC}} \propto R_\mu^2 \cdot \underbrace{\sigma_{E_e} \cdot \sigma_{E_\gamma}^2 \cdot \sigma_{t_{e\gamma}} \cdot \sigma_{\Theta_{e\gamma}}^2}_{\text{Detector resolutions}}$$

E_e spectrum

52.8 MeV

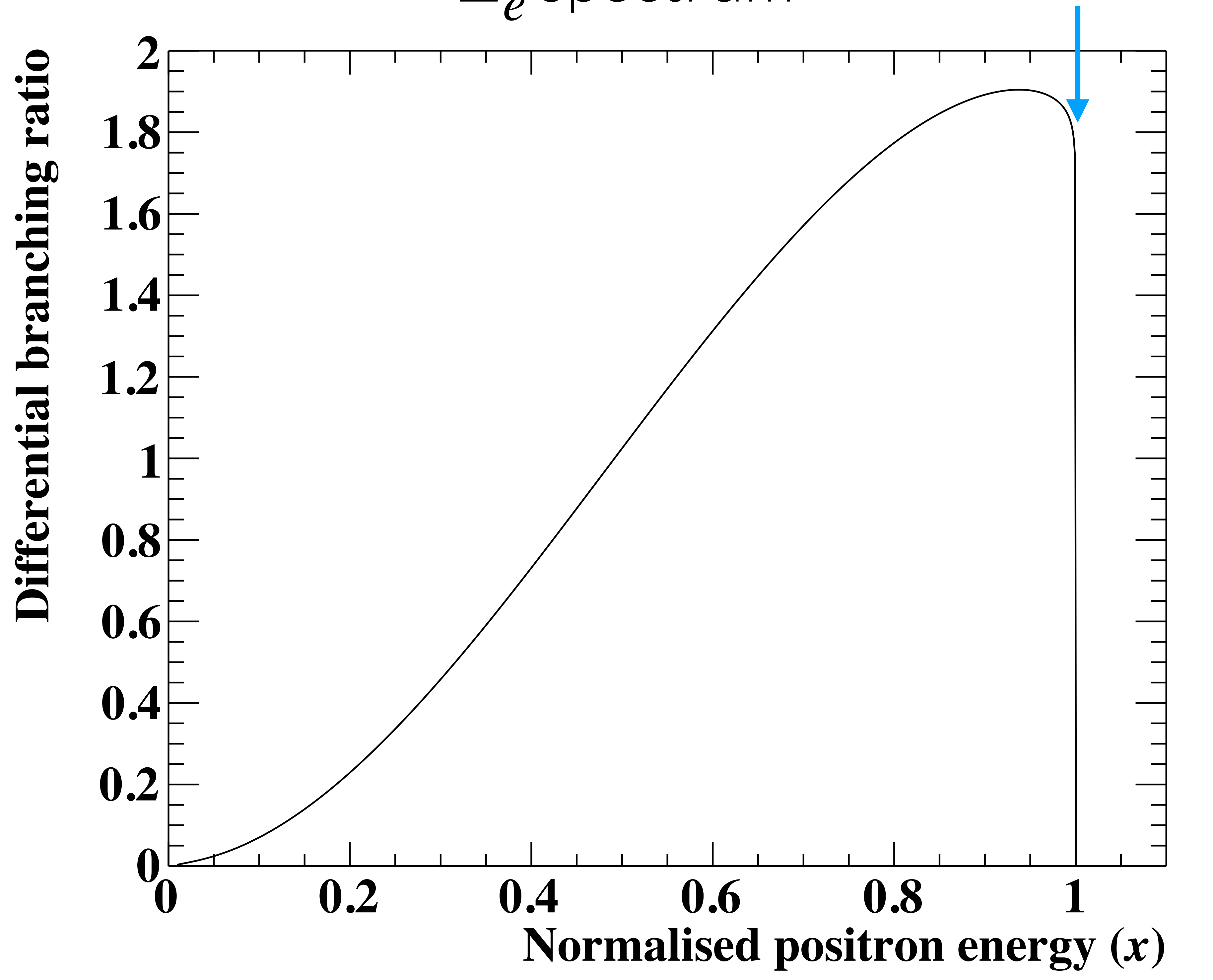

E_γ spectrum

52.8 MeV

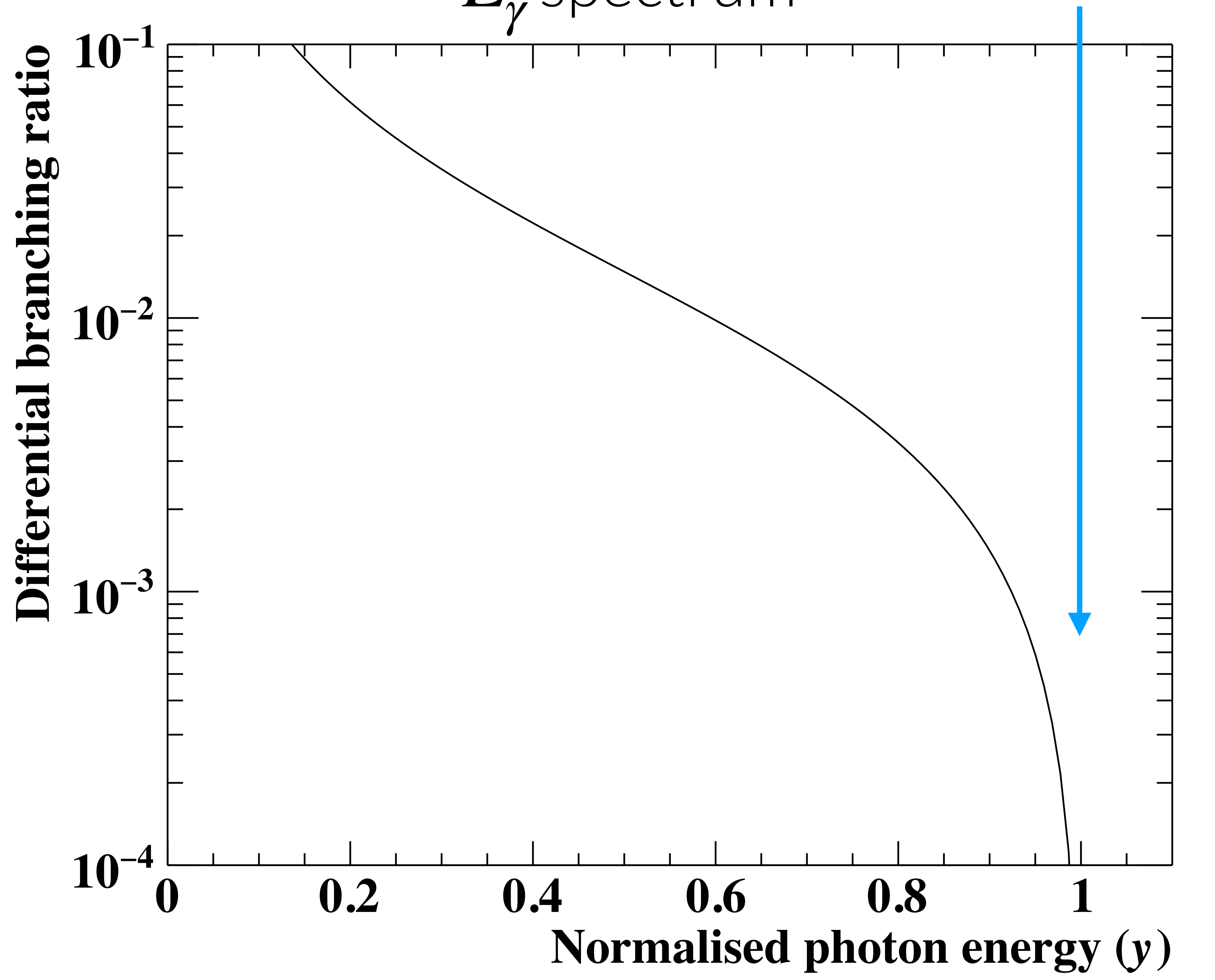

Muon beam and stopping target

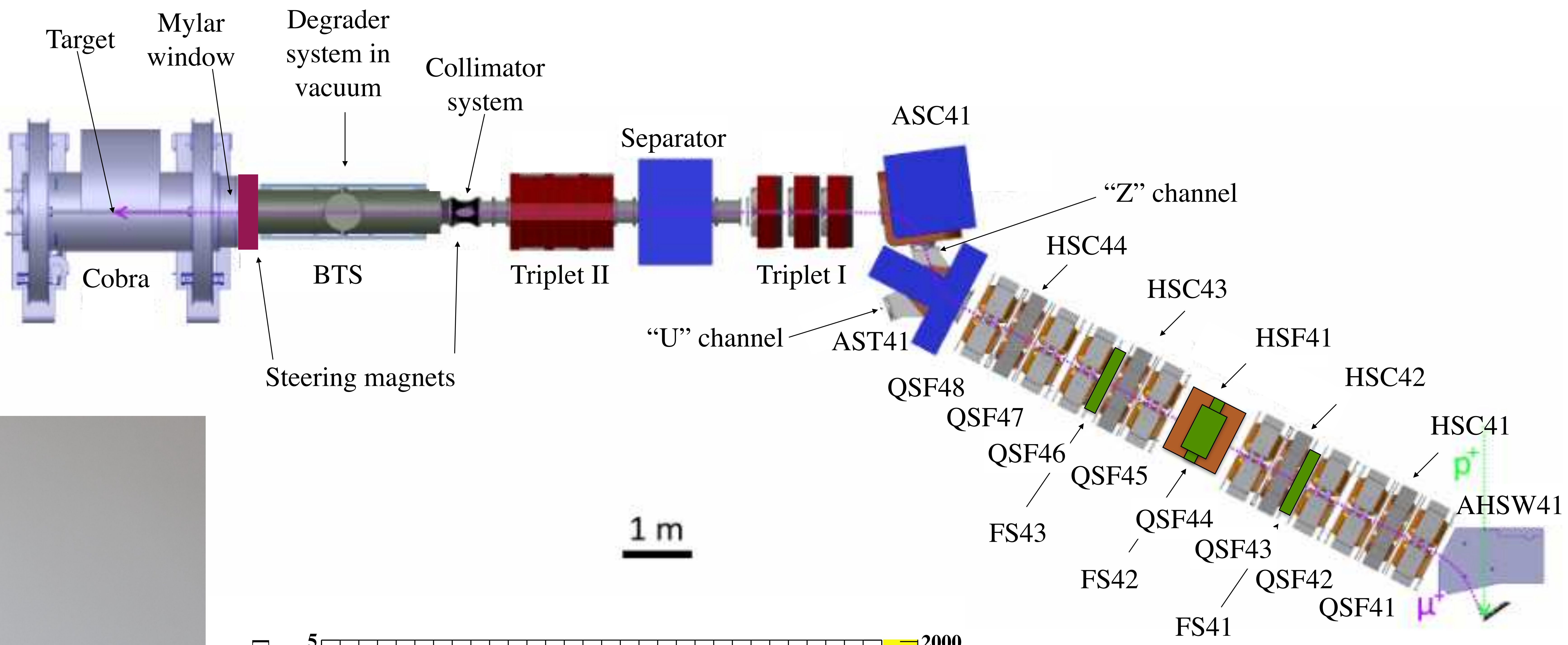

- Printing dots traced by camera
- Holes for alignment with CDCH

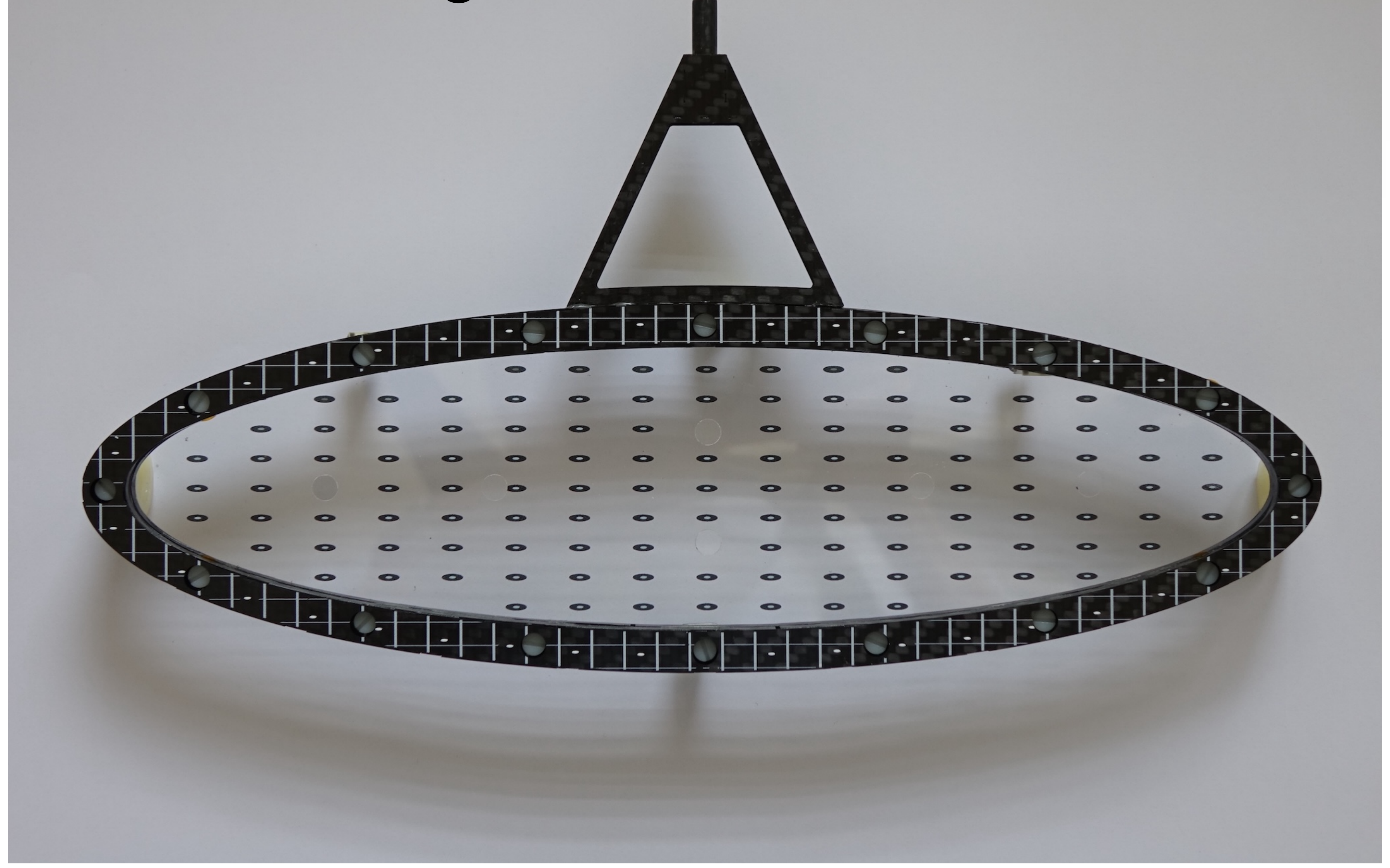

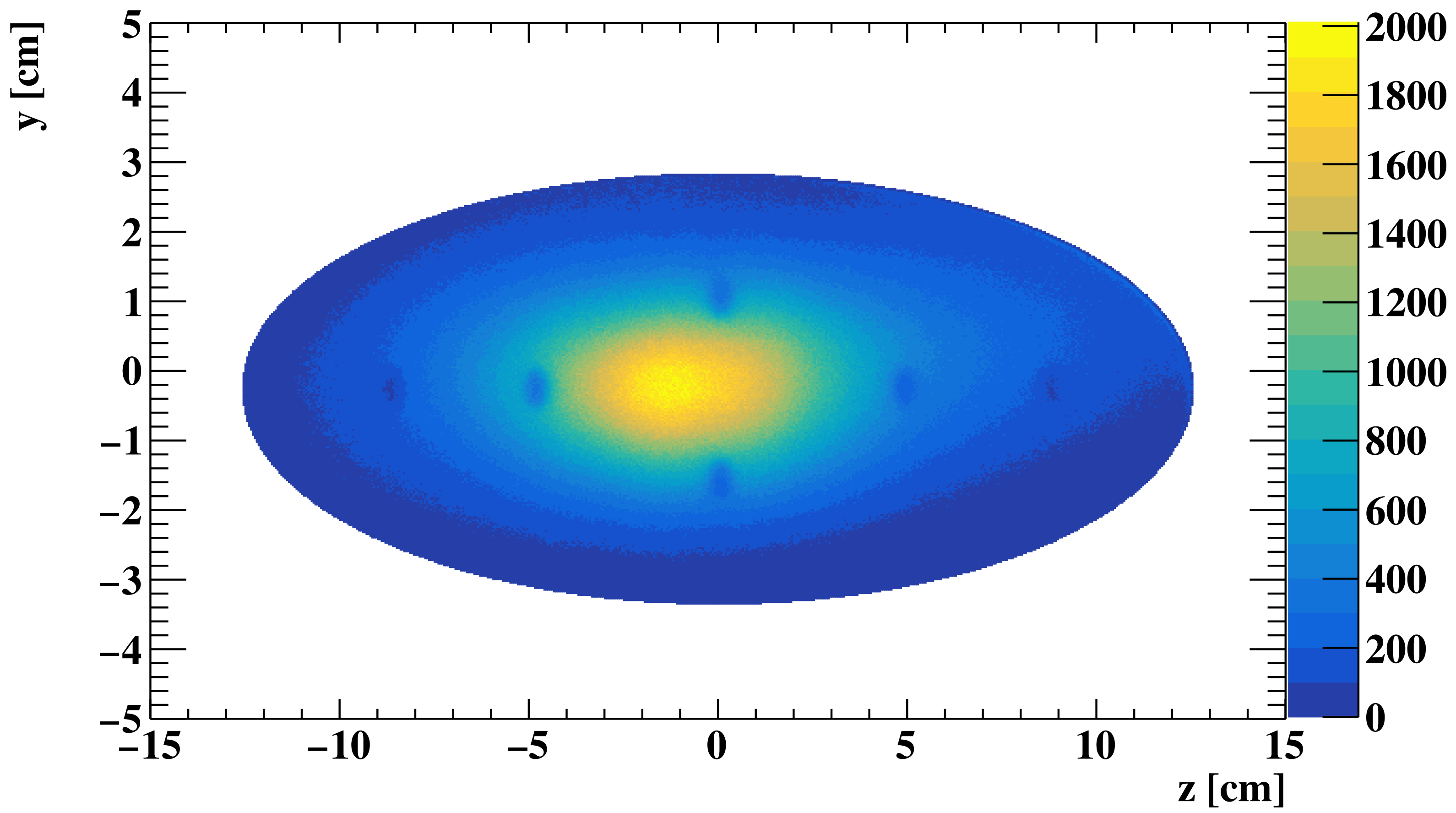

Positron spectrometer

- Designed to detect 52.8 MeV positrons under a high-rate environment

- Consists of
  - **Superconducting COBRA magnet**
    - Provide gradient magnetic field
    - Constant bending radius
    - Quickly sweeps positrons at $\theta \sim 90°$
  - **Cylindrical drift chamber (CDCH)**
  - **Pixelated timing counter (pTC)**

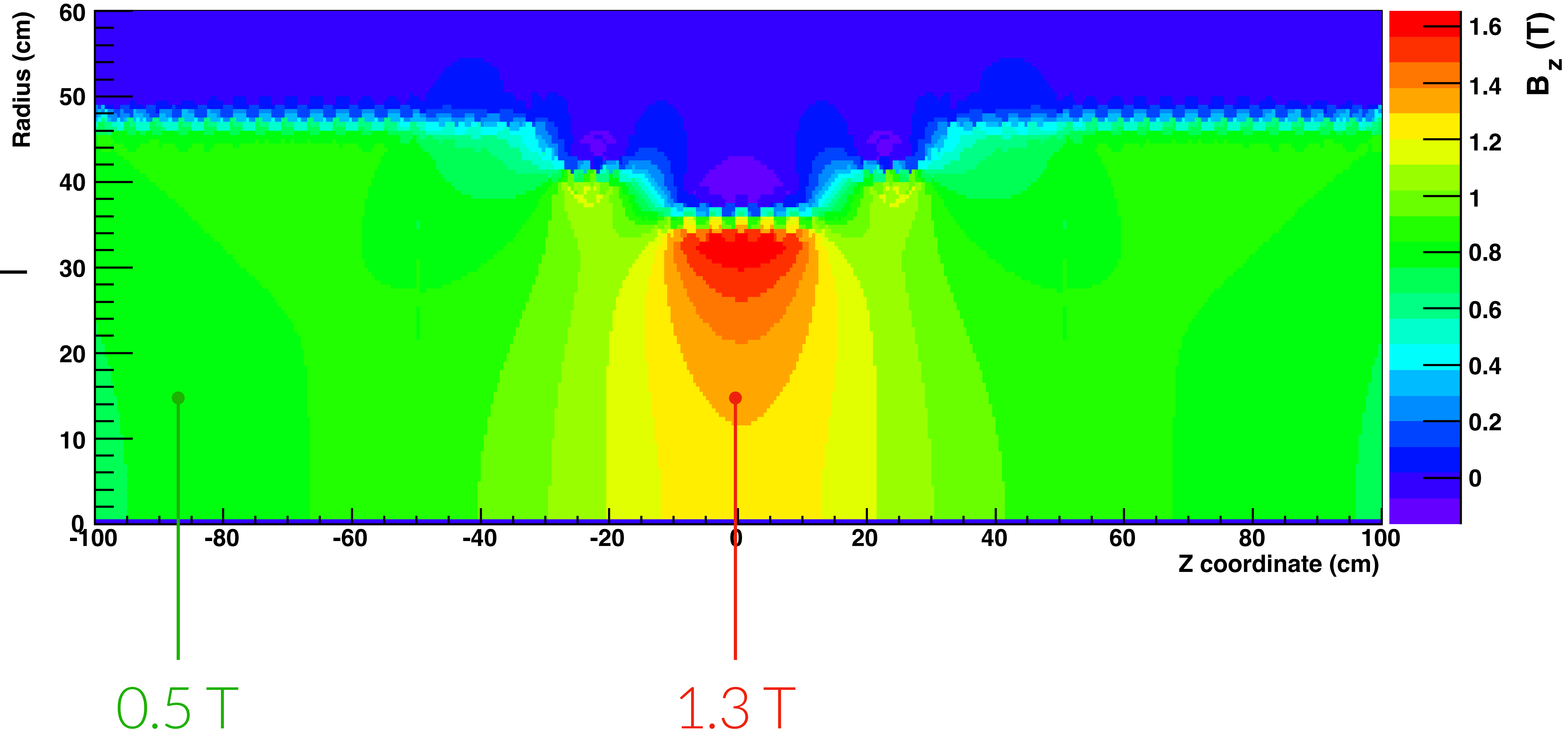

- Positron kinematics reconstructed based on
  - Positron tracks in CDCH ($\rightarrow p_e, \vec{x}_e, \theta_e, \phi_e$) and
  - Positron hits in pTC ($\rightarrow t_e$)

Cylindrical drift chamber (CDCH)

- Single-volume cylindrical drift chamber
- ~12,000 wires arranged in a stereo configuration

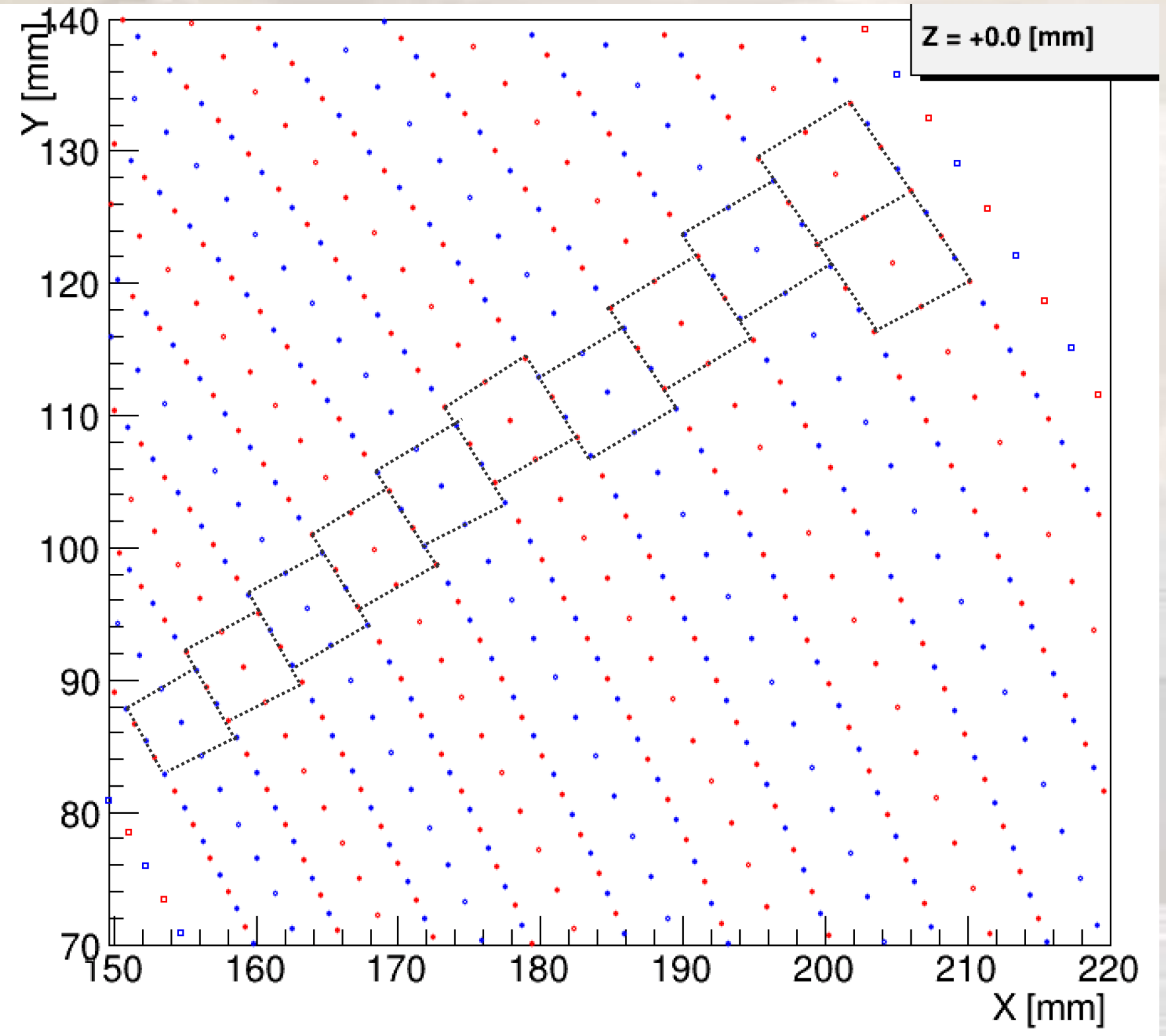

Pixelated timing counter

- 256 scintillation counters in each sub-module
- Multiple hits improve resolution

$$\sigma_{t_e} = \frac{\sigma_{\mathrm{single}}}{\sqrt{n_{\mathrm{pTC}}}}$$

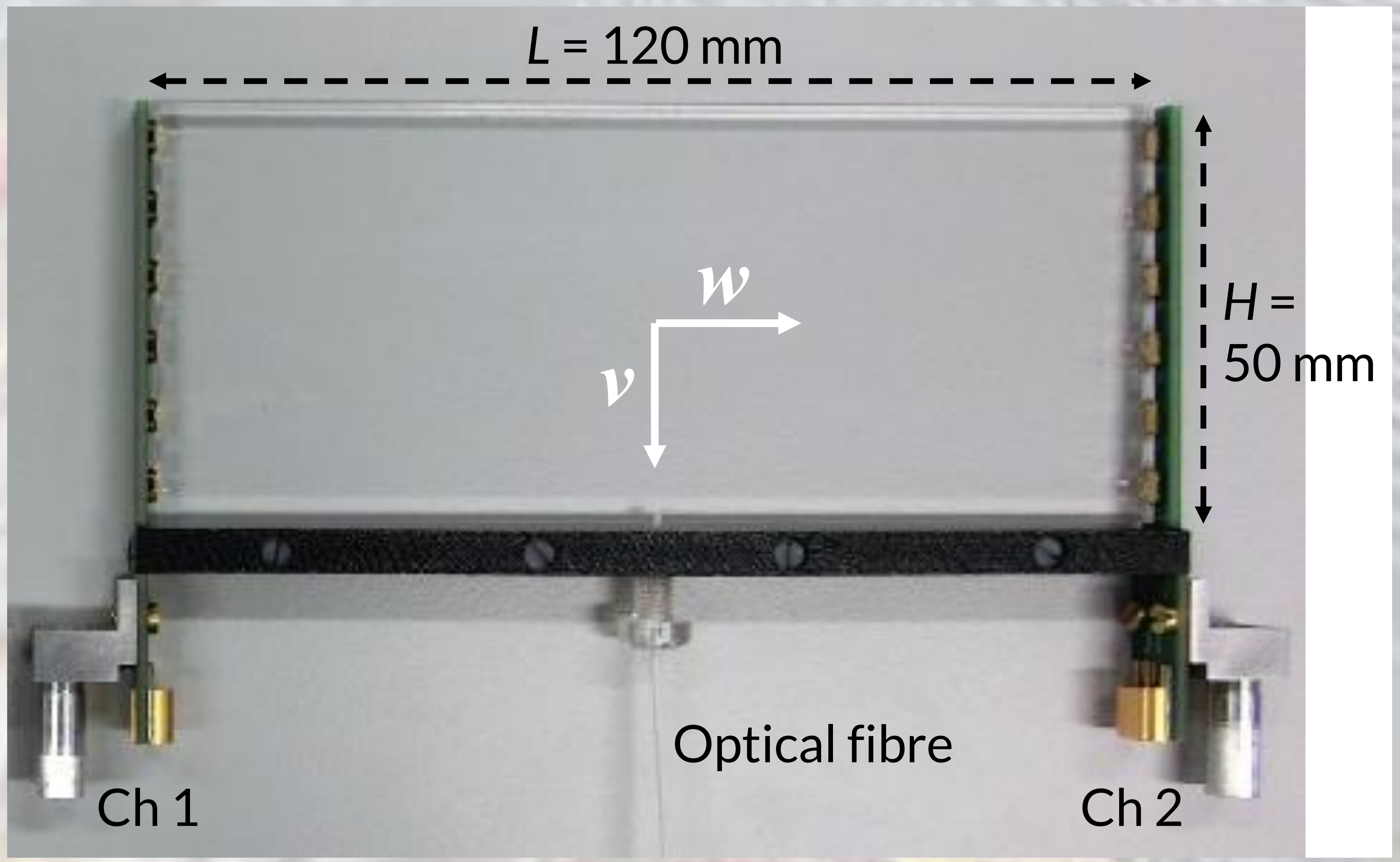

Scintillation light emission in LXe

Recombination process
with a time constant of 45 ns

$$
\begin{aligned}
Xe^+ + Xe &\longrightarrow Xe_2^+, \\
Xe_2^* + e^- &\longrightarrow Xe^{**} + Xe, \\
Xe^{**} &\longrightarrow Xe^* + \text{heat}, \\
Xe^* + Xe + Xe &\longrightarrow Xe_2^* + Xe, \\
Xe_2^* &\longrightarrow 2Xe + h\nu,
\end{aligned}
$$

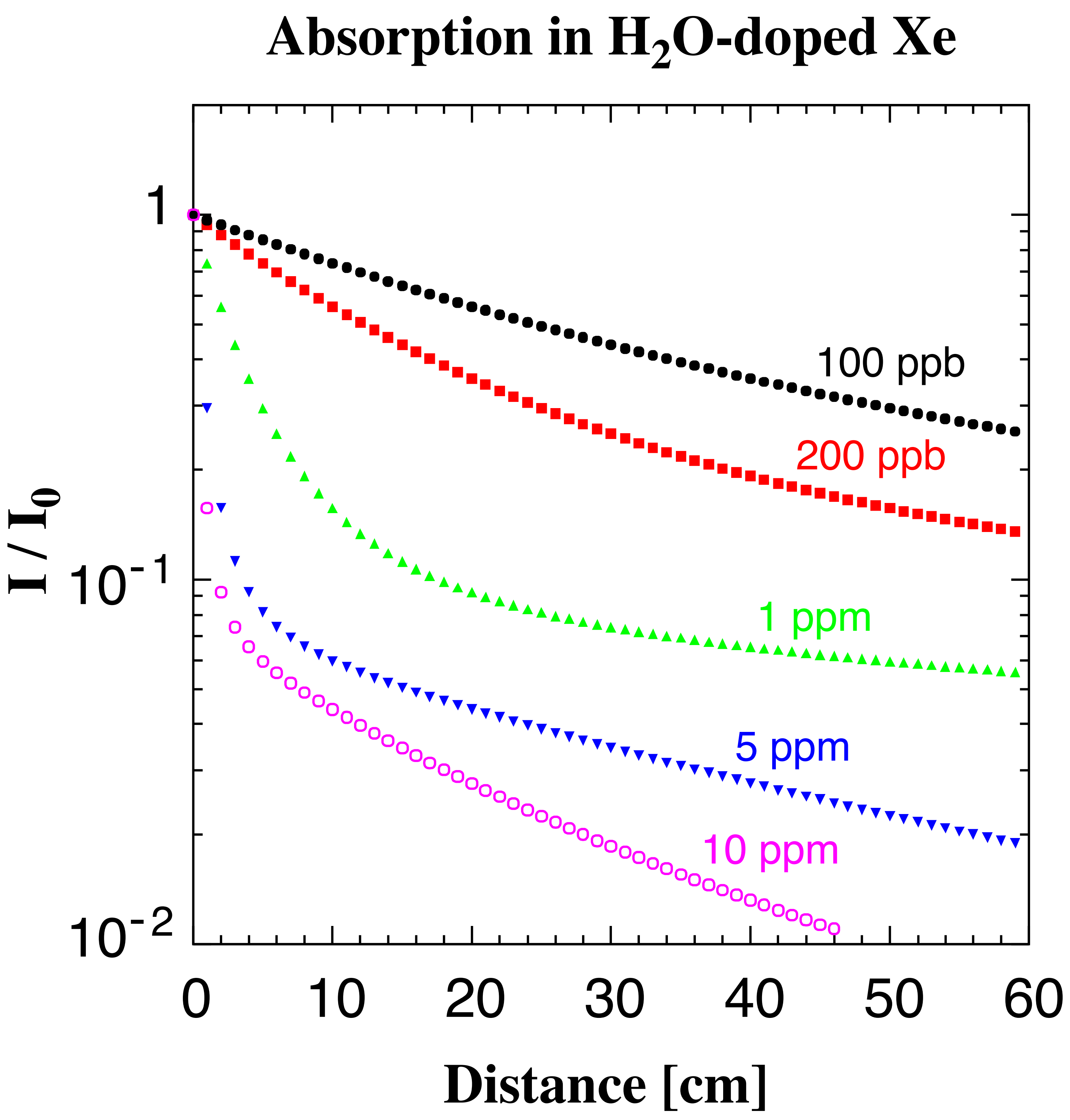

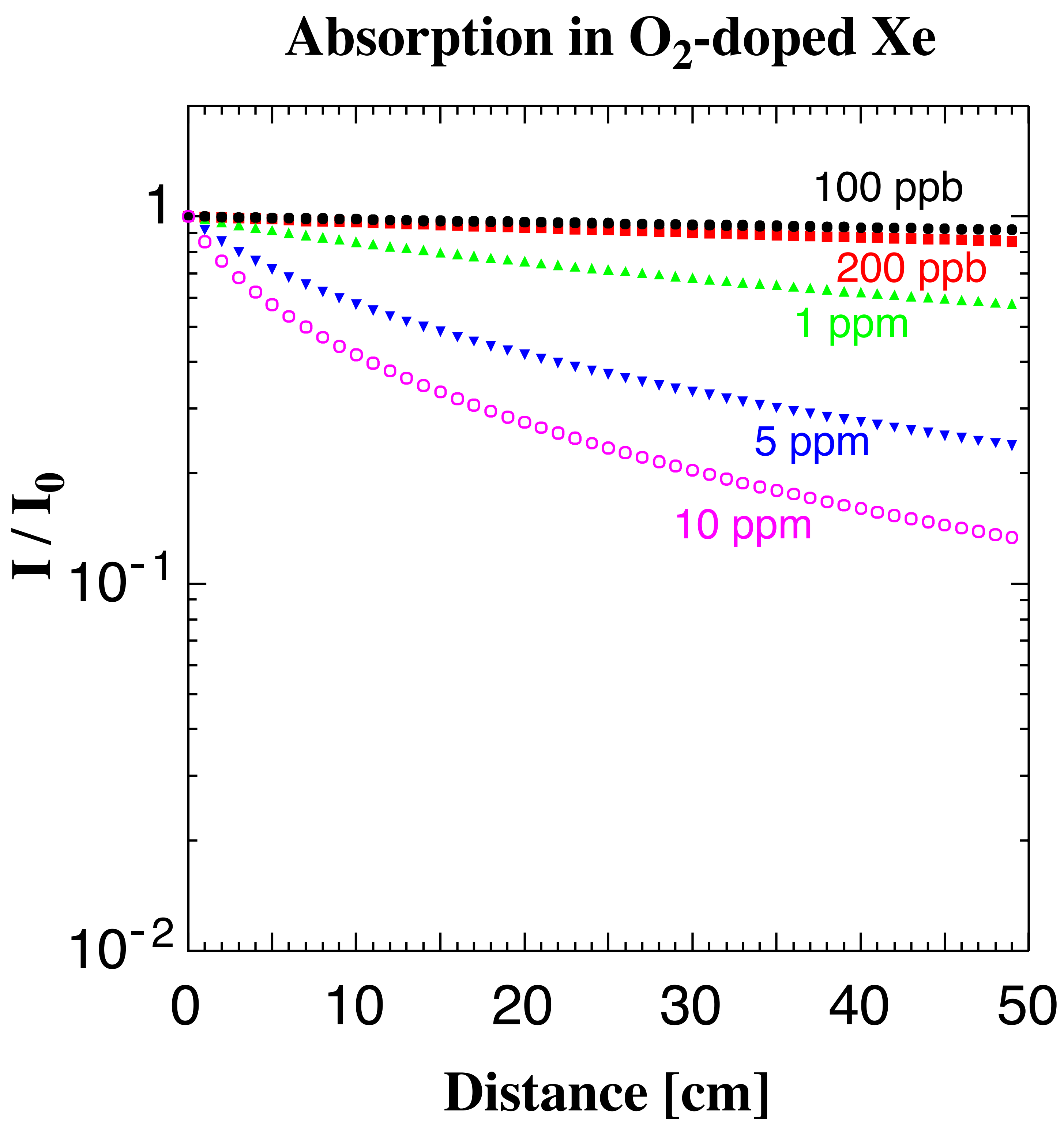

π^0 calibration

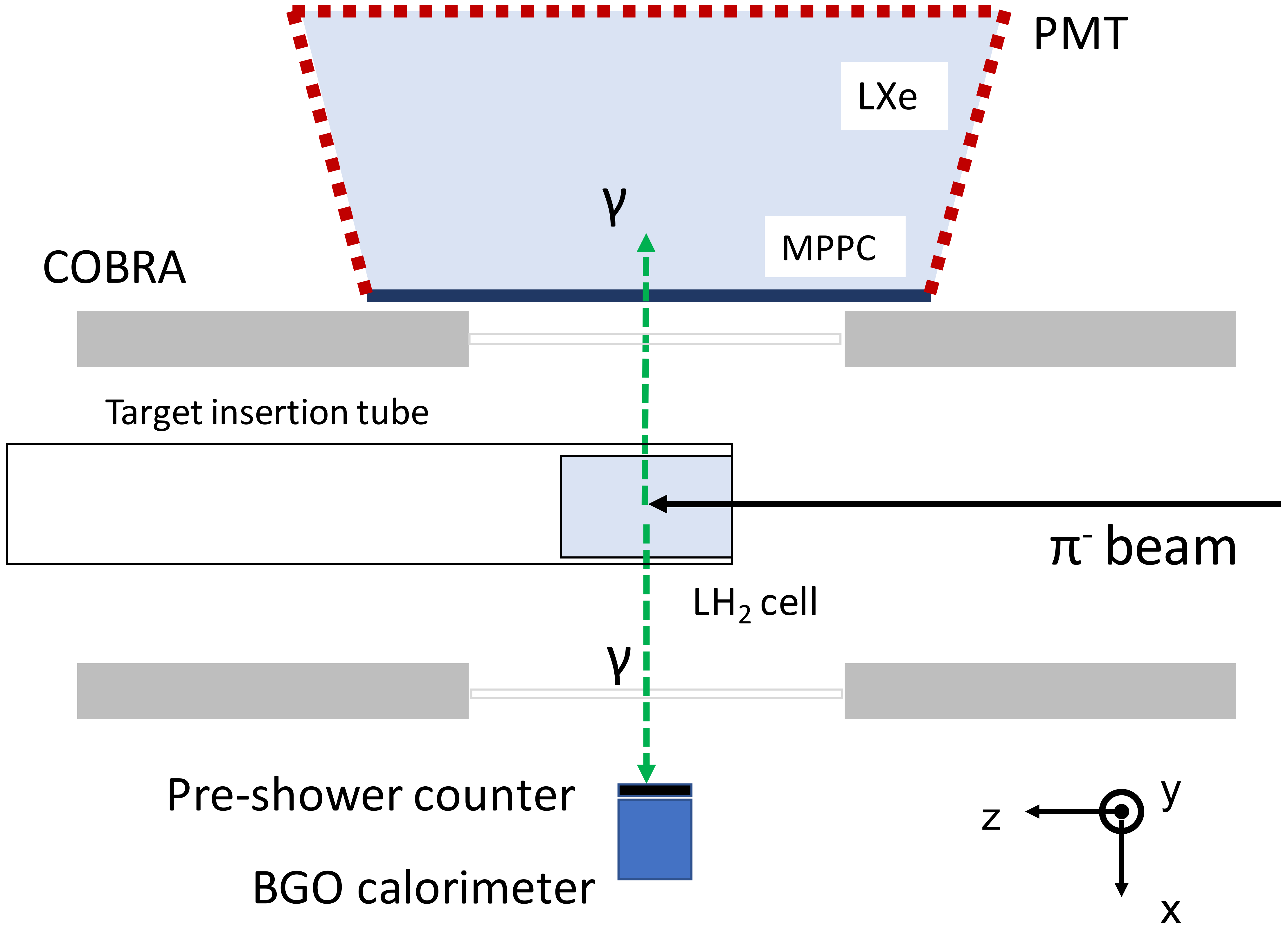

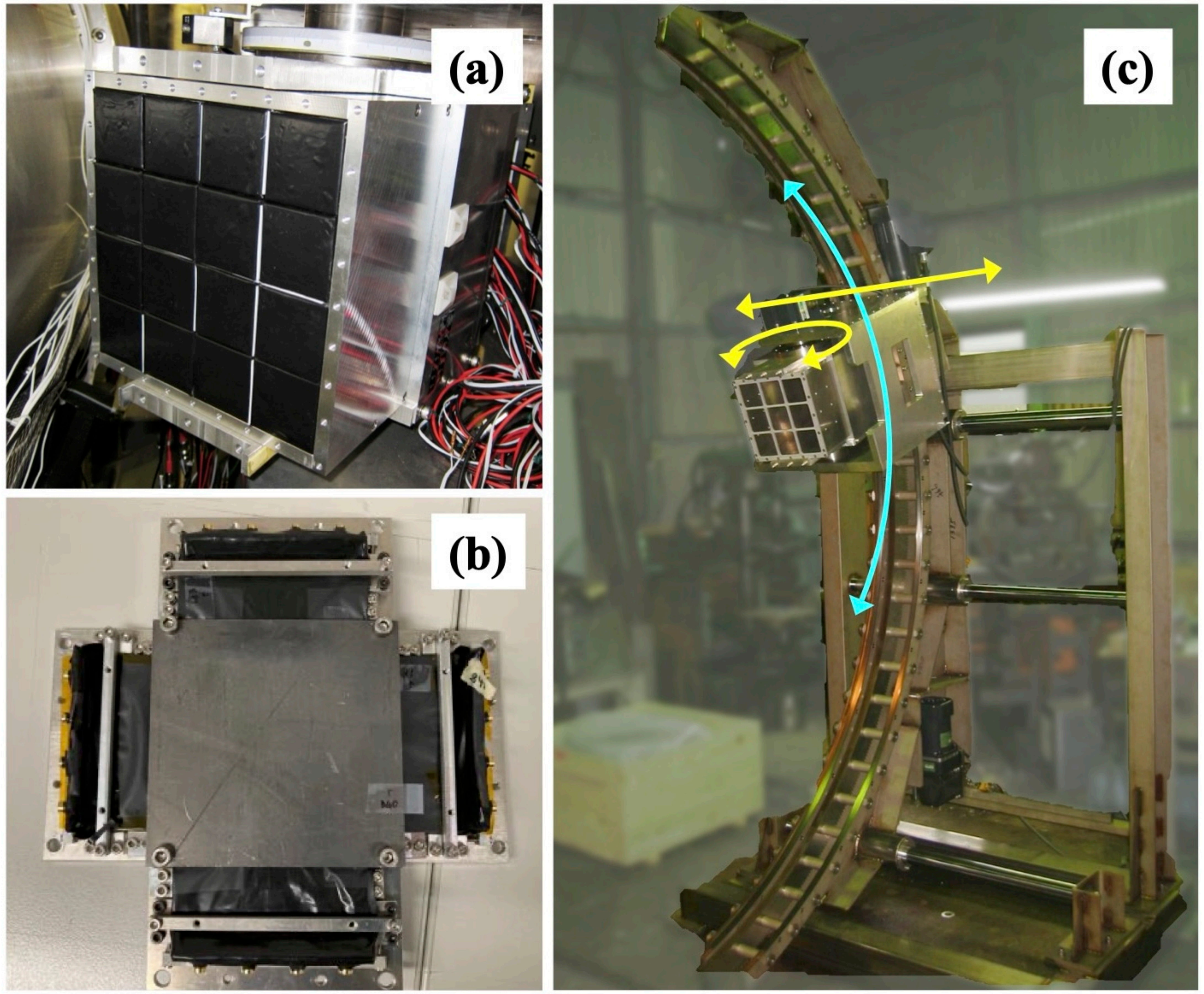

Trigger

Label	Logic
E_γ trigger	Weighted sum of all photosensors in the LXe detector
Time coincidence trigger	Time coincidence of pTC hit and LXe hit
DM trigger	Back-to-back hit positions in pTC and LXe detector
MEG trigger	(E_γ trigger) $\wedge$ (Time coincidence trigger) $\wedge$ (DM trigger)
Random trigger	Random timing
LED trigger	Signal from LED driver
α trigger	Pulse shape discrimination using outer PMTs
Neutron generator trigger	Neutron generator signal
pTC laser trigger	Laser pulser signal
pTC self trigger	$n_{\mathrm{pTC}} \geq 1$
RDC LYSO self trigger	One or more hits in RDC LYSO
BGO self trigger	Weighted sum of all PMTs in the BGO calorimeter
π^0 trigger	(E_γ trigger) $\wedge$ (BGO self trigger) $\wedge$ (Back-to-back photon positions) $\wedge$ (Time coincidence)

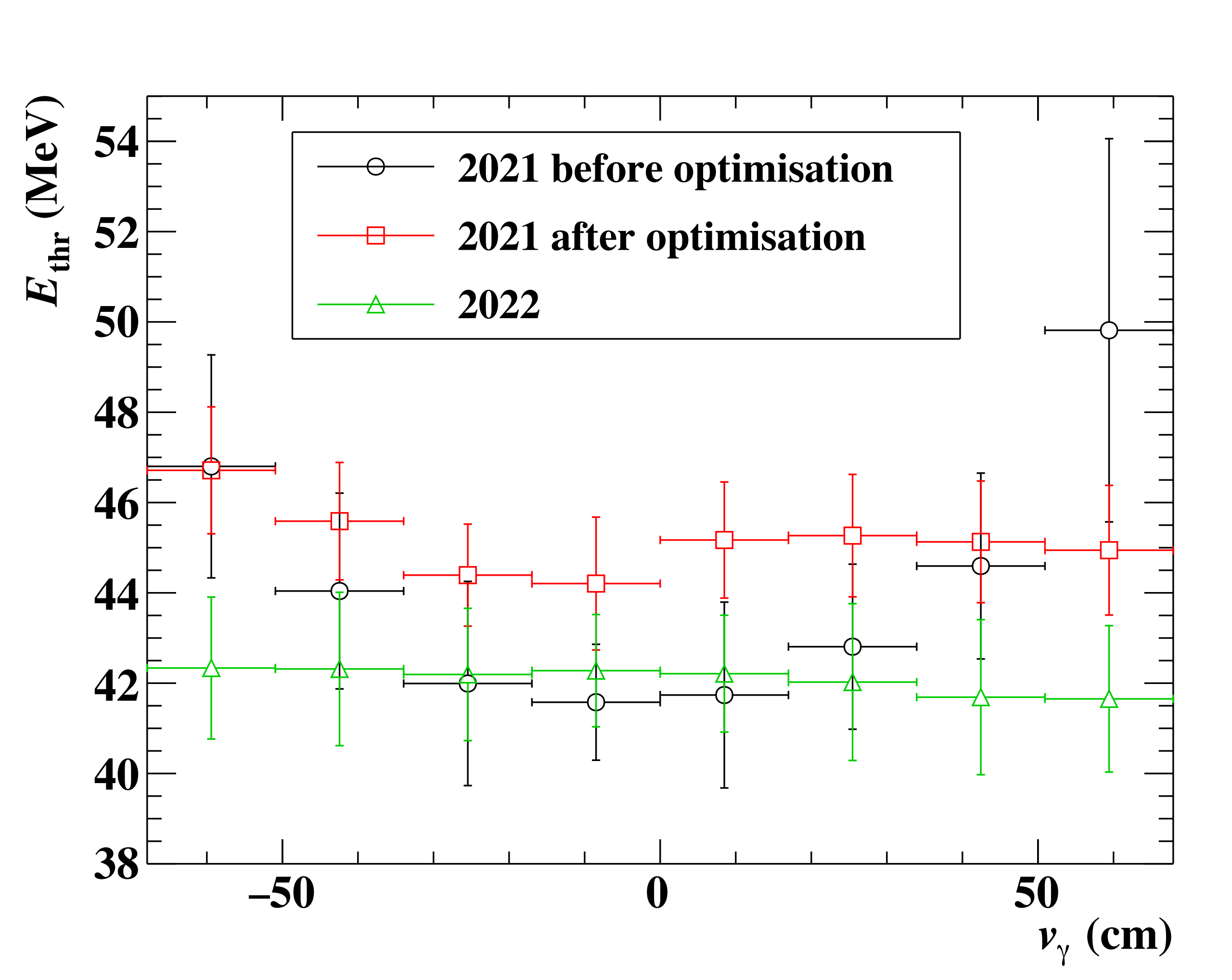

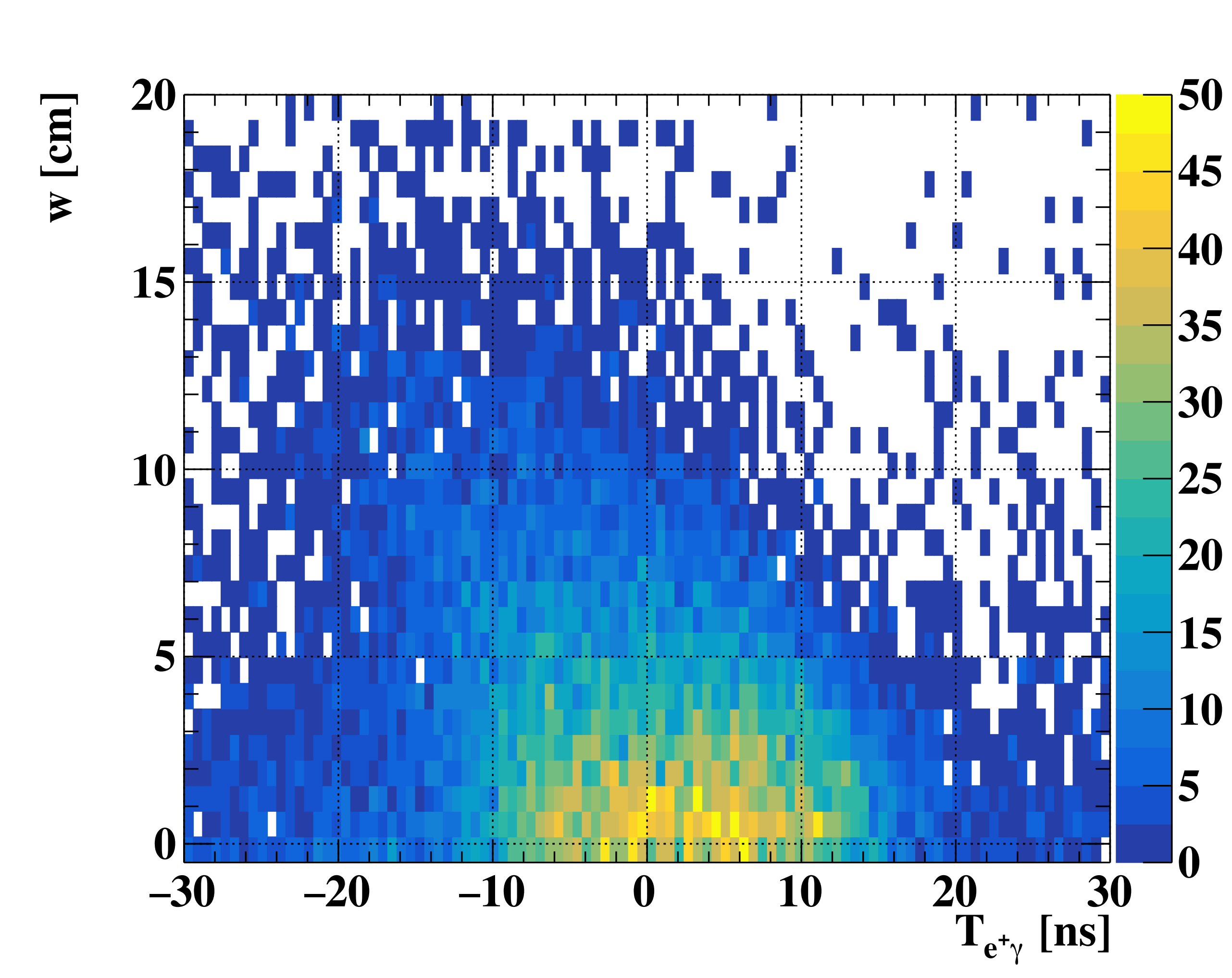

DAQ

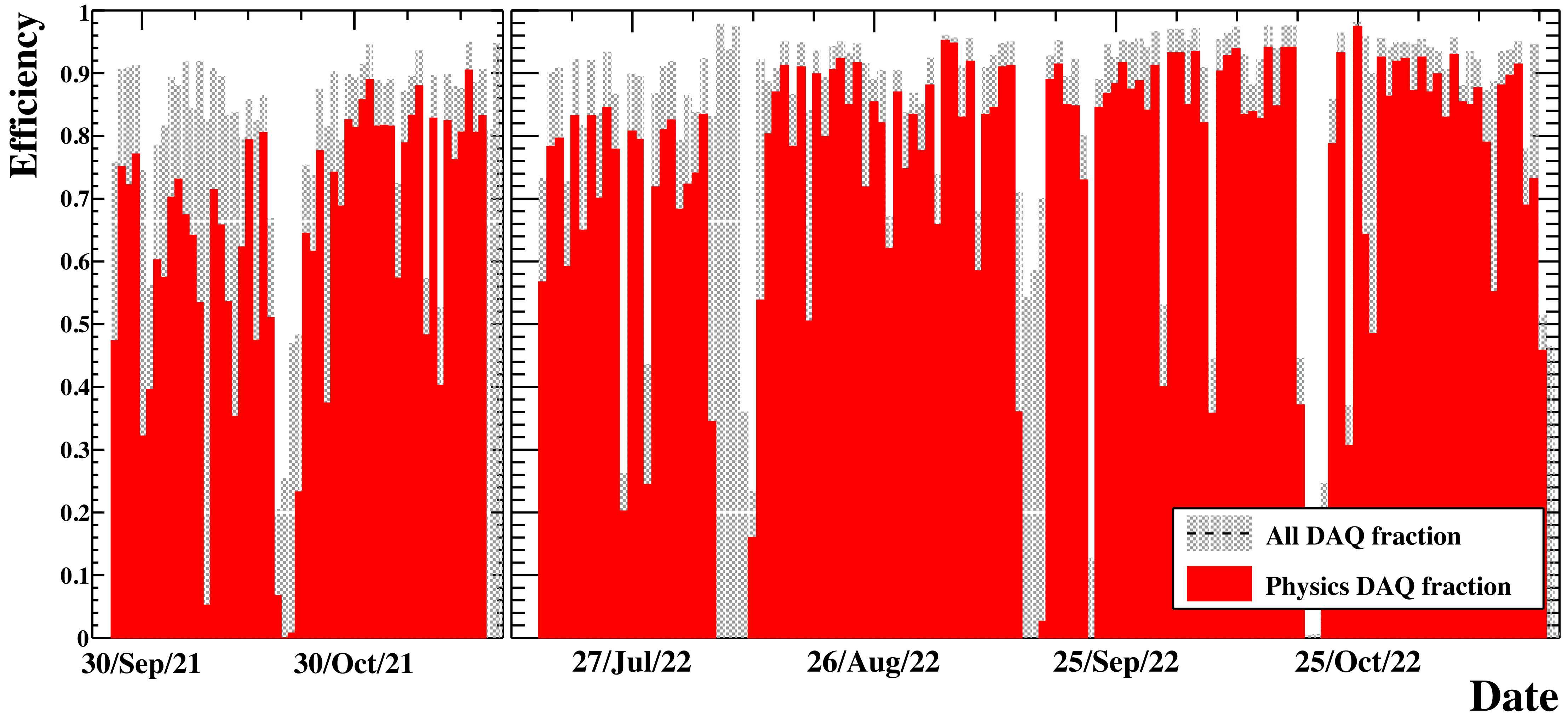

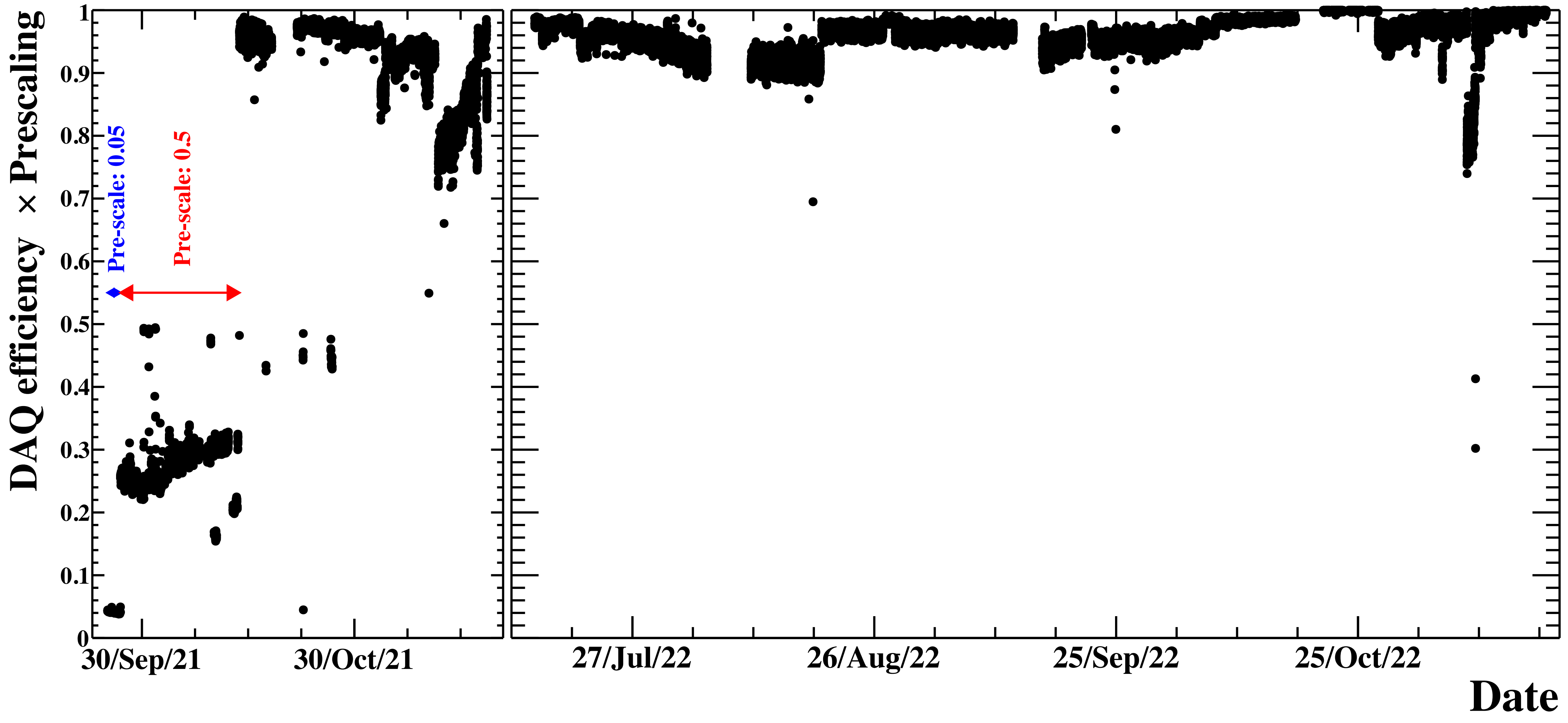

Dataset	DAQ frequency in 2021	DAQ frequency in 2022	Time comsumption
Random trigger data	2 day^{-1}	1 day^{-1}	10 min
LXe LED data (long)	1 day^{-1}	3 week^{-1}	40 min
LXe LED data (short)	1 day^{-1}	4 week^{-1}	10 min
LXe weak LED data		3 week^{-1}	30 min
LXe α-particle data	2 day^{-1}	1 day^{-1}	10 min
Cosmic-ray data	1 day^{-1}	3 week^{-1}	10 min
9 MeV photon data	3 week^{-1}	3 week^{-1}	15 min
17.6 MeV photon data	3 week^{-1}	3 week^{-1}	1 hour
pTC laser data	1 day^{-1}	3 week^{-1}	10 min

Ghost track selection

- Rating the ghost tracks is improved by adding information on the last half turn

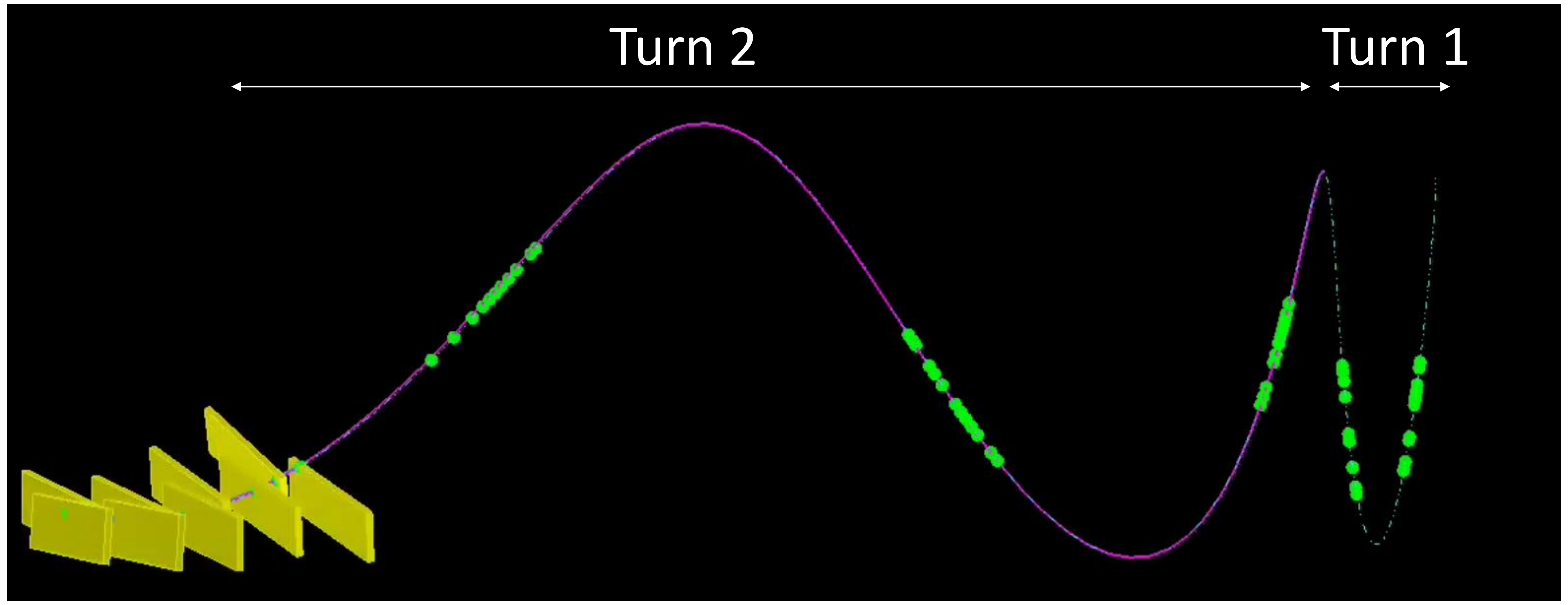

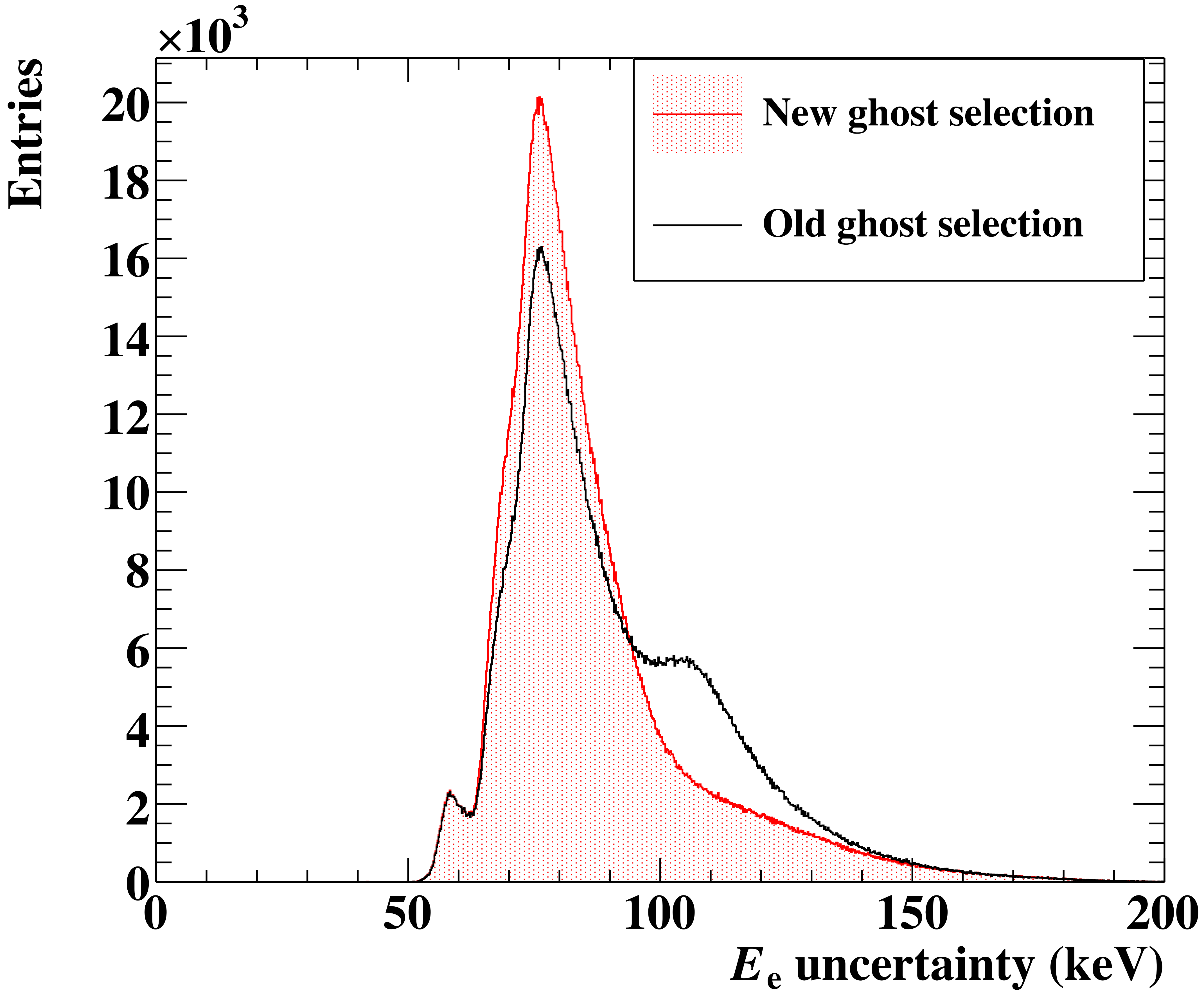

Pileup unfolding algorithm

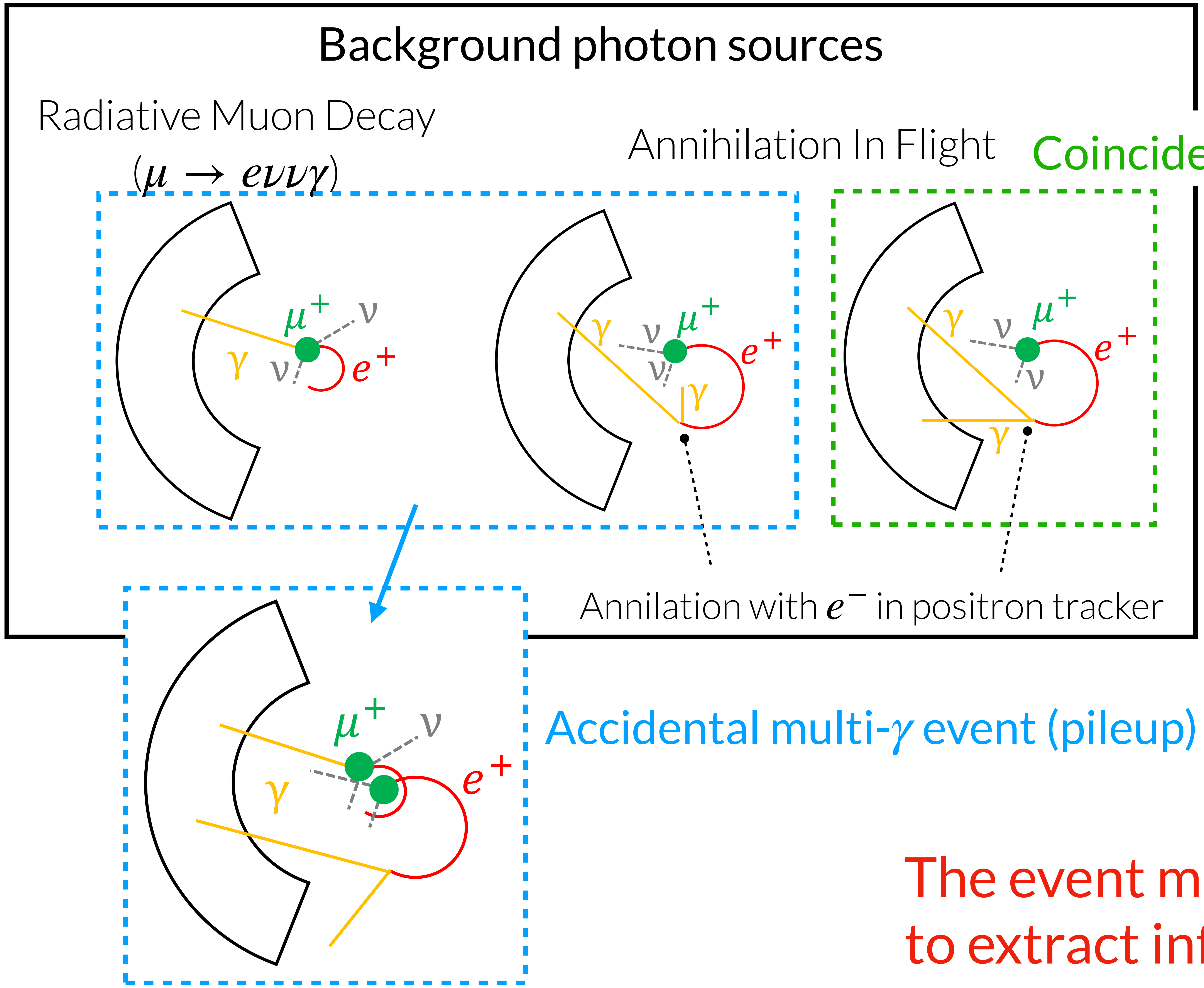

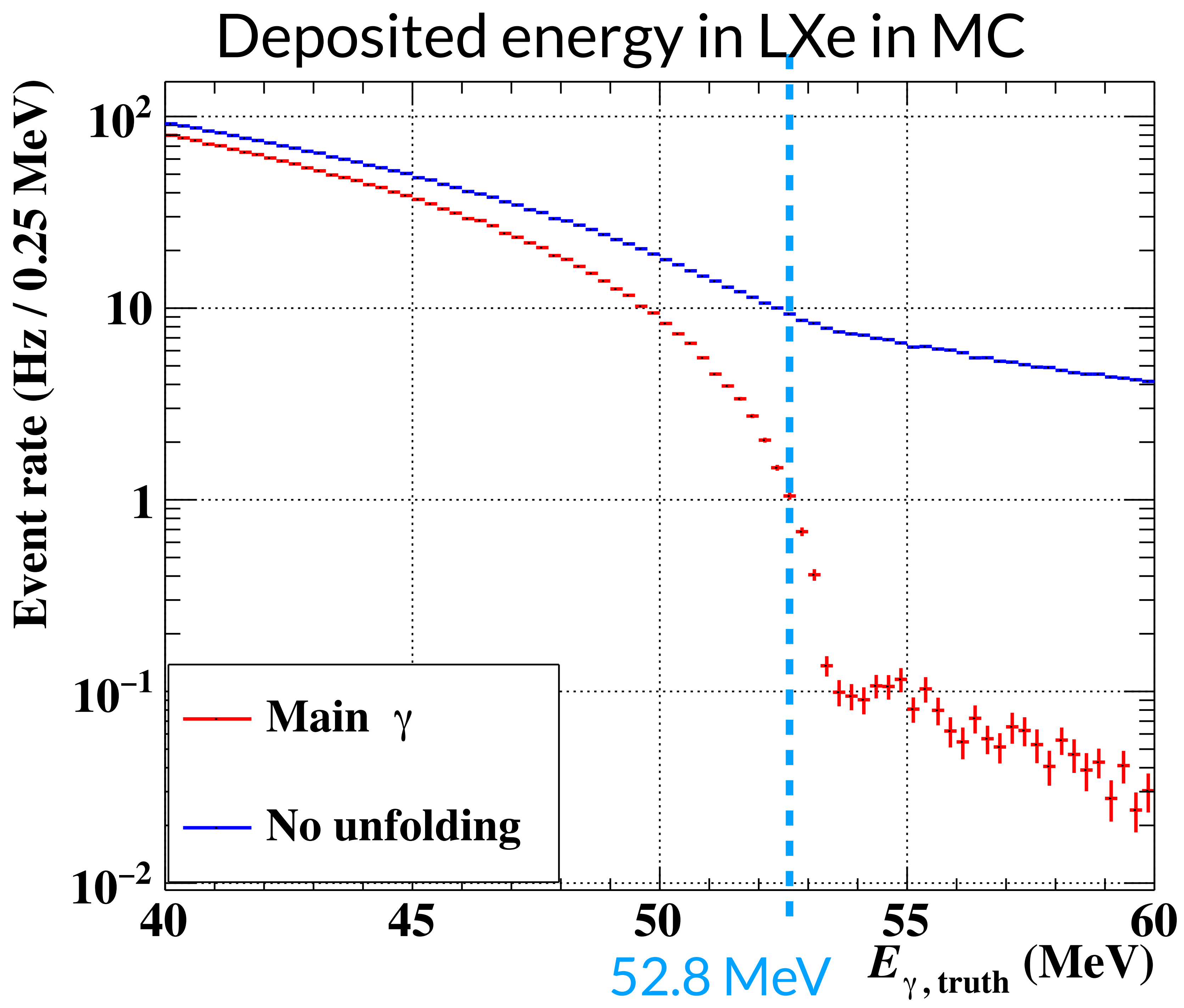

The event must be unfolded
to extract information of each individual photon

Pileup analysis inefficiency

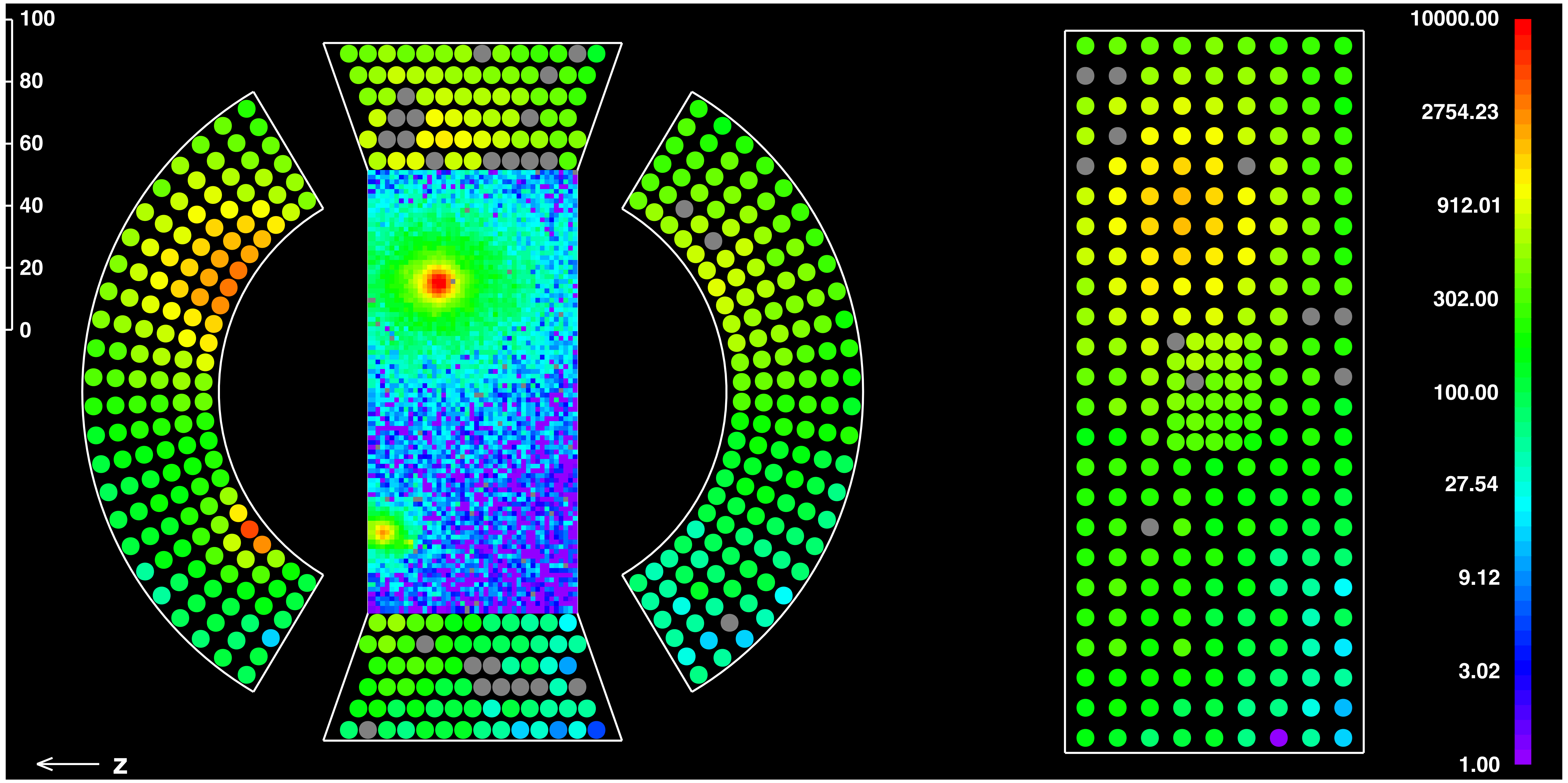

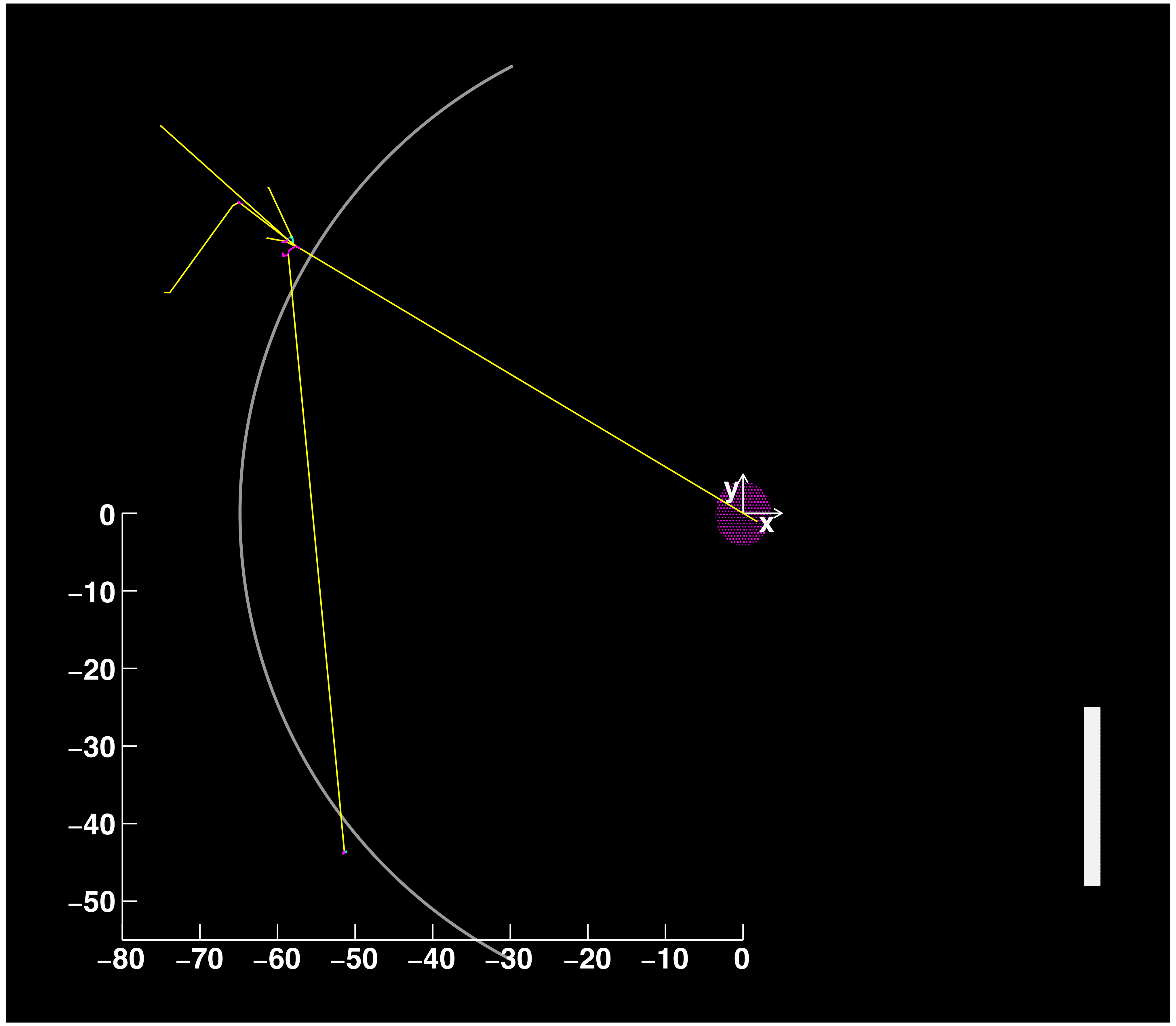

RDC detection efficiency improvement

Lower pulse search threshold for plastic scintillators

- Offline noise reduction methods allow for a halved pulse search threshold

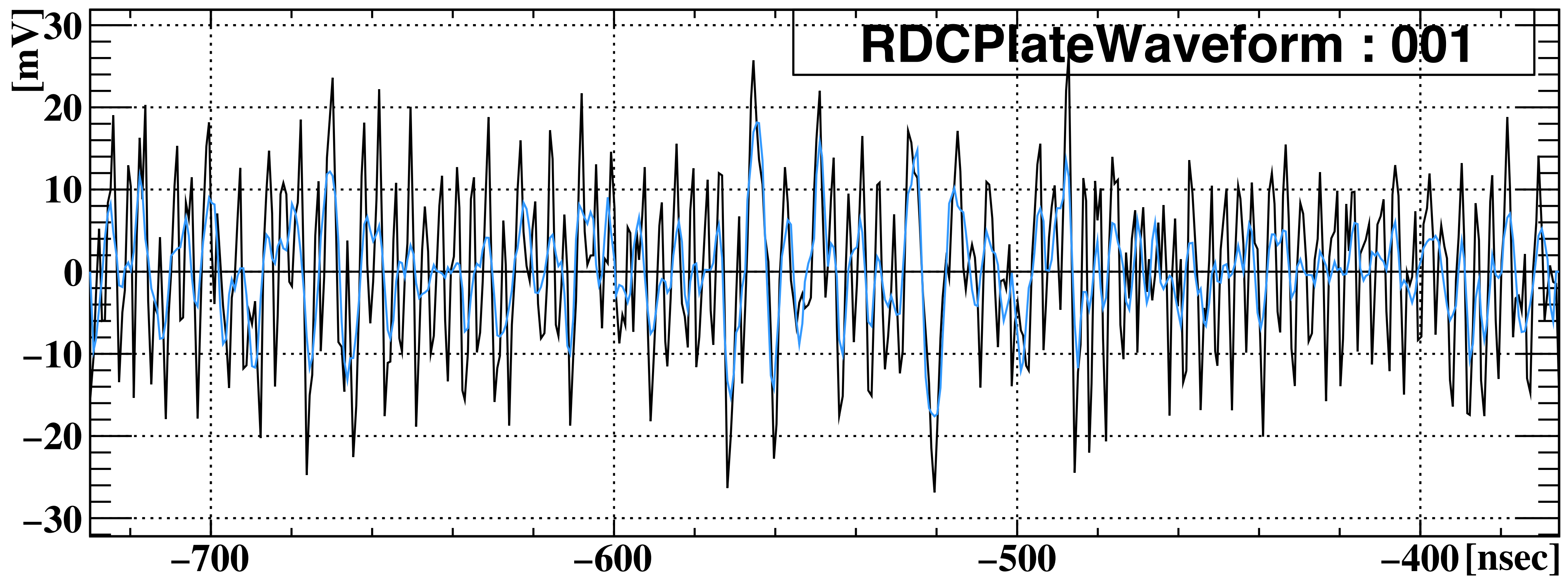

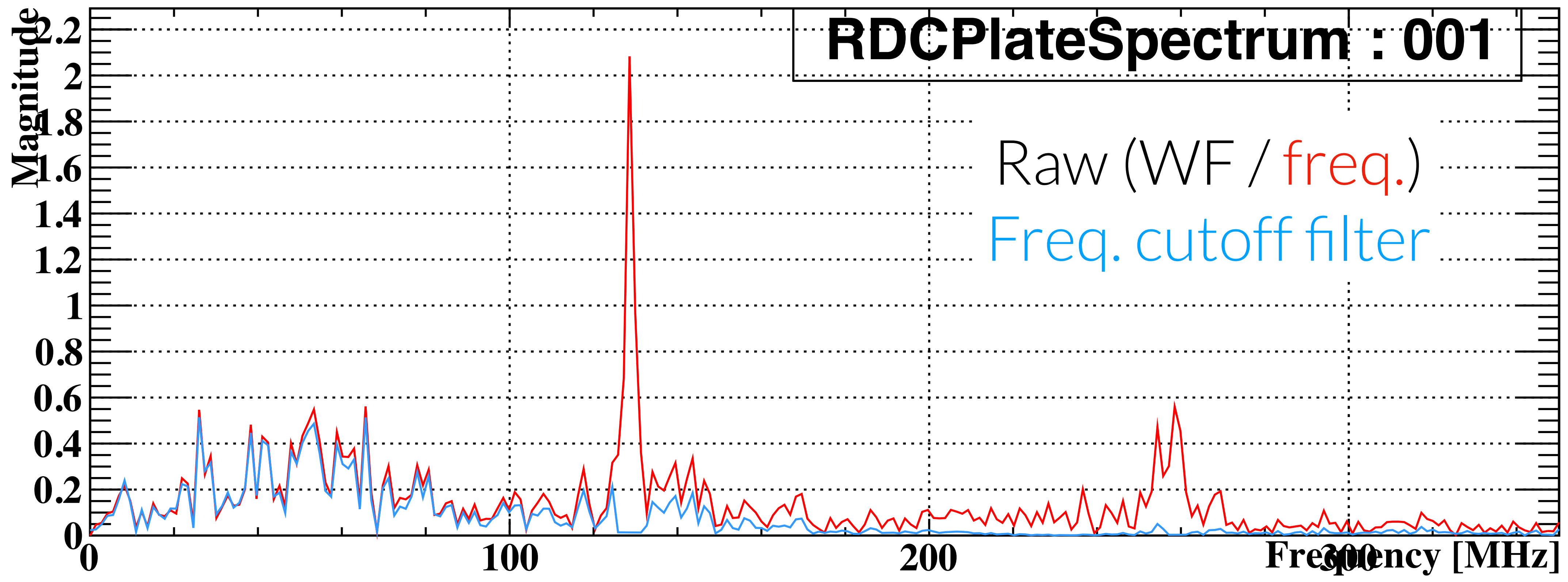

Template waveform fit for LYSO crystals

- Template waveform fit to suppress inefficiency due to pileup pulses

$$\text{Minimise } \Delta V^2 = \sum (V_{\mathrm{fit},i} - V_{\mathrm{raw},i})^2$$

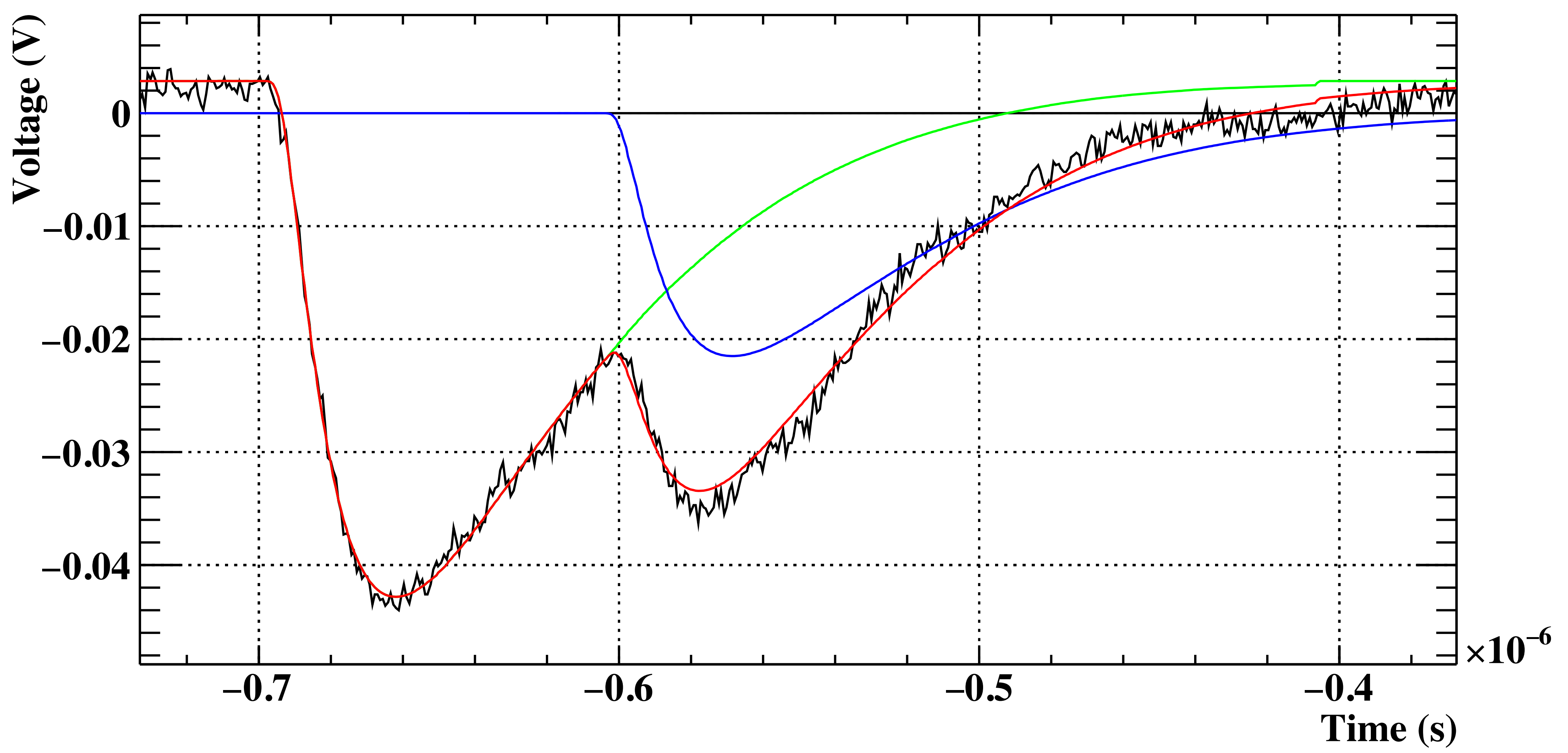

RDC detection efficiency improvement

- Detection efficiency improved by 17%
  - Thanks to offline waveform filter
  - Tagged-RMD fraction improved as well

Hit rate map in plastic scintillators

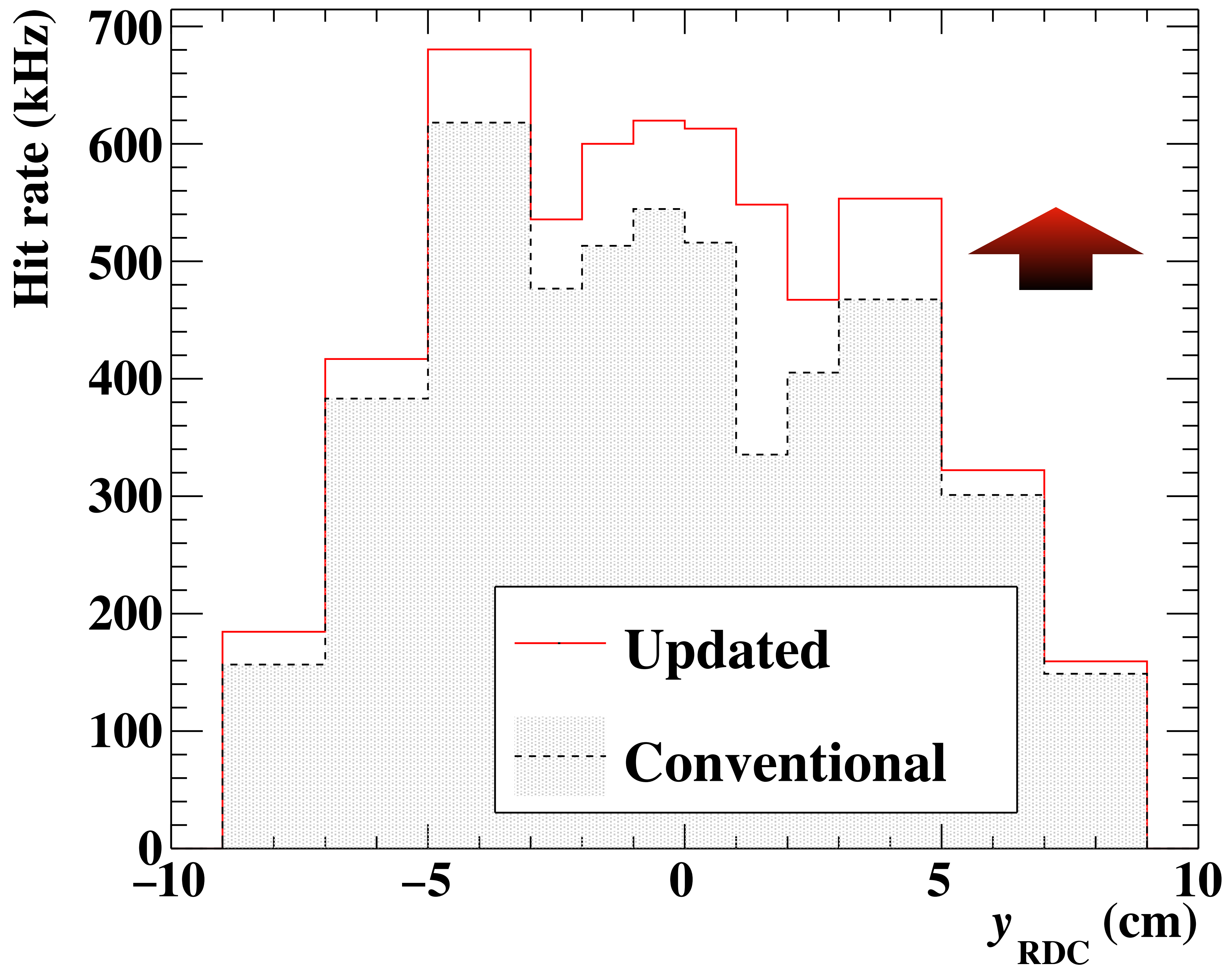

Tagged-RMD fraction as a function of E_γ

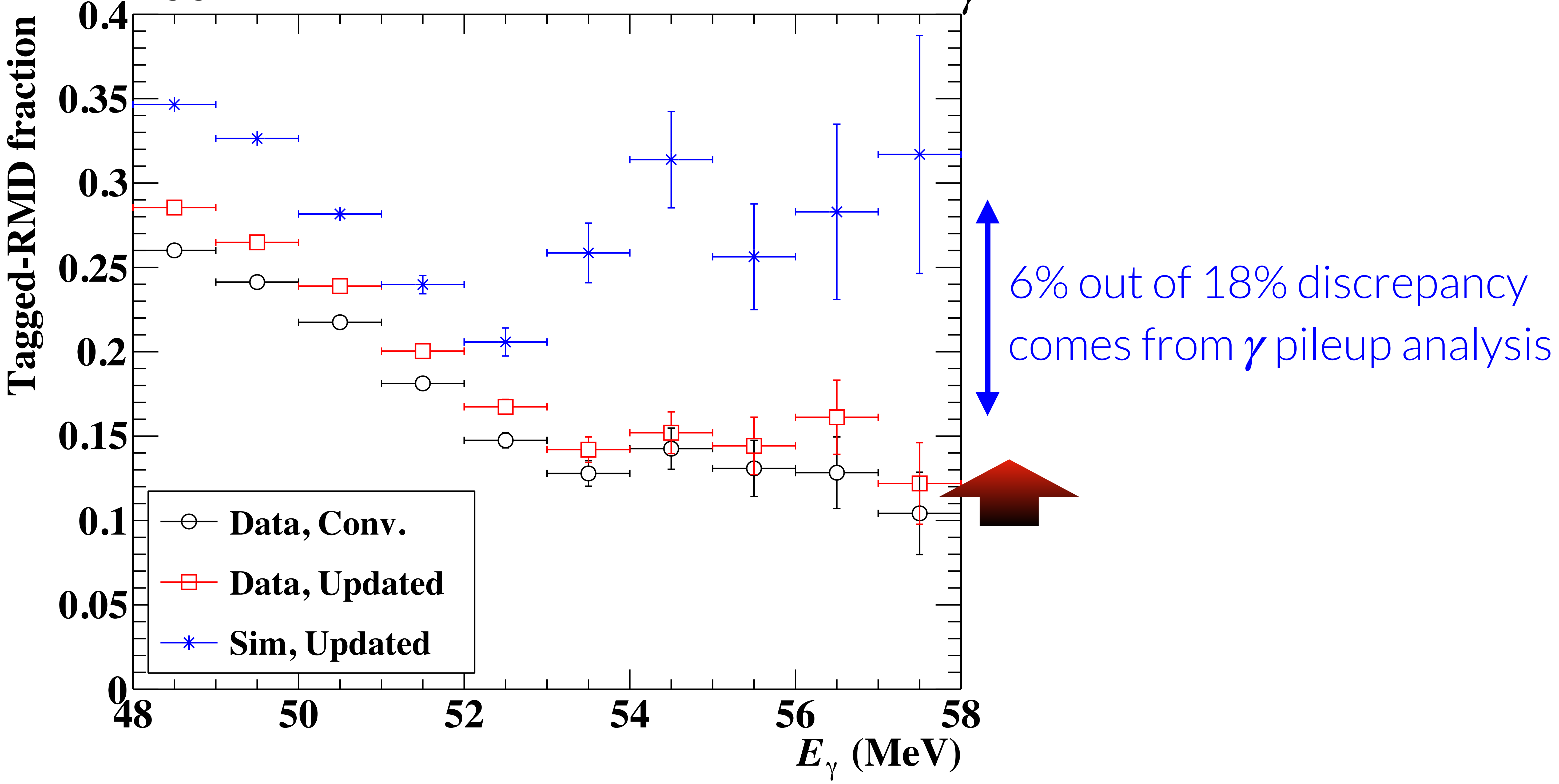

Photosensor calibration in LXe detector

PMT gain

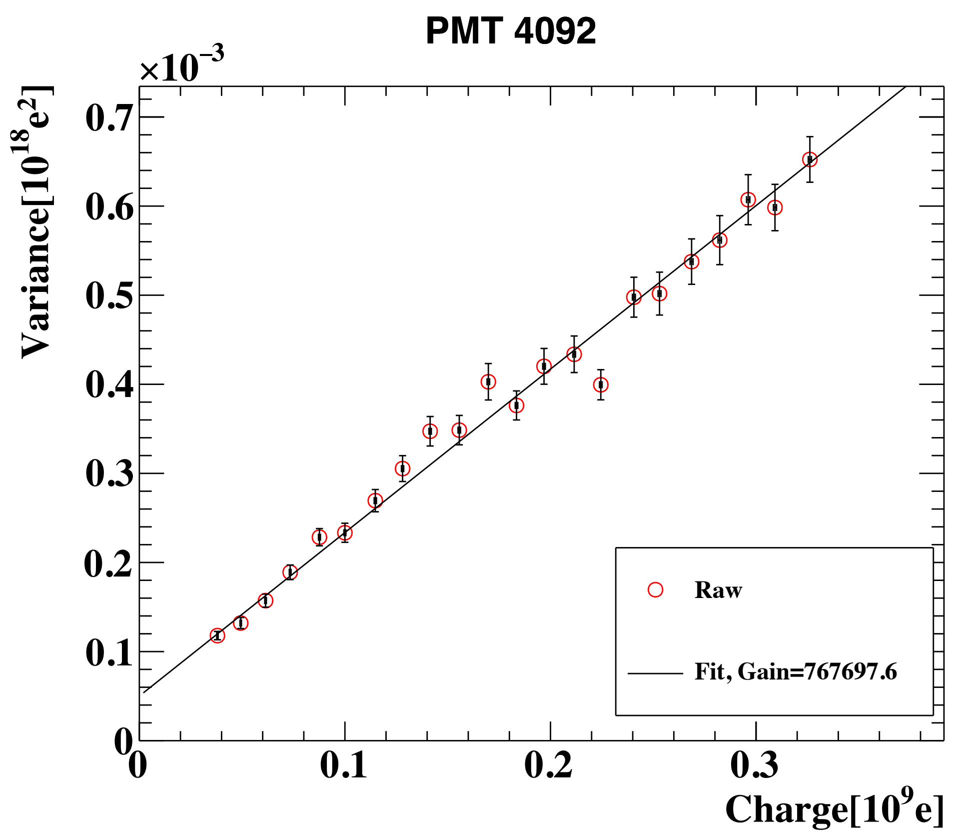

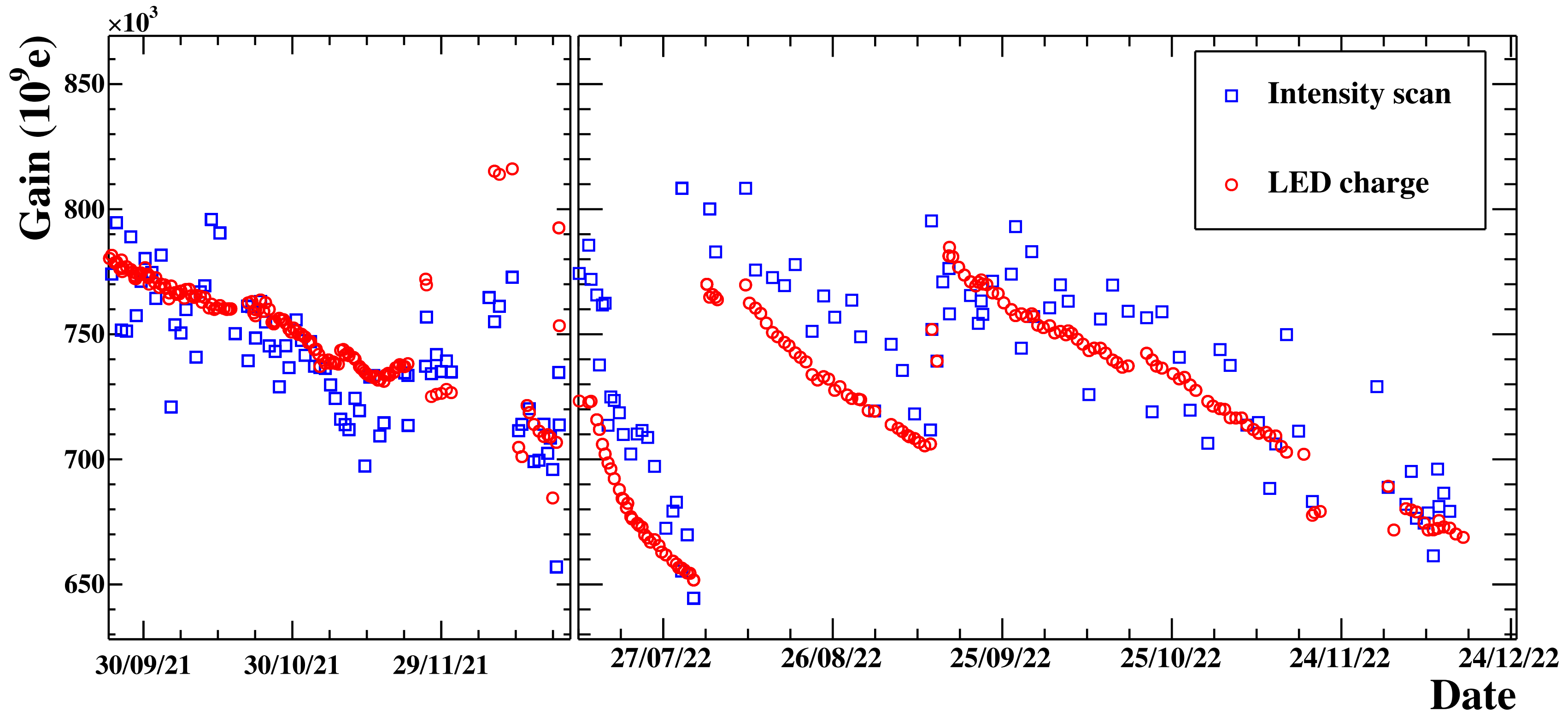

MPPC gain

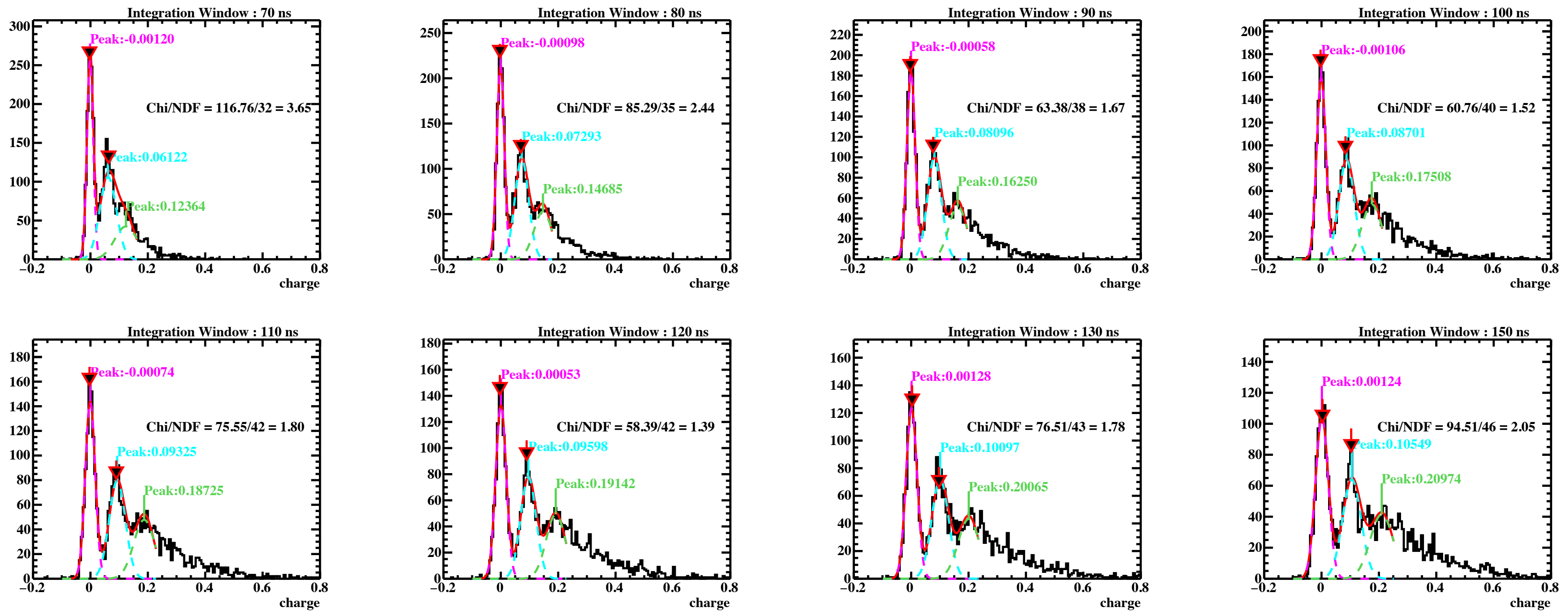

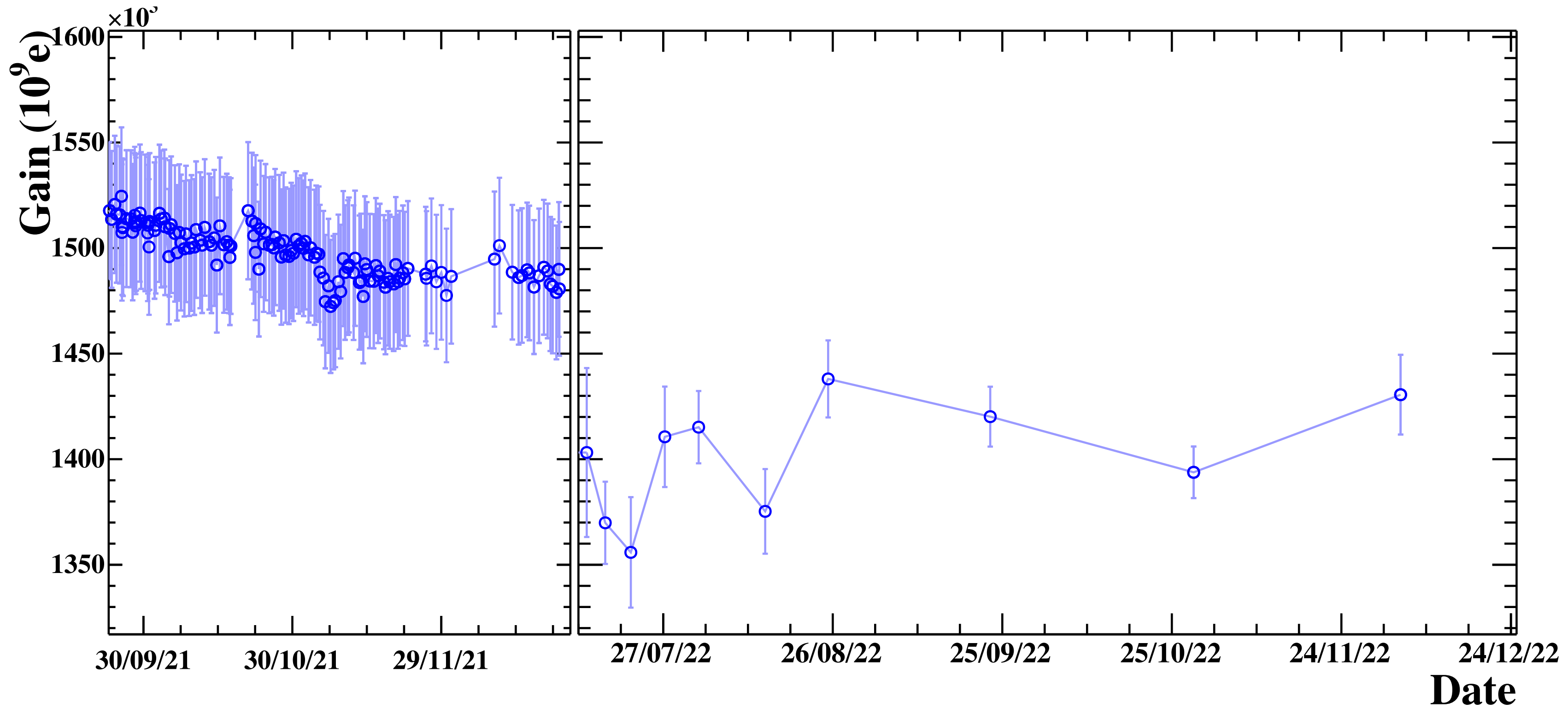

MPPC PDE

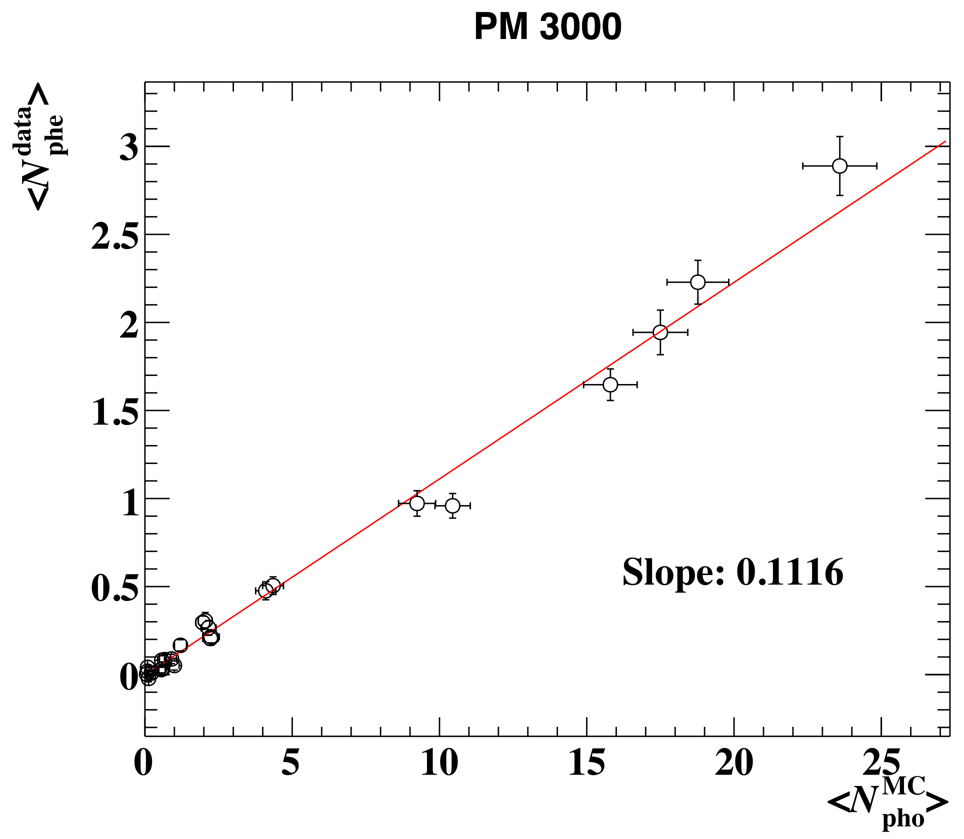

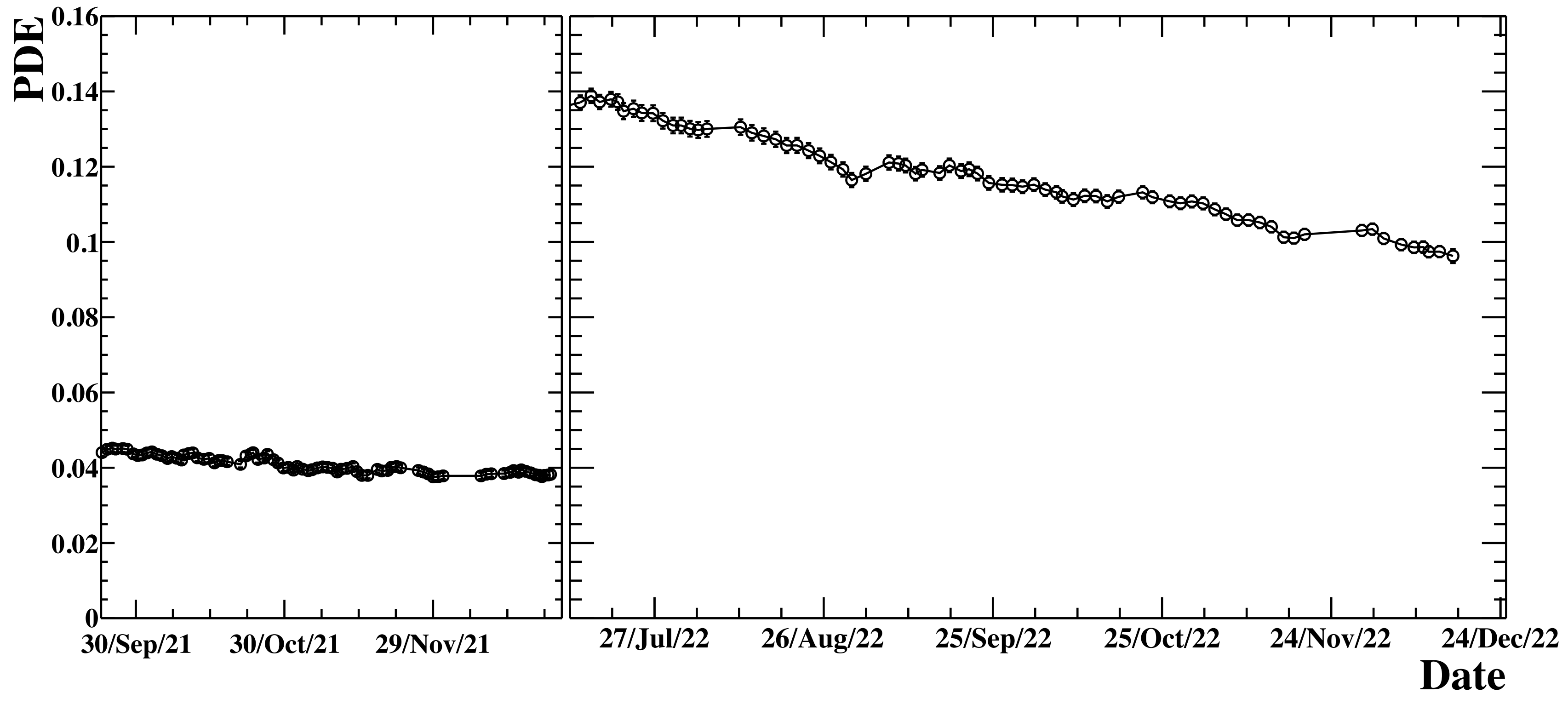

MPPC miscabling

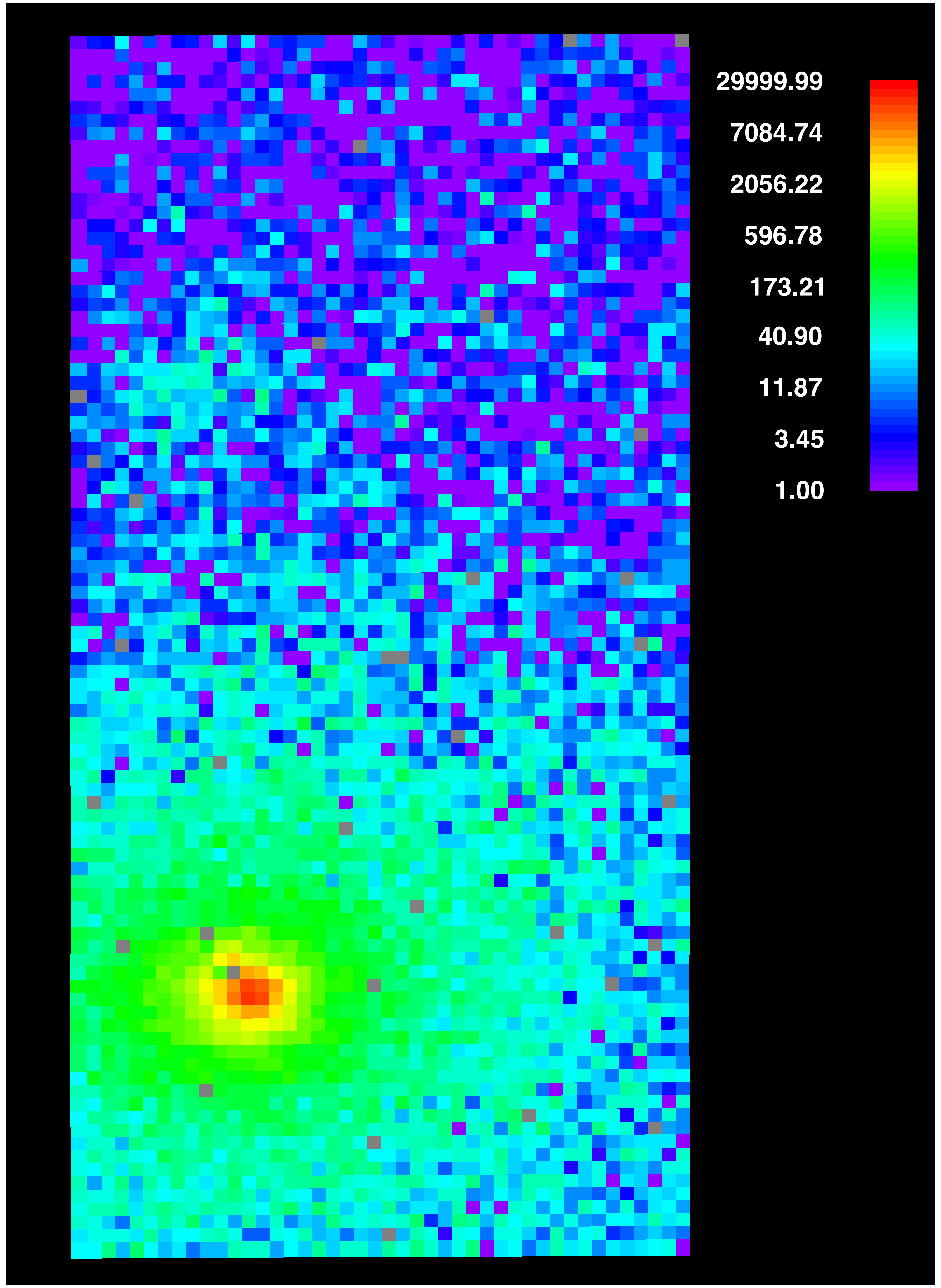

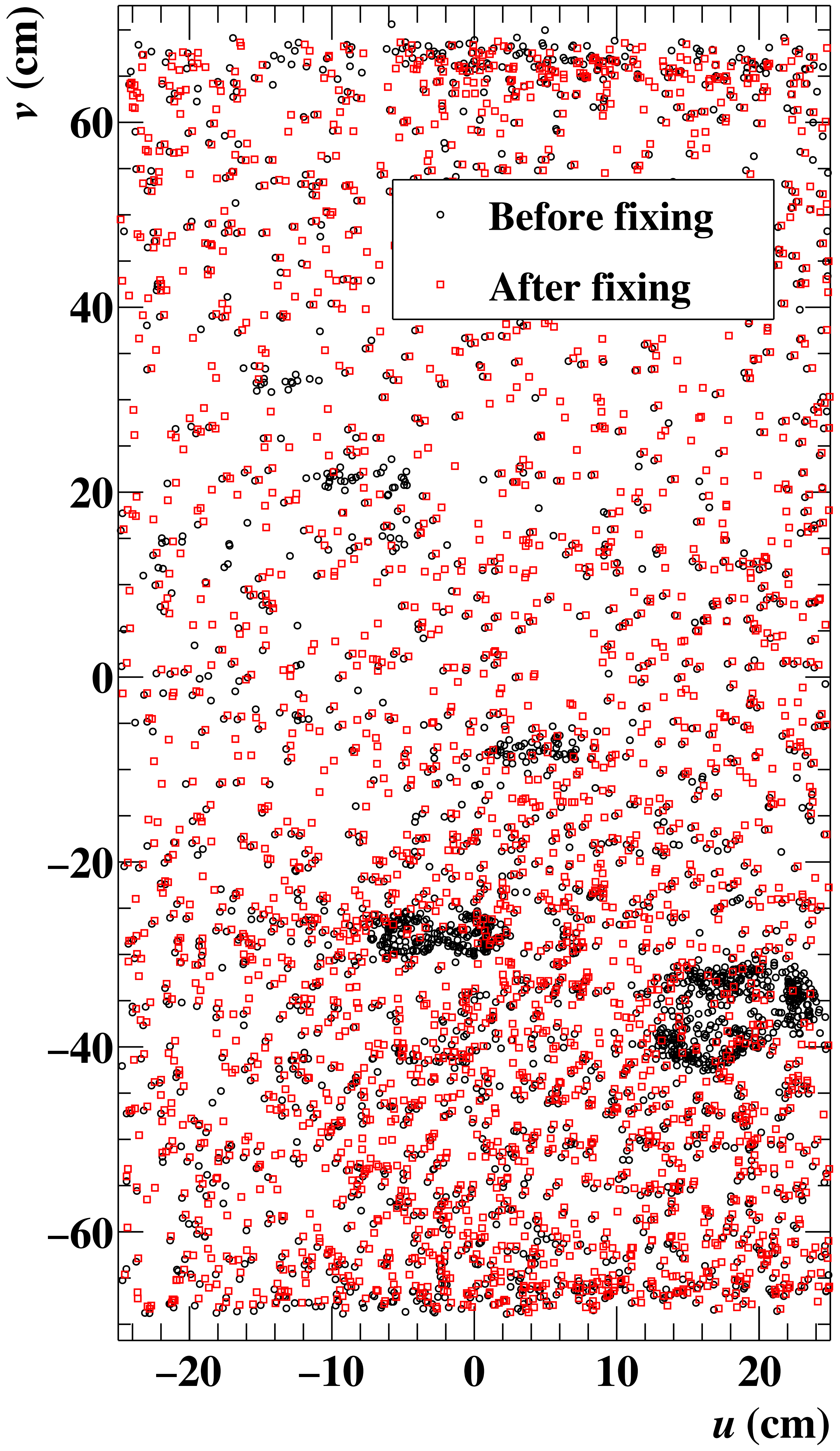

Detector alignment

(a) 2021.

Sub-detector		δx	δy	δz
Magnetic field	Sect. 6.4.2	(100 ± 100) µm	(700 ± 200) µm	(300 ± 100) µm
Muon stopping target	Sect. 6.7.1	(80 ± 100) µm	(860 ± 100) µm	(500 ± 100) µm
LXe detector	Sect. 6.7.2	No evaluation	No evaluation	(540 ± 410) µm

(b) 2022.

Sub-detector		δx	δy	δz
Magnetic field	Sect. 6.4.2	(100 ± 100) µm	(700 ± 200) µm	(300 ± 100) µm
Muon stopping target	Sect. 6.7.1	(80 ± 35) µm	(240 ± 35) µm	(570 ± 100) µm
LXe detector	Sect. 6.7.2	No evaluation	No evaluation	(560 ± 290) µm

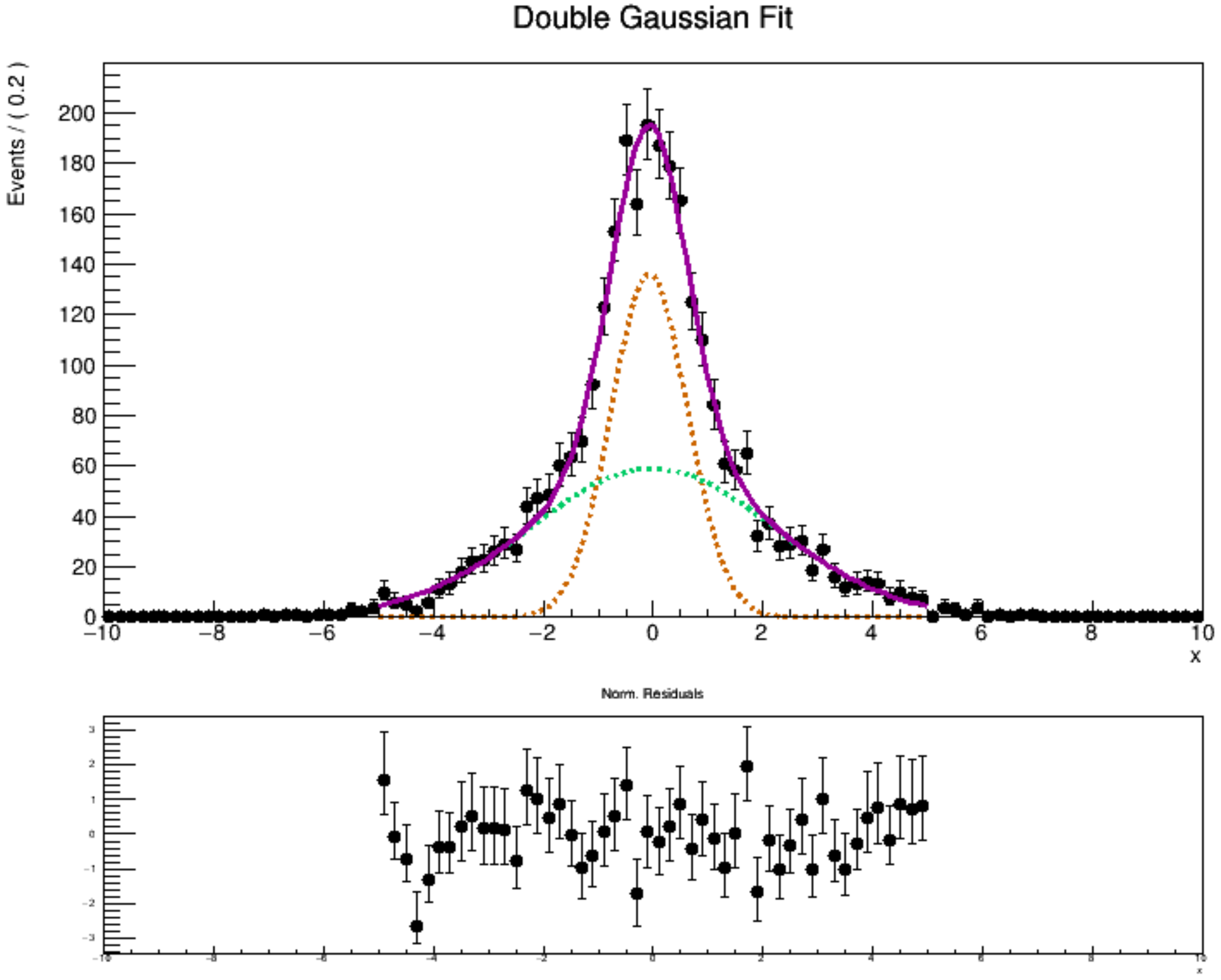

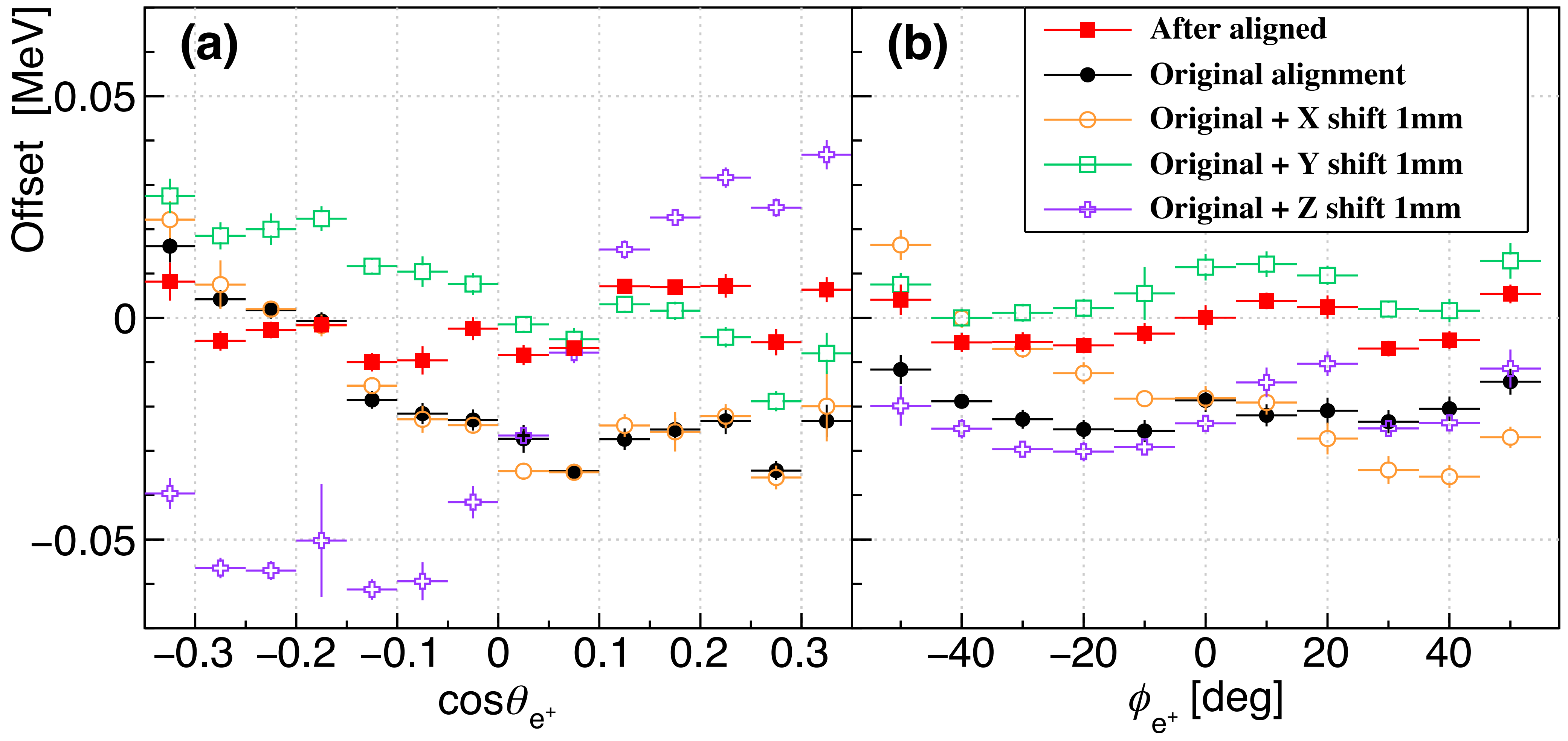

$t_{e\gamma}$ offset calibration

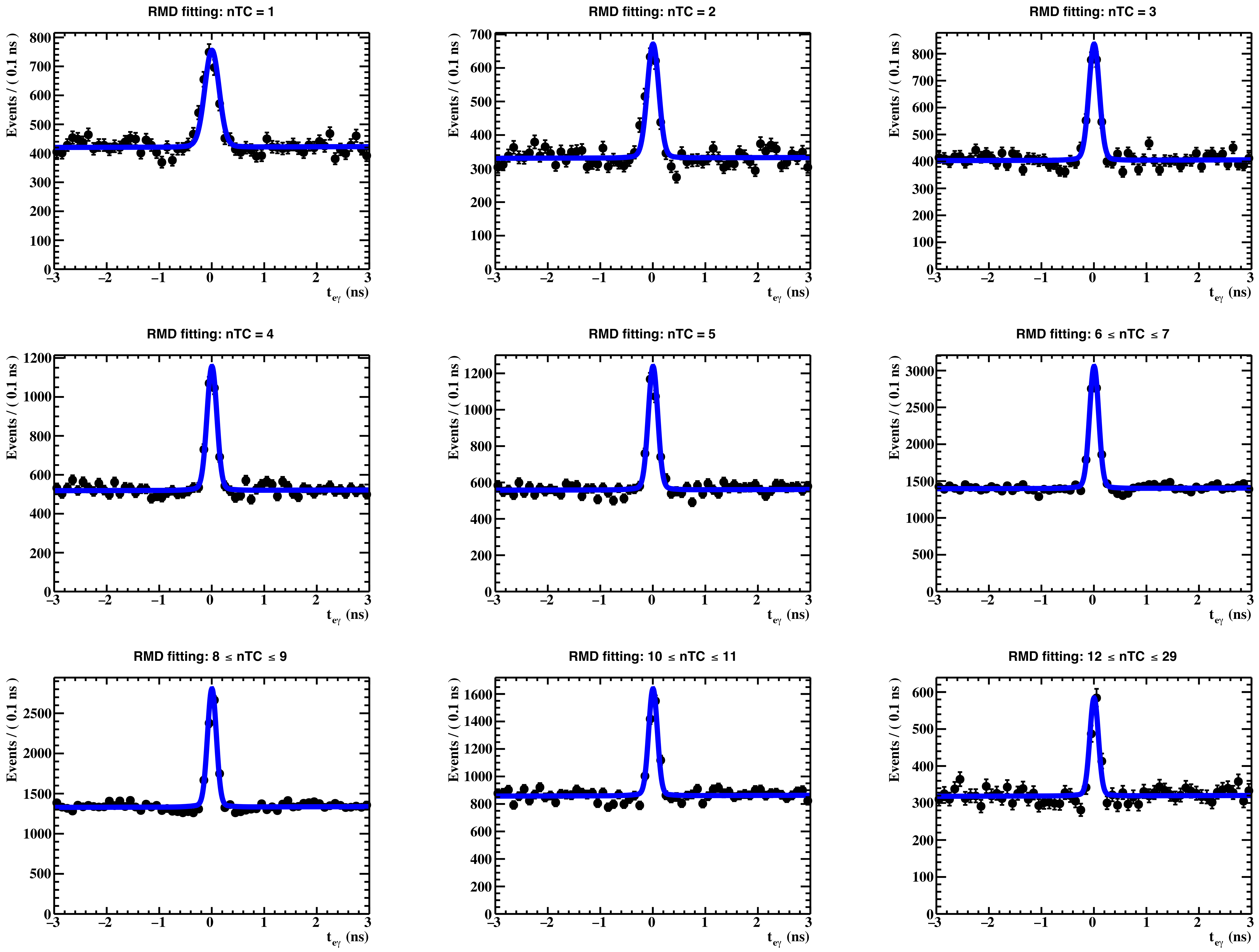

MPPC non-linearity

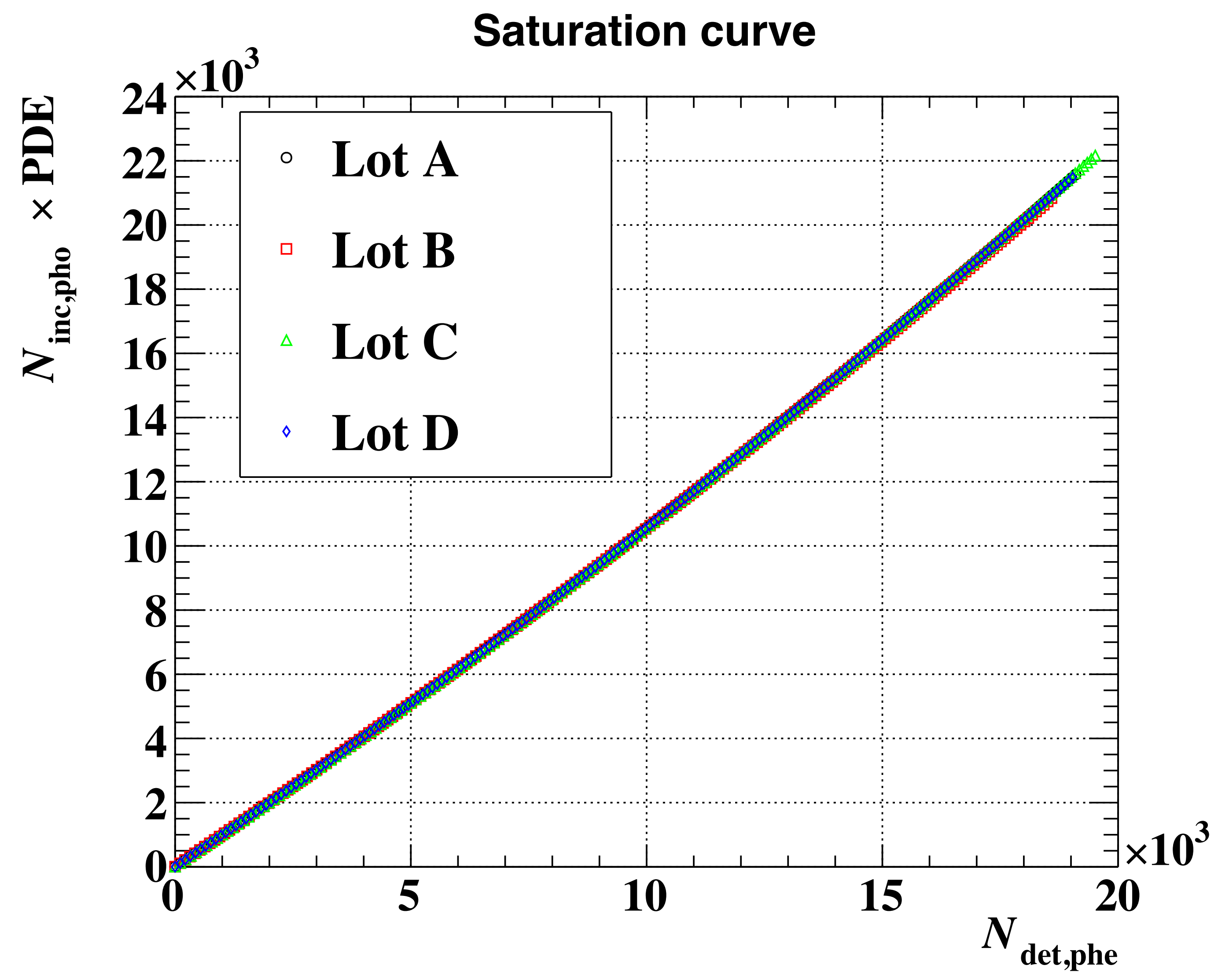

55 MeV in 2021

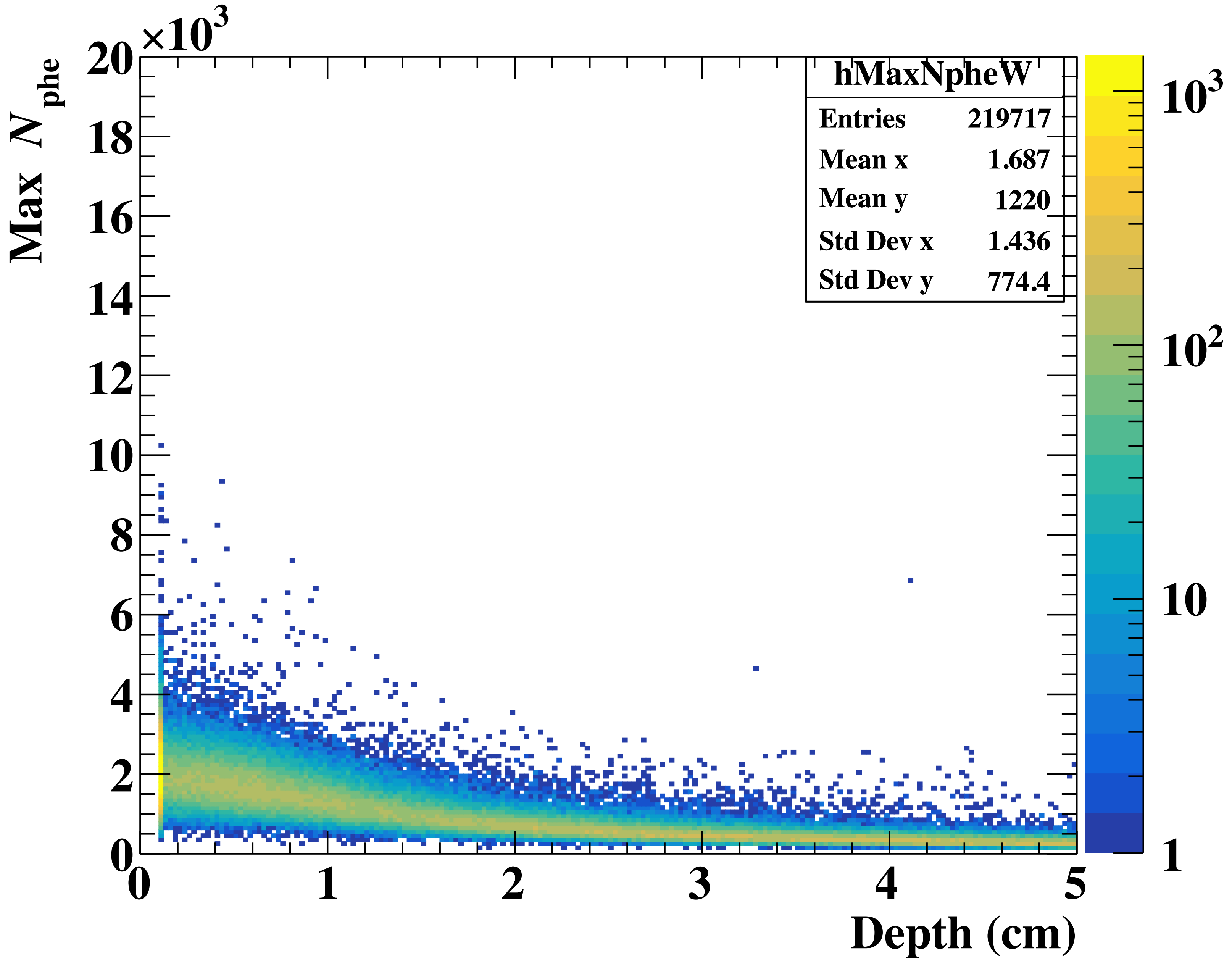

55 MeV in 2022

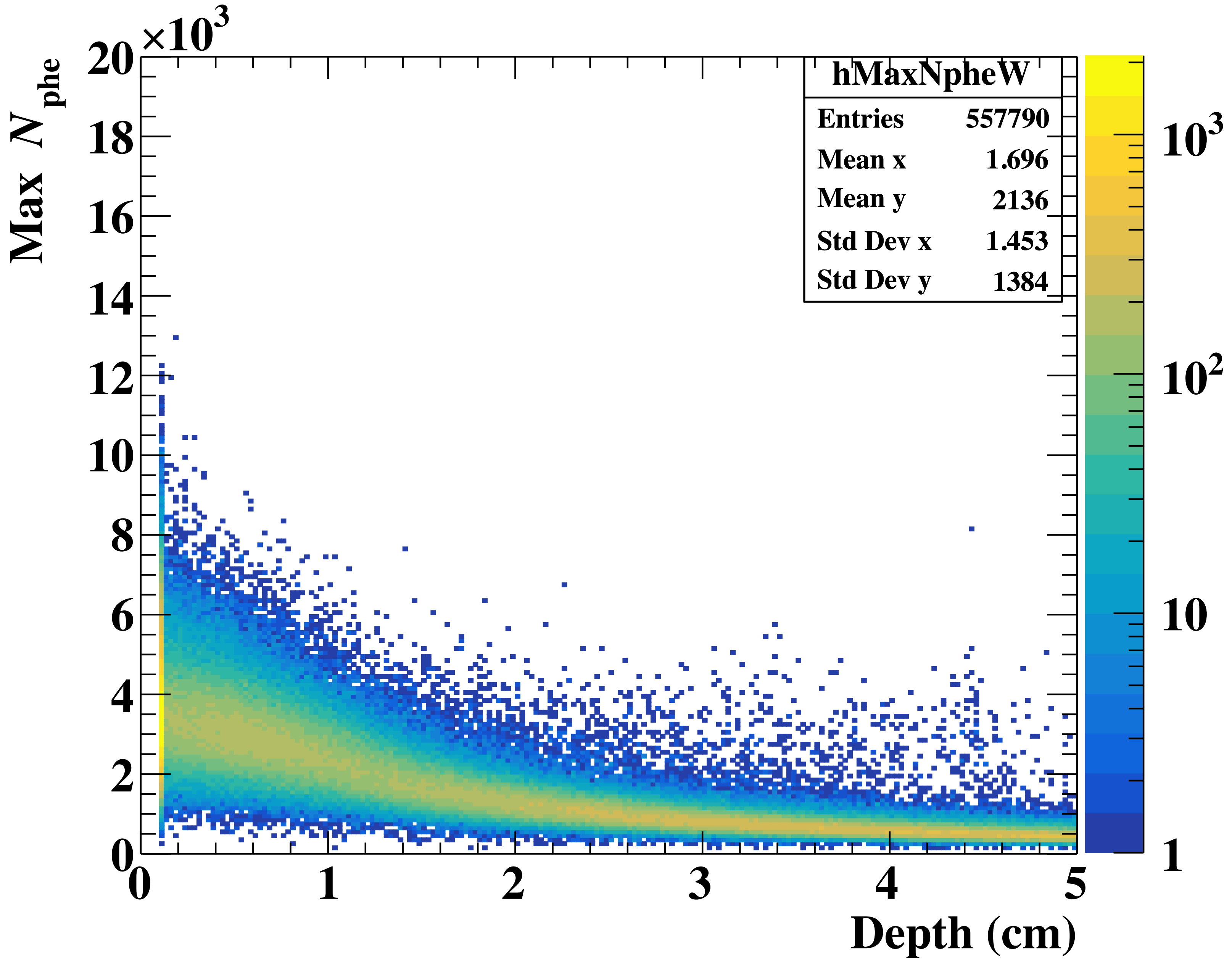

Signal γ MC in past study

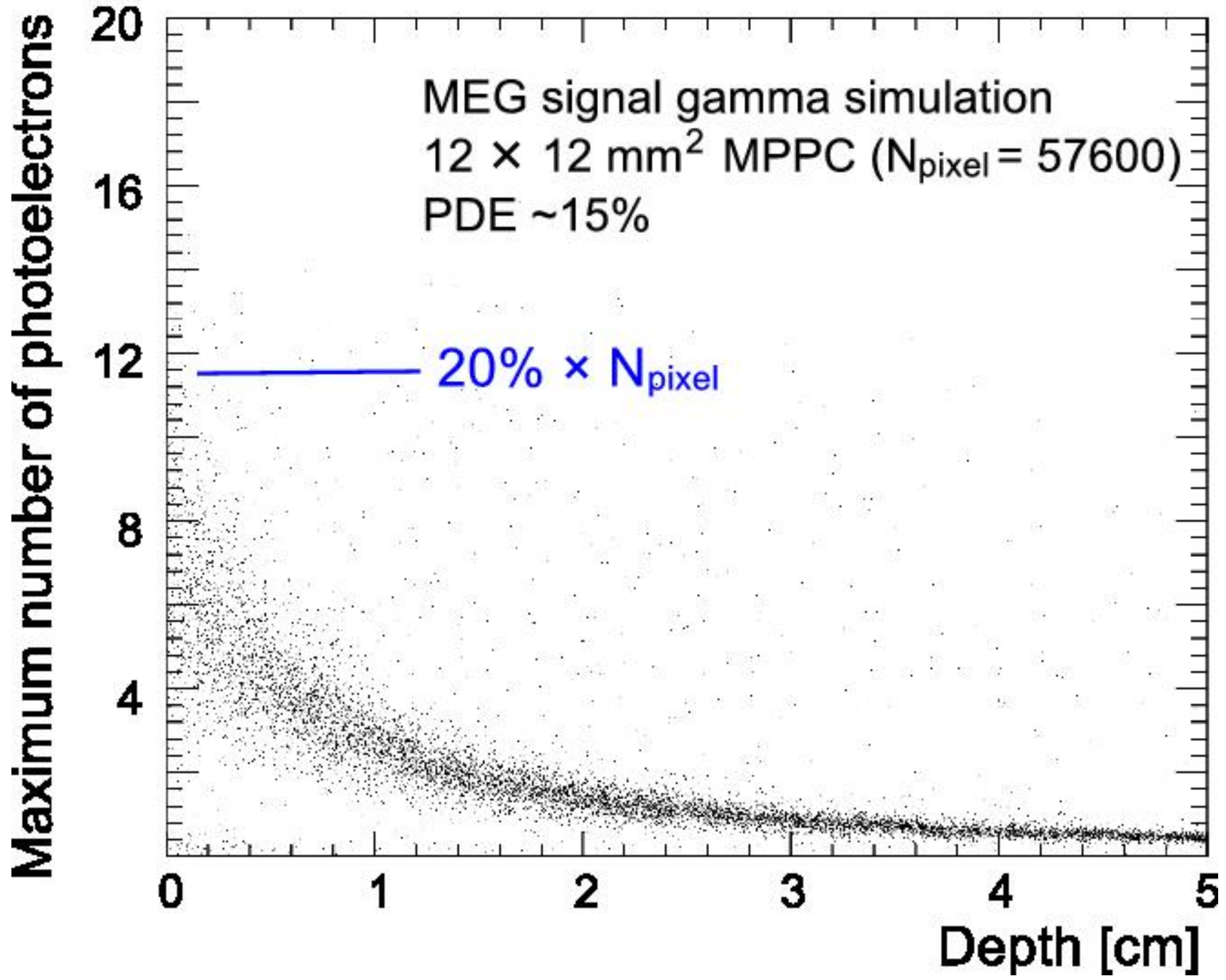

Analysis strategy

- Blind analysis
  - To prevent any biases in the analysis
  - Blind box fully covers analysis window

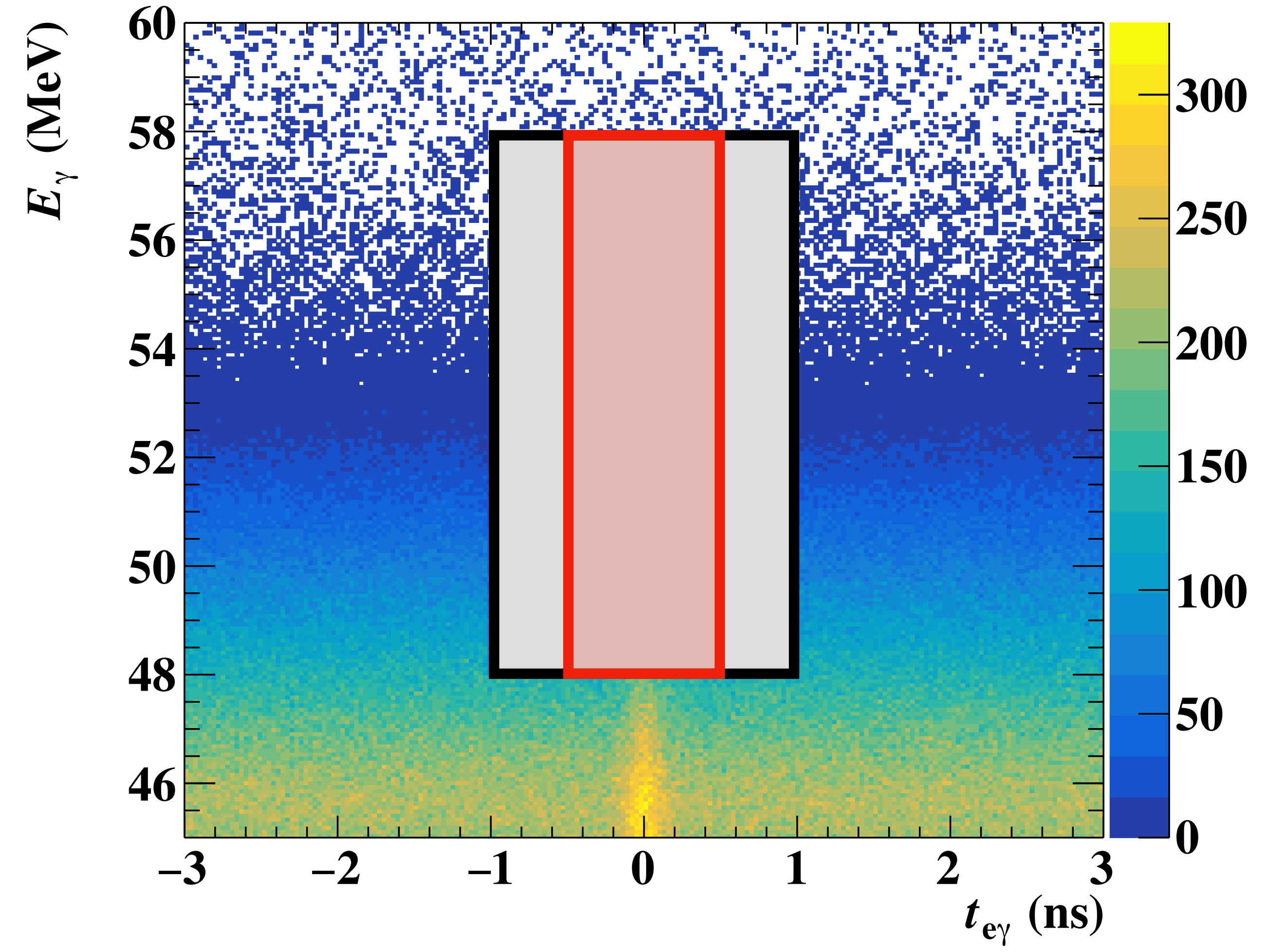

Analysis window

- 48 MeV < E_γ < 58 MeV
- 52.2 MeV < E_e < 53.5 MeV
- $|t_{e\gamma}|$ < 0.5 ns
- $|\theta_{e\gamma}|$ < 40 mrad
- $|\phi_{e\gamma}|$ < 40 mrad

- Maximum likelihood analysis estimates the number of signal events N_{sig}
- N_{sig} converted to $\mathcal{B}(\mu \to e\gamma)$ by number of effectively measured muons k

$$\mathcal{B}(\mu \to e\gamma) = \frac{N_{\mathrm{sig}}}{k}$$

- Confidence interval calculated by the Feldman-Cousins approach with profile-likelihood ordering
  - N_{sig} 90% C.L. upper (lower) limit normalised to $\mathcal{B}$ 90% C.L. upper (lower) limit

Maximum likelihood fit to estimate N_{sig}

What we want to estimate

Nuisance parameters

$$\mathcal{L}(N_{\mathrm{sig}}, N_{\mathrm{RMD}}, N_{\mathrm{ACC}}, X_{\mathrm{T}}) = \exp\left[-\frac{X_{\mathrm{T}}^2}{2\sigma_{\mathrm{T}}^2}\right]$$

Profiling for angle PDF uncertainty

$$\times \exp\left[-\frac{(N_{\mathrm{RMD}} - \langle N_{\mathrm{RMD}}\rangle)^2}{2\sigma_{\mathrm{RMD}}^2}\right] \times \exp\left[-\frac{(N_{\mathrm{ACC}} - \langle N_{\mathrm{ACC}}\rangle)^2}{2\sigma_{\mathrm{ACC}}^2}\right]$$

Gaussian constraints

$$\times \frac{e^{-N}}{N_{\mathrm{obs}}!}\prod_{i=1}^{N_{\mathrm{obs}}}\left[N_{\mathrm{sig}}S(\vec{x}_i) + N_{\mathrm{RMD}}R(\vec{x}_i) + N_{\mathrm{ACC}}A(\vec{x}_i)\right]$$

Extended likelihood

PDFs $S(\vec{x}_i), R(\vec{x}_i), A(\vec{x}_i)$

- Event-by-event PDFs to account for some dependences on resolutions

Observables $\vec{x}_i$

- E_γ
- $t_{e\gamma}$
- $\theta_{e\gamma}$
- $t_{\mathrm{RDC}-\gamma}$
- E_e
- n_{pTC}
- $\phi_{e\gamma}$
- E_{RDC}

Side-bands and background estimation

- Side-bands defined to study background
- $\langle N_{\mathrm{ACC}} \rangle$ and $\langle N_{\mathrm{RMD}} \rangle$ estimated with side-bands

Count events in time side-bands
→ $\langle N_{\mathrm{ACC}} \rangle$ = 364 ± 9.54

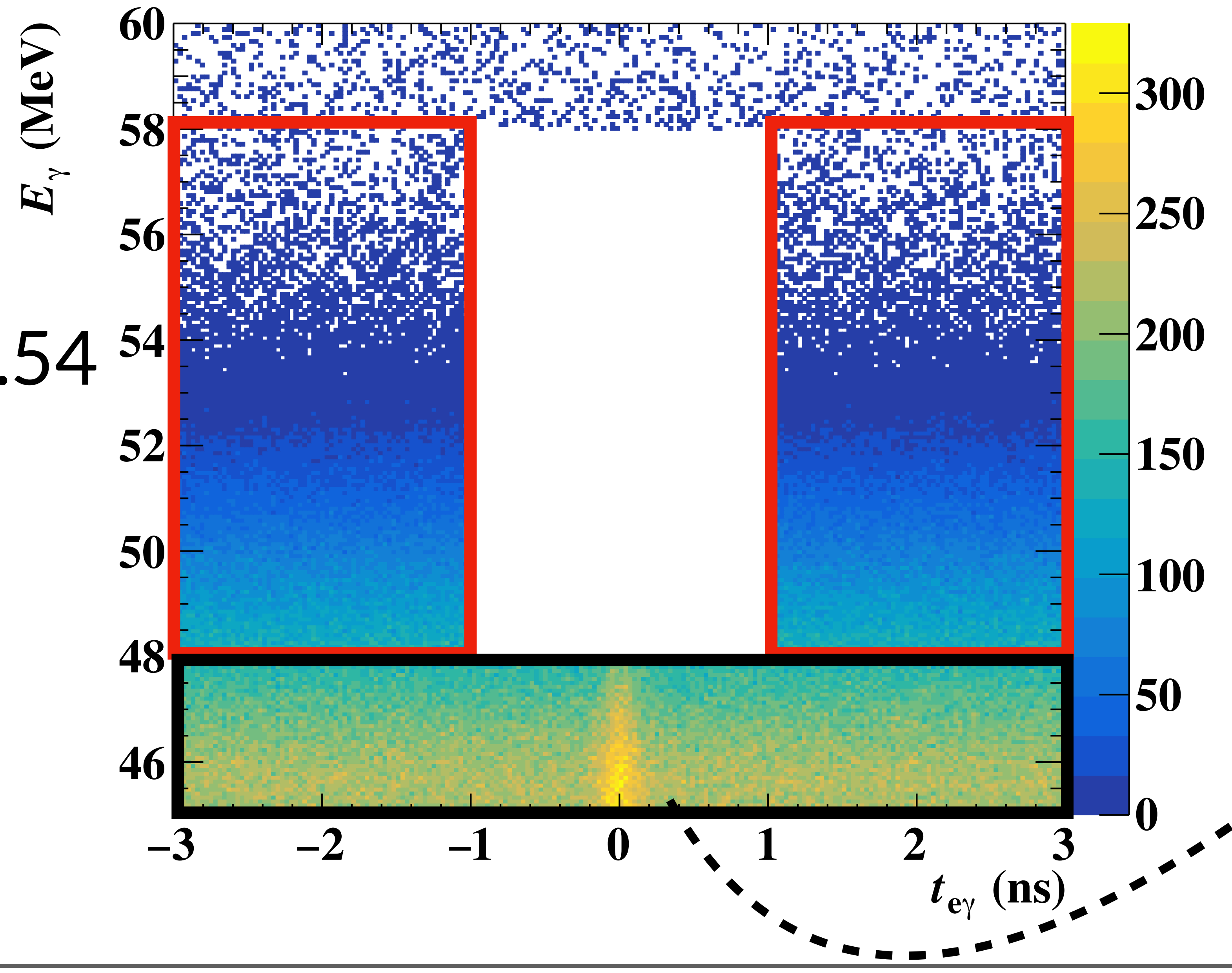

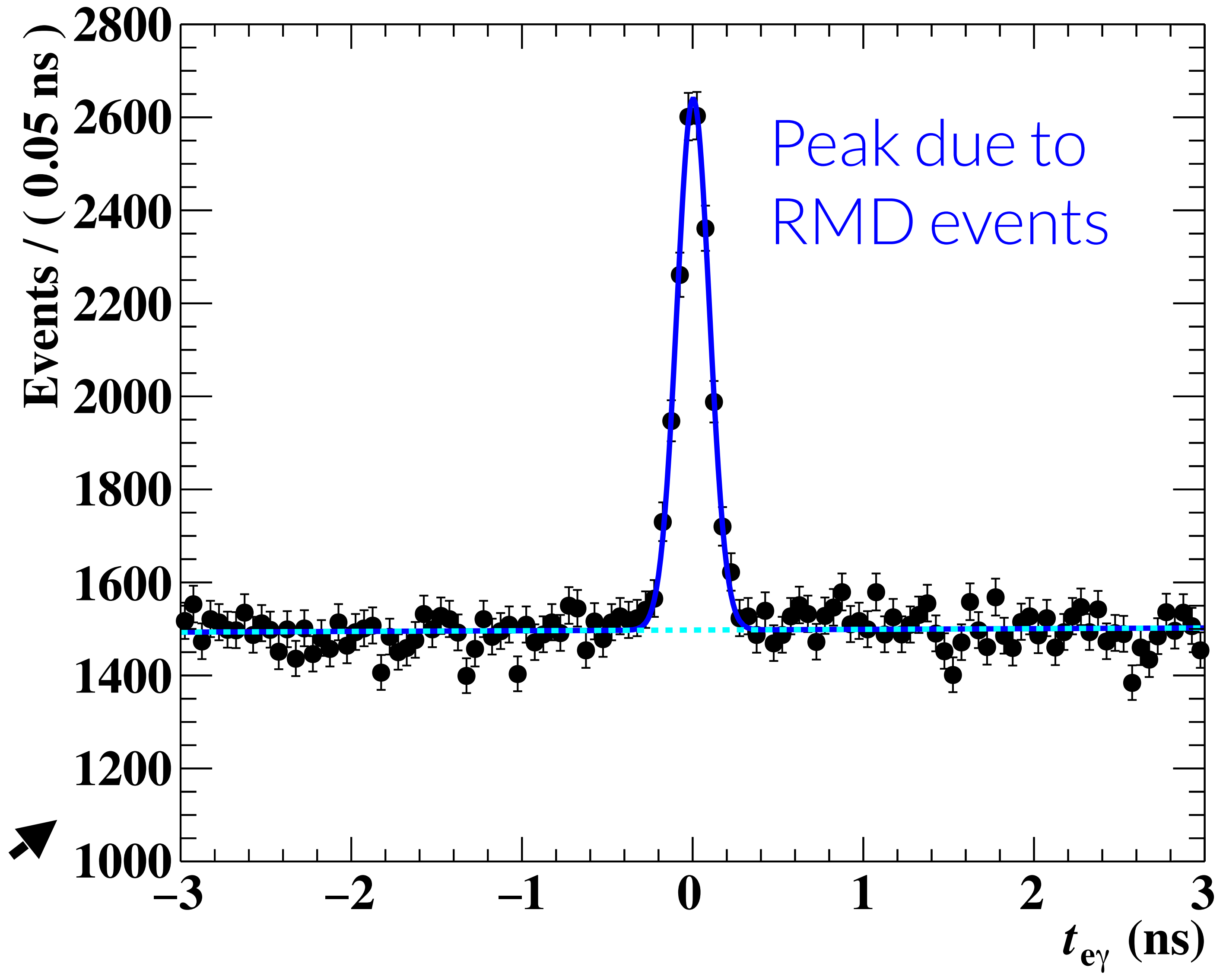

Count on-peak events in energy side-band and extrapolate it
→ $\langle N_{\mathrm{RMD}} \rangle$ = 10.1 ± 1.7

E_γ resolution uniformity

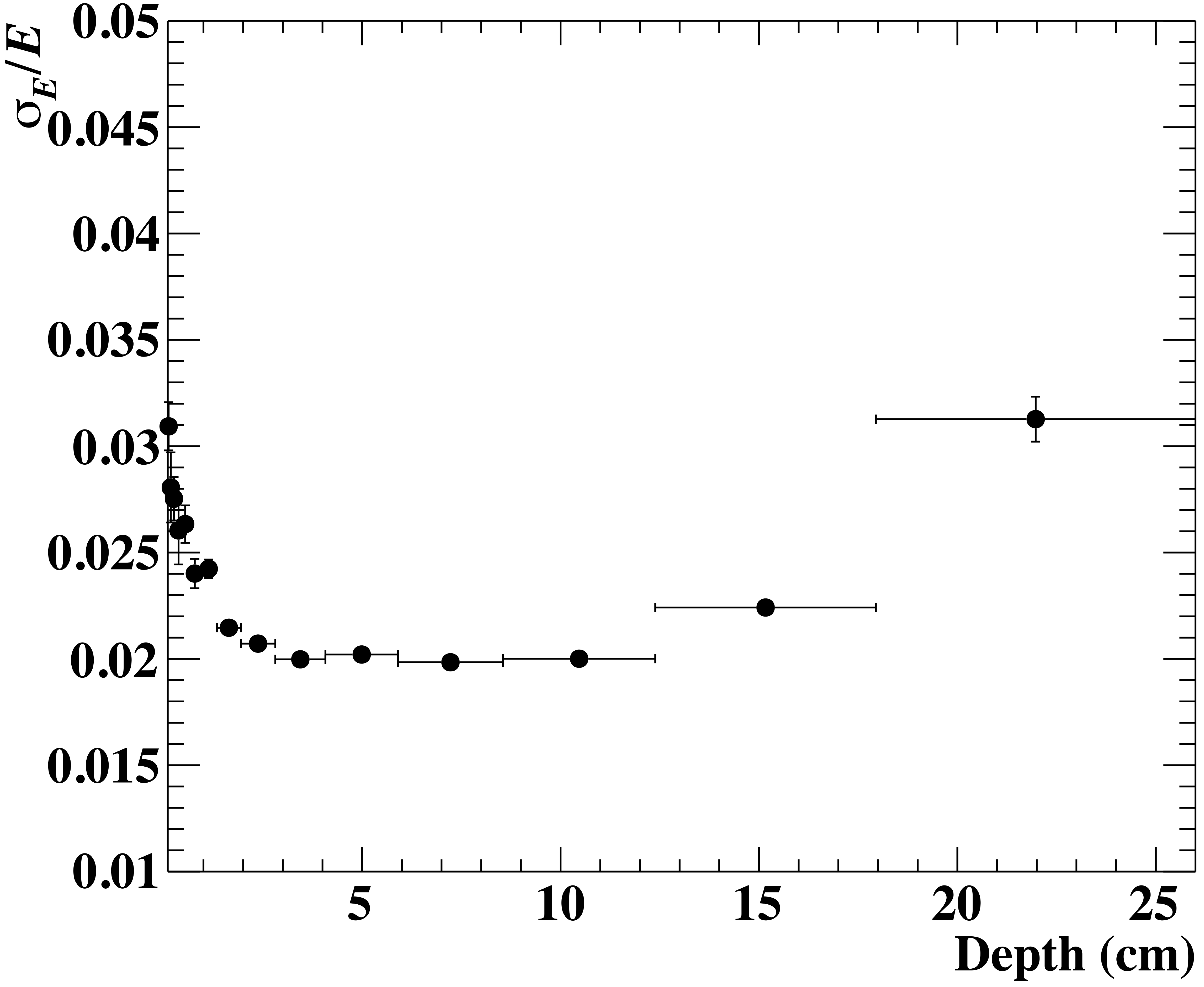

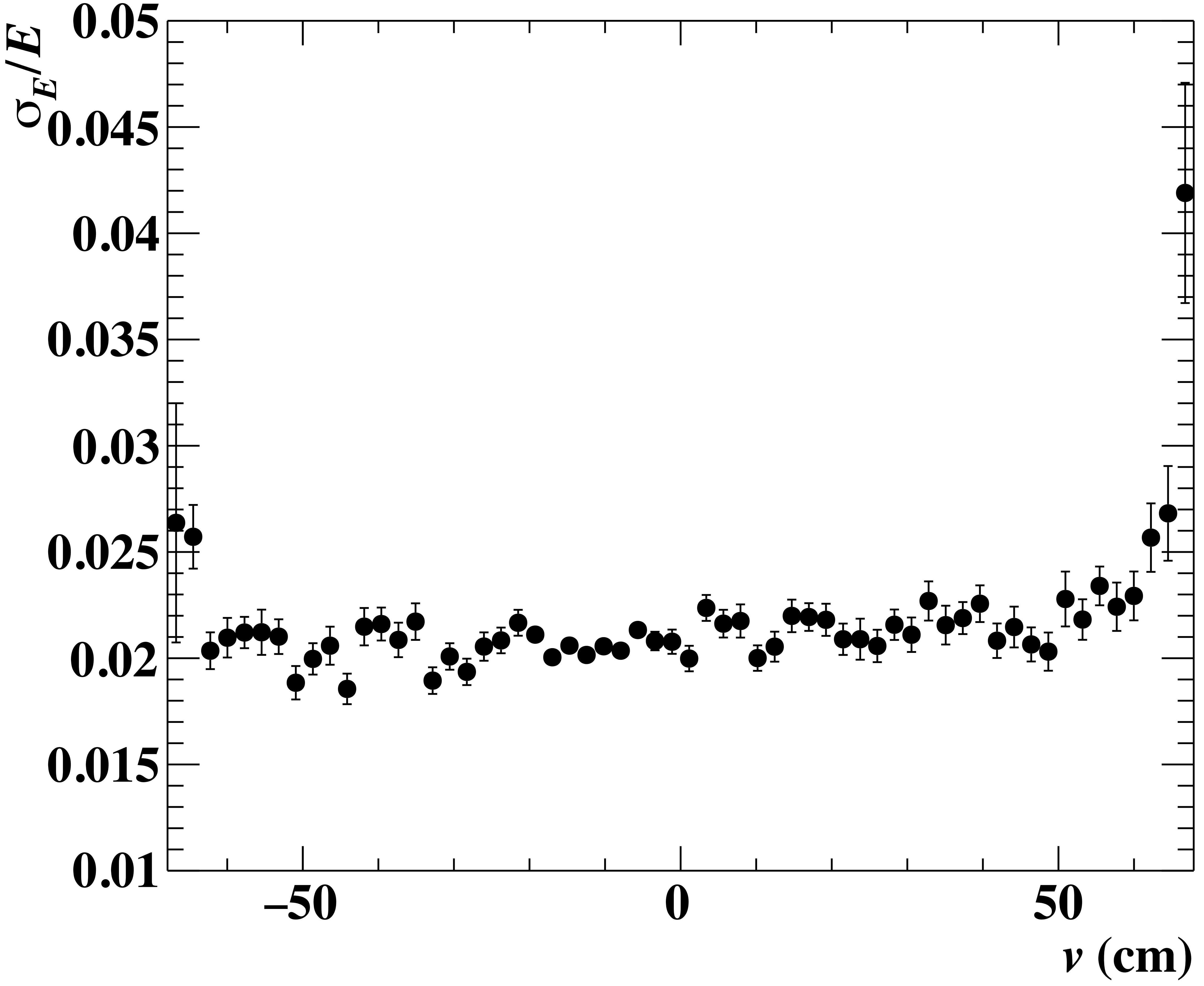

$t_{e\gamma}$ PDFs

- Signal PDF based on
  - $t_{e\gamma}$ peak originating from $\mu \to e\nu\bar{\nu}\gamma$ events
  - Number of pTC hits n_{pTC}

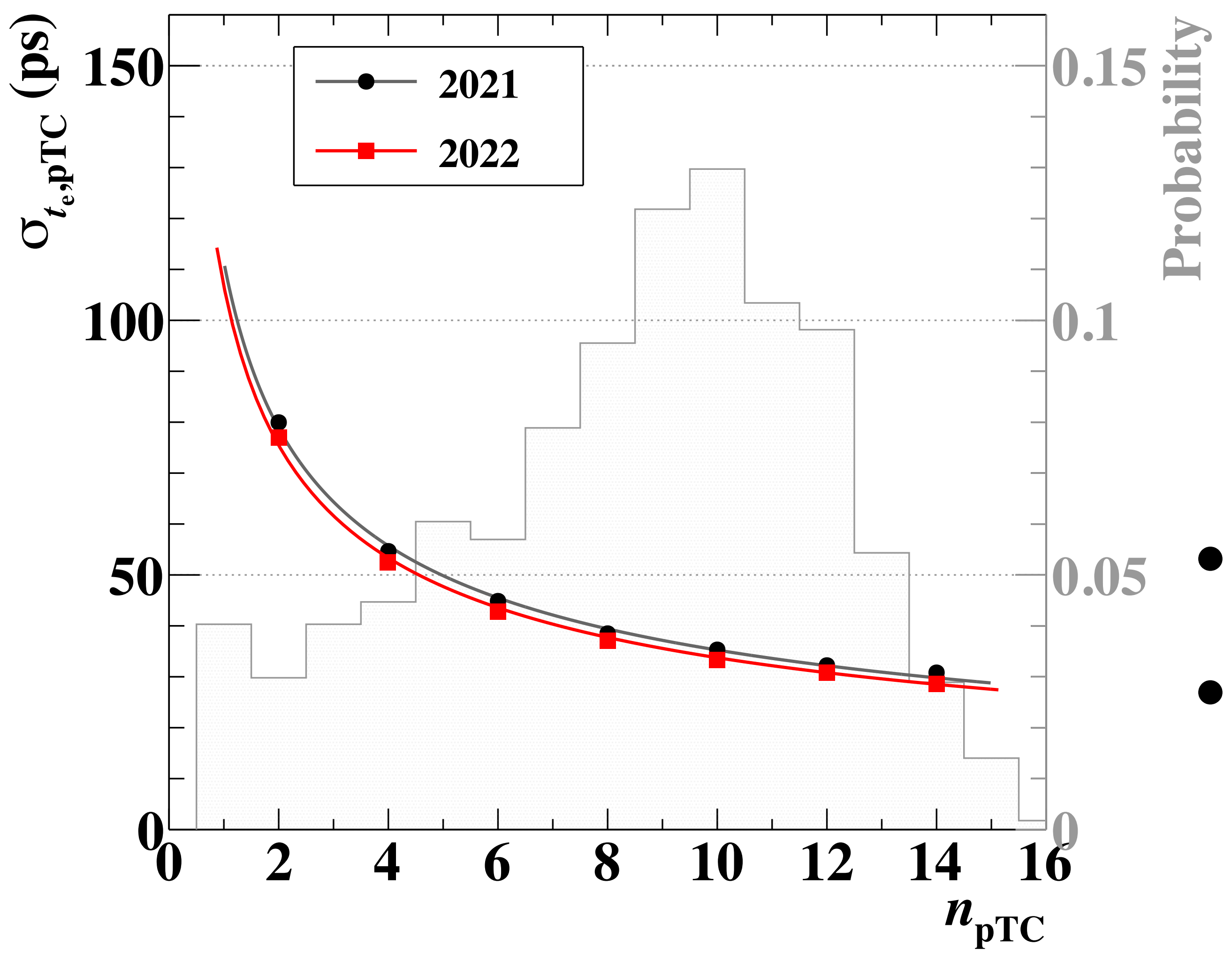

$$\sigma_{\mathrm{const}} \oplus \frac{\sigma_{\mathrm{single}}}{\sqrt{n_{\mathrm{pTC}}}}$$

- σ_{const}: Dominated by t_γ resolution (65 ps)
- σ_{single}: pTC single counter resolution (110 ps)

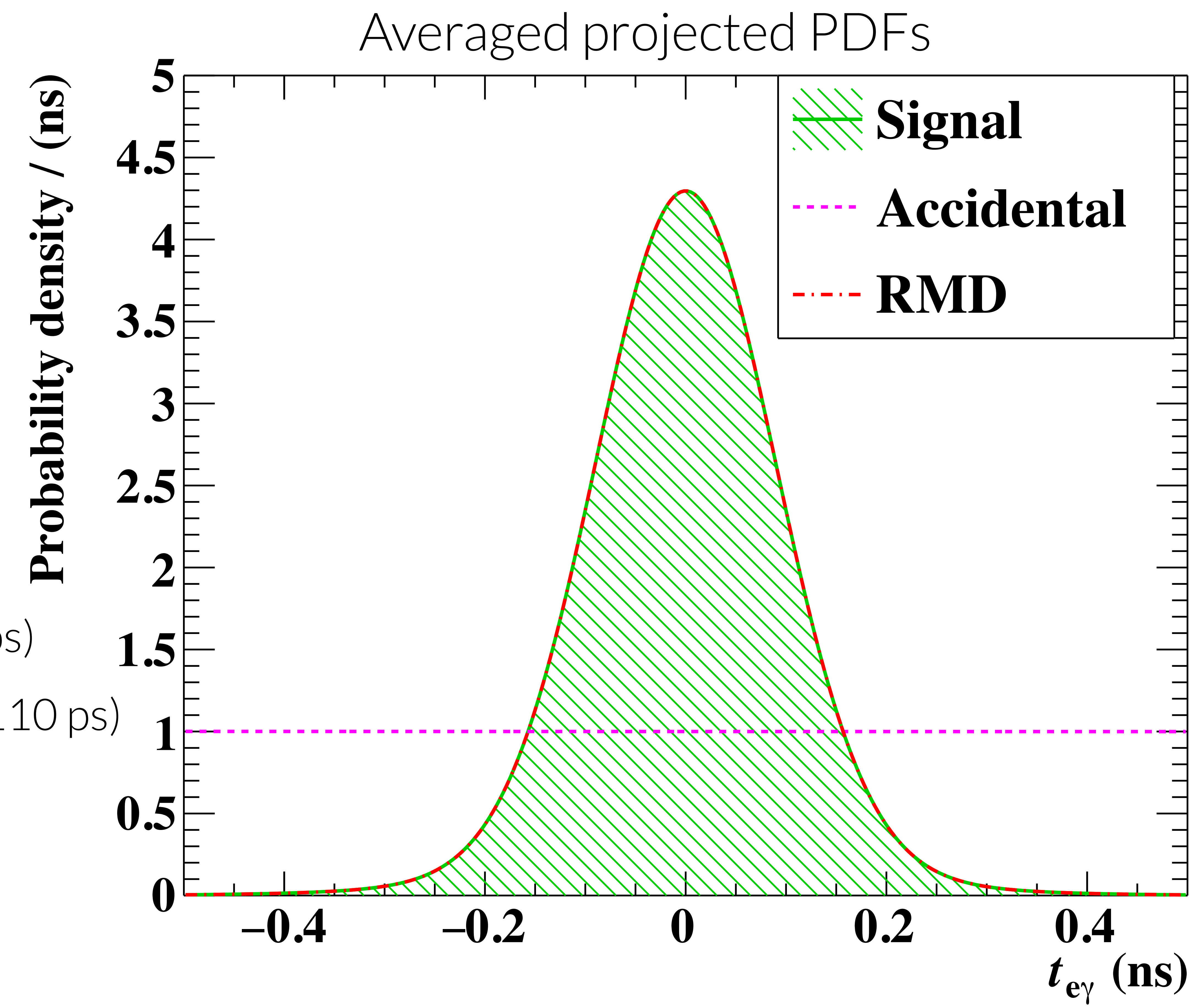

- Accidental BG PDF
  - Flat

Angle PDFs

$$\theta_{e\gamma} = (\pi - \theta_e) - \theta_\gamma$$
$$\phi_{e\gamma} = (\pi + \phi_e) - \phi_\gamma$$

- Signal PDFs parametrised by the combination of
  - **Positron angle & vertexing resolutions**

$\sigma_{y_{\mathrm{e}}}$ (mm)	$\sigma_{z_{\mathrm{e}}}$ (mm)	$\sigma_{\theta_{\mathrm{e}}}$ (mrad)	$\sigma_{\phi_{\mathrm{e}}}$ (mrad)
0.61	1.76	5.2	6.2

  - **Photon position resolution**
    - 2.5-4 mm depending on conversion depth
- $\theta_{e\gamma}$ vs $\phi_{e\gamma}$ correlation taken into account
- The largest systematics: **Detector alignment**
  - Profiling approach adopted
- Accidental PDFs extracted from time side-bands

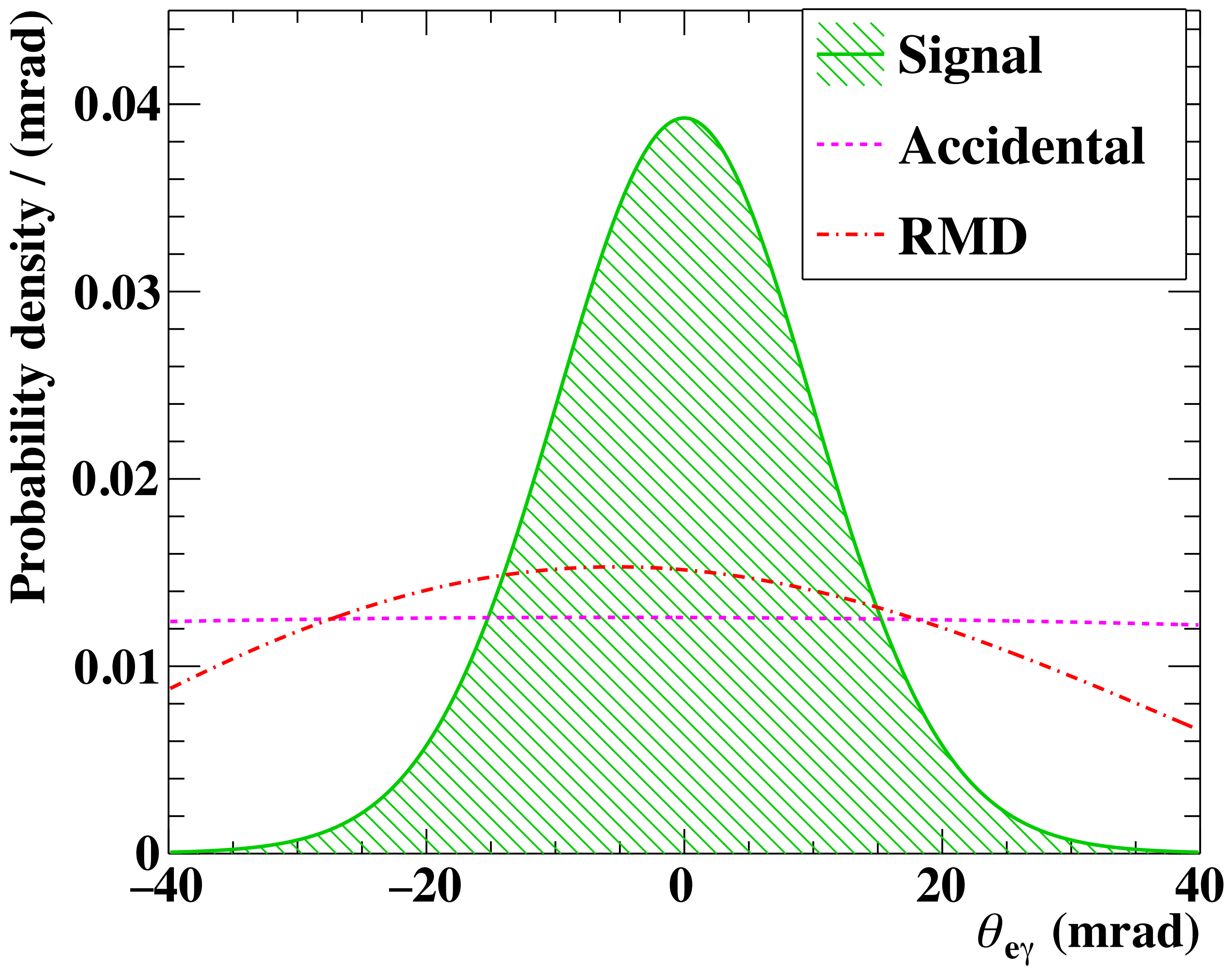

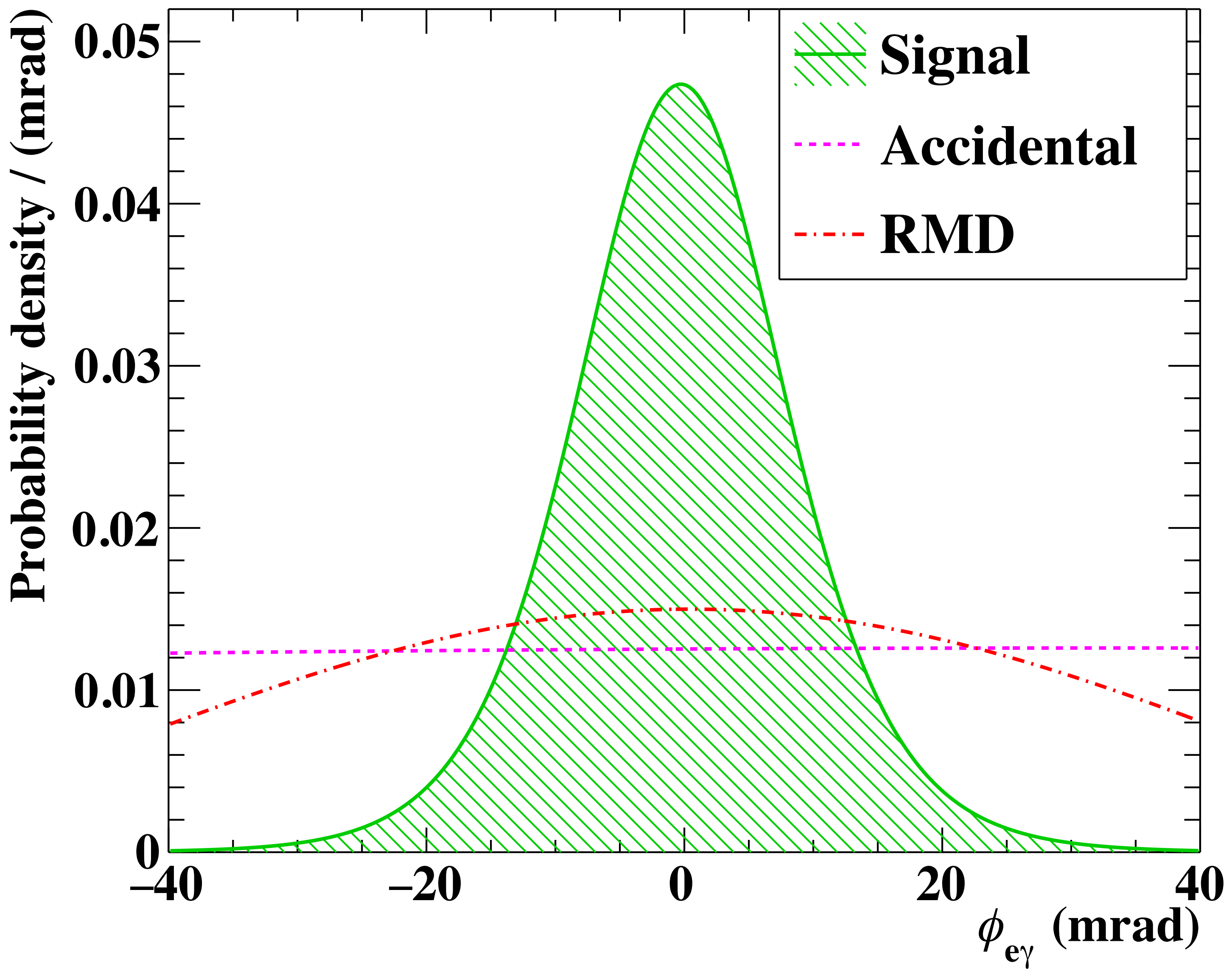

Combined angle resolutions

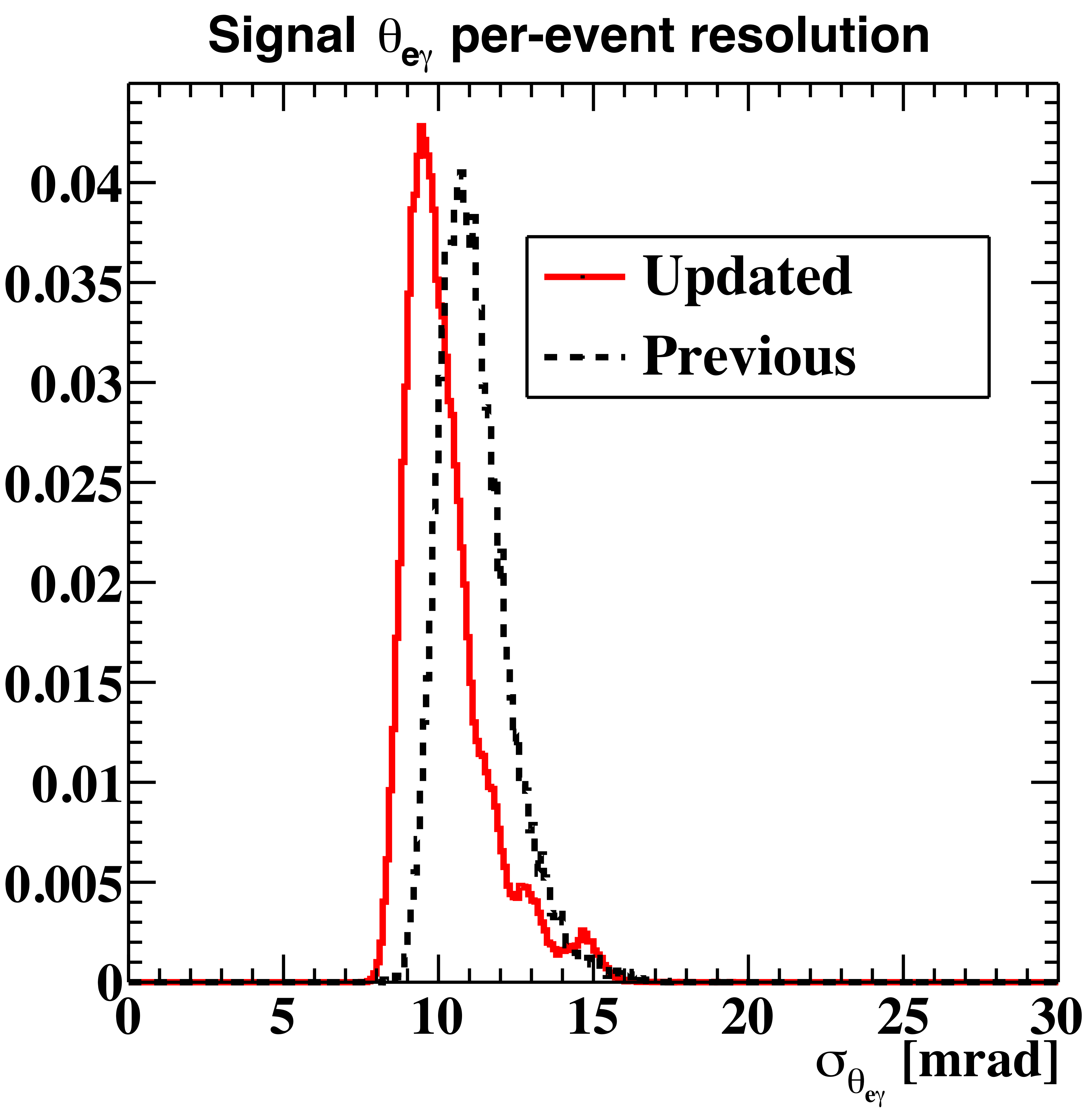

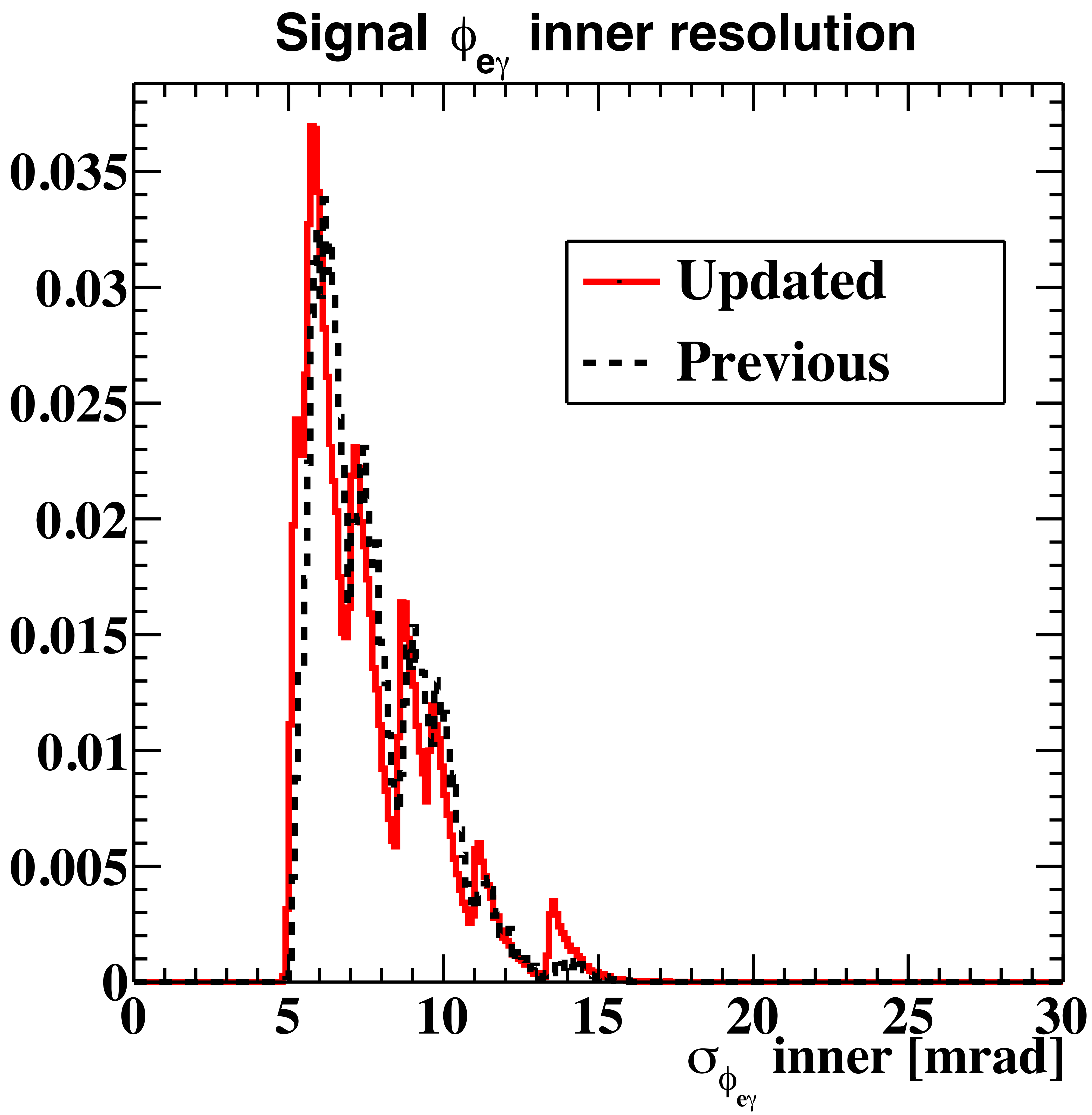

Unblind results: Confidence interval

- No signal excess observed
- Set an upper limit on the branching ratio to 1.5×10^{-13} at 90% C.L.

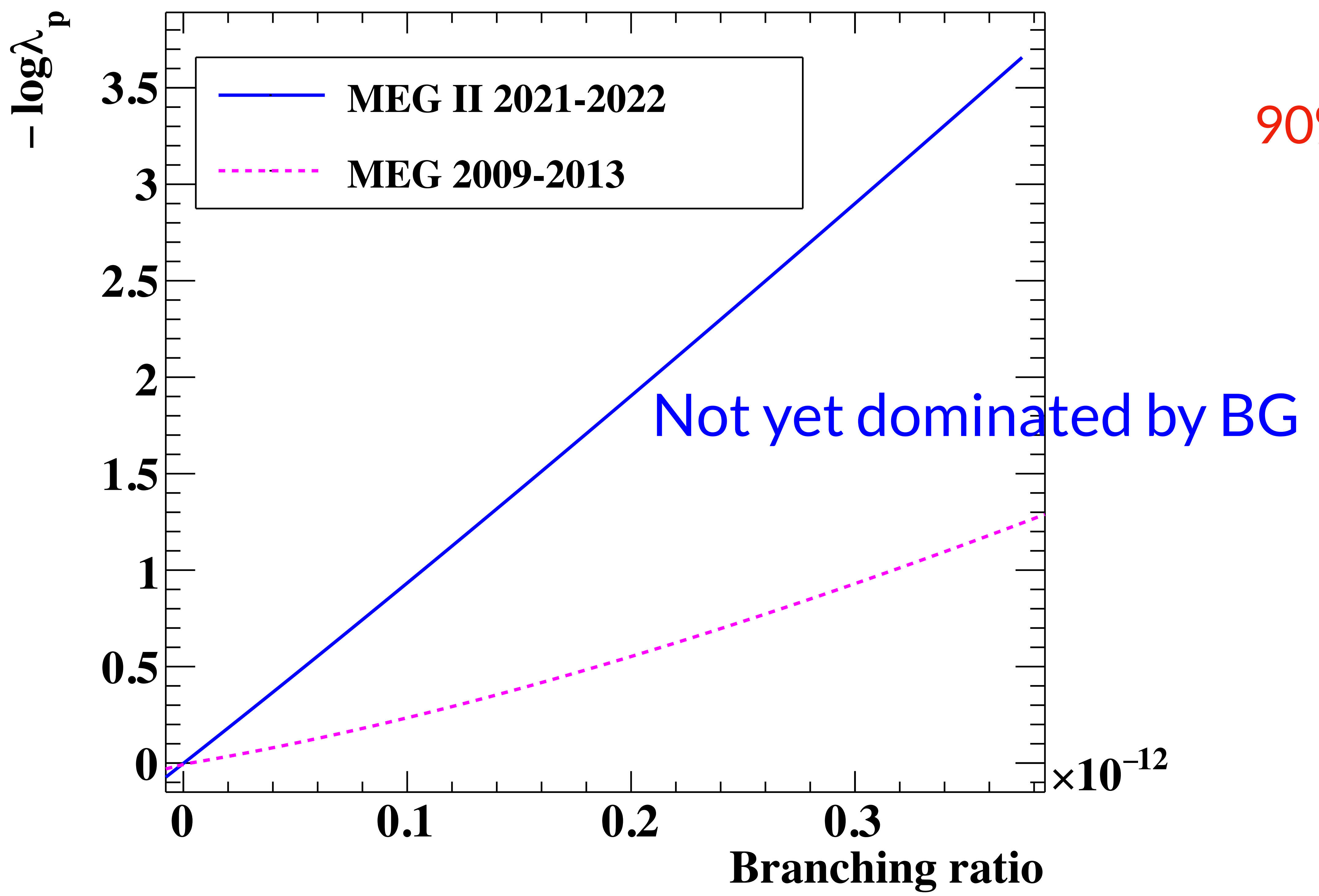

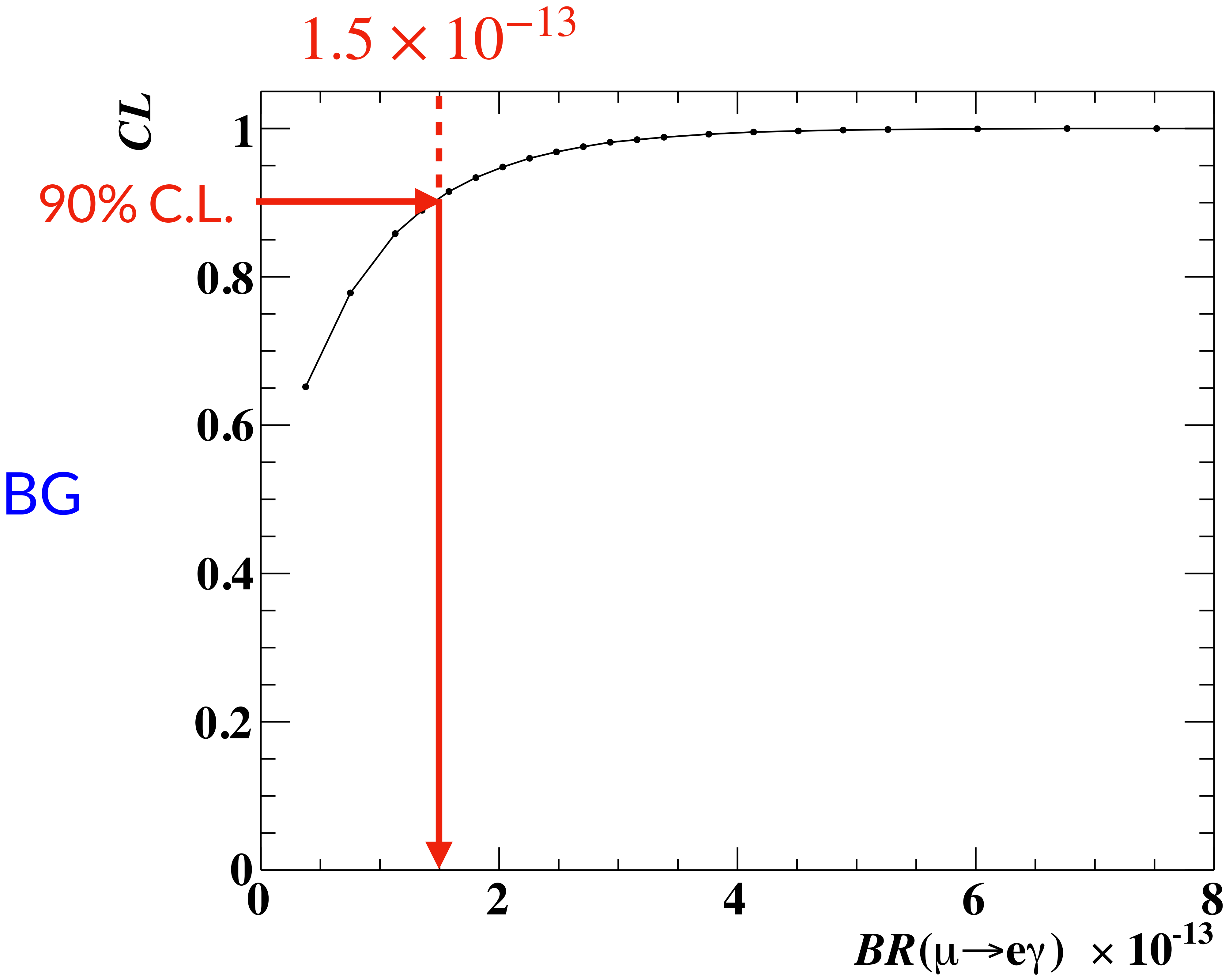

2021 data

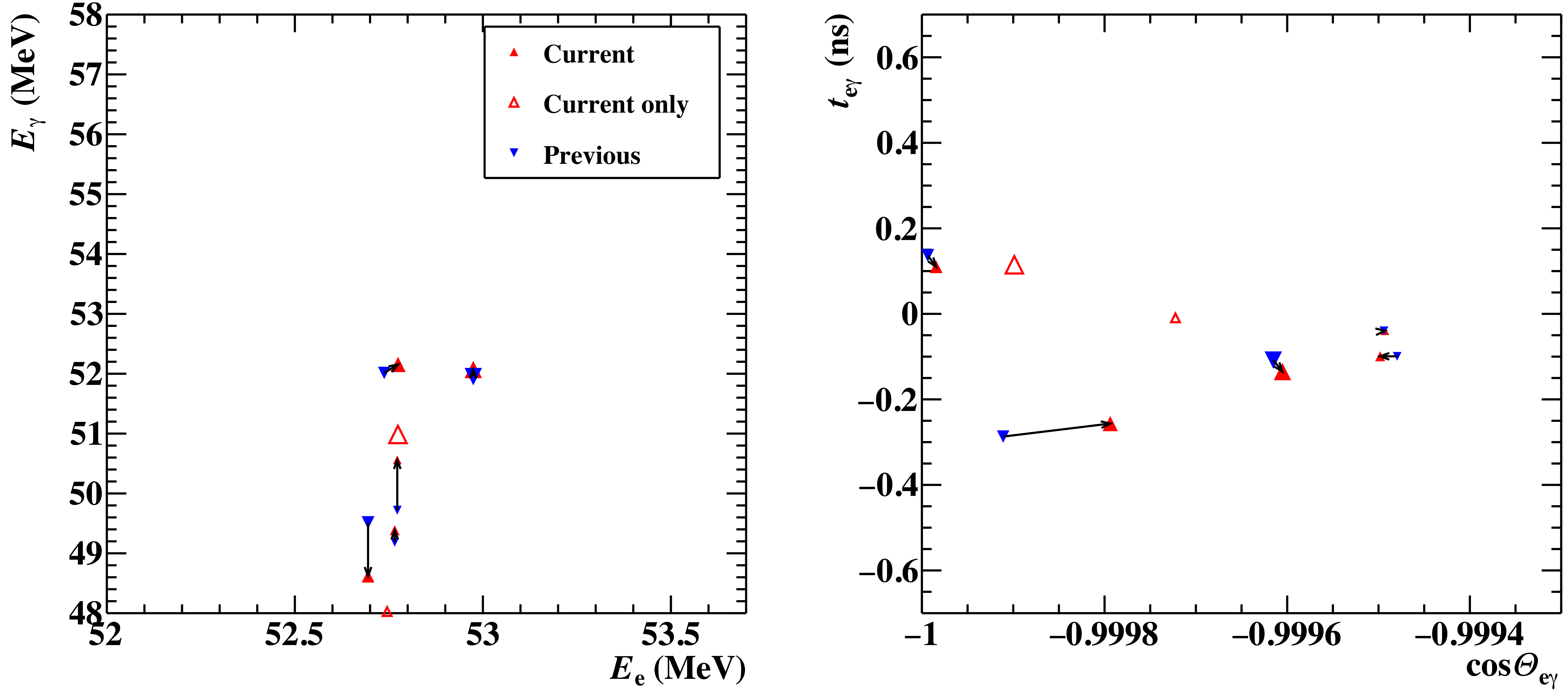

Current
Current only
Previous
E_γ (MeV)
E_e (MeV)
58
57
56
55
54
53
52
51
50
49
48
52
52.5
53
53.5
$t_{e\gamma}$ (ns)
$\cos\Theta_{e\gamma}$
0.6
0.4
0.2
0
−0.2
−0.4
−0.6
−1
−0.9998
−0.9996
−0.9994